Efficacy of a Novel Thoracopelvic Orthosis in Reducing Lumbar Spine Loading and Muscle Fatigue in Flexion: A Study with Weighted Garments

by

Daniel D. Johnson

A dissertation submitted in partial fulfillment
of the requirements for the degree of
Doctor of Philosophy
(Mechanical Engineering)
in the University of Michigan
2012

Doctoral Committee:

Professor Albert J. Shih, Co-Chair
Professor James A. Ashton-Miller, Co-Chair
Professor Thomas J. Armstrong
Assistant Professor Paul Park

from: Iron Man Vol. 1, No. 300, Jan. 1994 (pp. 39-42)
New York: Marvel Comics

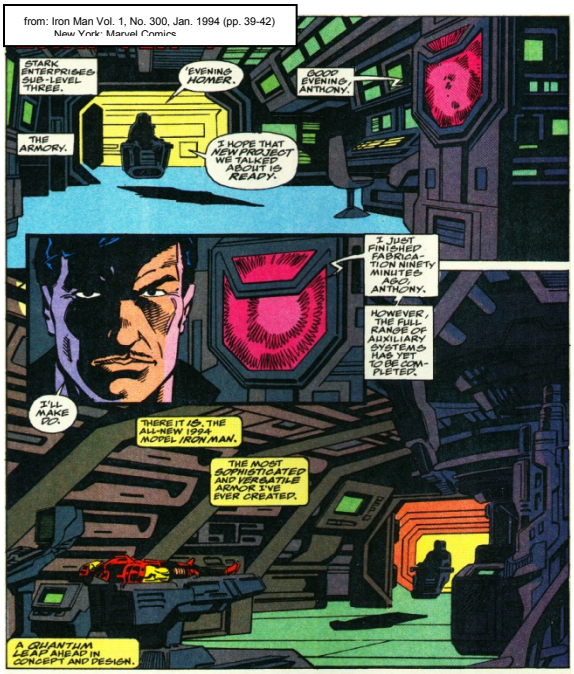

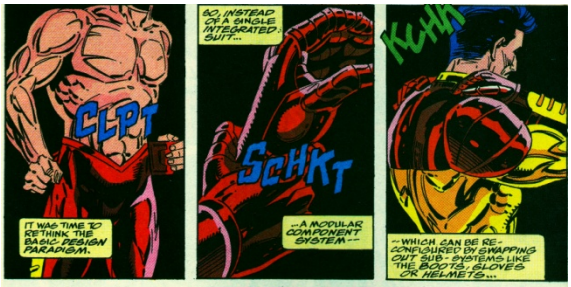

For my parents and students
…Oh, and Sheamus

Acknowledgements

I'd like to thank all those who have supported and assisted me along the way to completing the work for my doctoral program, including: Leah Buechley, Adam Brzezinski, Robert Coury, Alicia Davis (and the orthotists at the University of Michigan Orthotics & Prosthetics Center), Robert Dodde, Toby Donajkowski, Patrick Hughes, Jennifer Keller, Janet Kemp, Anne Kirkpatrick, Achin Masli, Ronald McCarty, Connor Moelmann, Hannah Perner-Wilson, Mary Ramirez, Corwin Stout, and Grace Wu…not to mention all of my long-suffering test subjects.

I also owe a special thanks to Massimo Banzi (and the entire team behind the Arduino™ platform), as well as SparkFun® Electronics: two pioneers of open-source hardware design.

Table of Contents

List of Figures

List of Tables

List of Appendices

Abstract

The purpose of this thesis was to design and test a novel electromechanical thoracopelvic orthosis. We tested the overall hypothesis that the activity of the postural muscles of the lower back in erect and flexed postures, both with and without the wearing of a weighted garment, can be reduced through the wearing of this thoracopelvic orthosis, which was called the Exoskeletal Spinal Support, or ESS. Two experiments informed the design of the orthosis. The first experiment was a repeated-measures study of the effect of a weighted garment (a lead vest) on shoulder and lower back muscle activity of 19 young healthy adults. The results showed that use of the lead vest did not significantly increase muscle activity in any of the three muscle groups studied. However, the adoption of a 25° forward-flexed posture significantly increased the activity of all muscle groups, especially the erector spinae muscles. The second experiment was a repeated-measures study of factors contributing to the normal contact stress developed at the interface between a partial thoracic orthosis and the skin of 20 healthy young men. The results showed stress magnitudes of 8-28 kPa, and the magnitudes were found to increase in proportion to the normalized applied distraction force and moment, as well as respiration phase. The ESS was designed and programmed so that its microcontroller monitored the interface contact stress and commanded its four linear actuators to adjust the orthosis configuration so as to maintain a near-constant trunk extensor moment over a range of trunk flexion. A final experiment was a preliminary validation study of the ESS on a single subject in a variety of loading conditions and flexed postures, with lumbar muscle activity as the primary outcome. The results suggest that at 5° forward flexion, the ESS reduced normalized erector spinae muscle activity by up to 11%. However, when the lead vest was worn over the ESS, muscle activity increased, perhaps due to artifact. We conclude that the ESS has promise as the first “active” orthosis. It allows one to program its mechanical interaction with the trunk via software alone. This interaction includes the use of a constant corrective moment, as was demonstrated here, but the potential exists to program any linear or curvilinear relationship between applied moment and thorax inclination in the sagittal or coronal planes. In addition, it

is possible to change the damping behavior of the ESS through software commands as well. This technology allows for the possibility of telemanagement of orthotic treatment in the future.

Chapter 1

Background and Introduction

1.1 ANATOMY, INJURY, AND BIOMECHANICS OF THE SPINE

The spine is one of the most important structures in the human body. The bones and tissues of the spine serve as the only structures that bear compressive load from the upper body down to the pelvis and legs, making these structures vital to maintaining an upright posture and the overall shape of the body. The rigid elements of the spine also serve as a protective conduit for the spinal column, the bundle of nerve fibers that connects the brain to every other region of the body. The muscles of the back work in concert with the rigid structural elements of the spine to balance the upper body over the pelvis, as well as allowing for a large degree of maneuverability.

1.1.1 Overview of the Spine

The spine is made up of a combination of bone and soft tissues and spans the length of the body from the base of the skull to the coccyx, or tailbone. The spine contains 25 distinct bones: the 24 vertebrae, and the sacrum and coccyx at the base. These bones are connected by the soft tissues of the spine, including the intervertebral discs and numerous tendons and ligaments. The spine is subdivided into four regions (cervical, thoracic, lumbar, and sacral & coccygeal) based on the curvature and morphology of the associated vertebrae. Figure 1.1 shows the vertebrae of the spine from a lateral (side) view, with the rear (posterior) facing to the right. The vertebrae are numbered from top to bottom of their respective regions.

The cervical region of the spine is made up of the uppermost seven vertebrae. The first of these vertebrae (C-1) is known as the Atlas, followed by the Axis (C-2). These two vertebrae have unique shapes and have the largest degree of flexibility in the spine, which allows for the full range of motion of the skull as it sits atop the vertebral column. In general, the cervical vertebrae are thinner, lighter, and more flexibly-connected than vertebrae in the other portions of the spine, and are arranged in a slight backward curvature, or lordosis.

The thoracic region of the spine is primarily characterized as where the ribcage connects to the spine. For all but the lowest "floating" ribs (which are loosely connected by cartilage), the thoracic spine connects to the ribs via ligaments anchored to facets on the thoracic vertebrae. Due to these connections with the ribs, as well as ligaments connecting the ribs to each other, the thoracic region of the spine is mostly rigid. The thoracic spine also has a slight forward curvature, or kyphosis.

The last flexible portion of the spine is the lumbar region. The five lumbar vertebrae are the largest in diameter and bear the largest compressive stresses of the vertebrae. Like the cervical spine, the lumbar region has a lordotic curvature.

The lowermost region of the spine consists of the sacrum and coccyx, which contains the sacral and coccygeal vertebrae. These bones are not distinct structures; rather, they form the semi-flexible, fused central region of the pelvis. This region of the spine only significantly flexes in women during childbirth, where the structure flattens to allow for enlargement of the birth canal (Ashton-Miller & Schultz, 1997).

1.1.2 Motion Segments: Mechanical Sub-units of the Spine

When discussing its behavior as a flexible mechanical structure, the spine is typically broken down into subunits known as motion segments, one of which is shown below in Figure 1.2. A motion segment consists of two vertebrae and the soft tissues connecting them. Foremost among these tissues is the intervertebral disc, which lies between the vertebral bodies: the thick, cylindrical portions of the vertebrae. The intervertebral discs are the largest avascular tissues in the body, meaning that they have no interval blood vessels; they rely entirely on nutrients and oxygen diffusing inwards from their outermost surfaces (Ashton-Miller & Schultz, 1997). The nucleus pulposus at the core of each disc and the innermost layer of the annulus fibrosis that surrounds it together act as a hydraulic cushion that provides uniform hydrostatic force to separate the two vertebrae of the motion segment. The pressure within and thickness of a disc are largely dependent on the amount of fluid contained in the intervertebral disc, which can decrease by as much as 20% over the course of a day of normal activity in healthy people (Adams, McMillan, Green, & Dolan, 1996).

At the posterior of each vertebra are bony structures known as processes, which serve as secondary links between the vertebrae (the articular processes) and attachment points for muscles and ligaments of the back (spinous processes). The processes are connected to the

vertebral body by an intermediate bony structure called the pedicle. The space enclosed by the processes, pedicle, and vertebral body is known as the intervertebral foramen, which is where the nerve fibers of the spinal column are enclosed (Ashton-Miller & Schultz, 1997).

1.1.3 Back Pain from Injury to the Spine

Back pain of the sort not caused by muscular strain/injury is caused by undue pressure being put on nerves in or around the spinal column, which can be caused by several factors. Acute injury to the spine (from impact, for example) can cause structures of one or more motion segments intrudes into the intervertebral foramen, thus applying pressure to (or in severe instances, severing) the nerves of the spinal column. Intrusion can occur from fractures of the processes or crushing of the vertebral bodies, but the more common form of damage occurs when an intervertebral disc bulges into the intervertebral foramen, a condition known as a herniated disc. Disc herniation is caused by a loss of structural integrity of the annulus fibrosis, which in turn can be caused by factors such as disease, age, and even chronic over-loading. Even for healthy discs, it has been shown that as water is squeezed out of the nucleus pulposus, stress concentrations can appear on the annulus fibrosis. If the stresses become high enough to cause individual lamellae (the tough, ring shaped layers of the annulus fibrosus) to fail, the disc will not be able to maintain shape, potentially bulging into the intervertebral foramen (Adams, McMillan, Green, & Dolan, 1996; Ashton-Miller & Schultz, 1997).

Apart from the spinal column, back pain can also come from other nerve tissue within the structure of the spine. Nerves in the outermost layers of the annulus fibrosis can be stimulated by high mechanical forces, and pain can also result from deformation of the vertebral endplates (at the top and bottom of each vertebral body). Pain from either one of these causes would be expected to increase over time, especially in a flexed posture, due to time- and load-dependent water depletion in the nucleus pulposus (Adams, McMillan, Green, & Dolan, 1996).

1.1.4 Morphology and Kinematics of the Lumbar Spine

The lumbar spine is the focus of this study, and thus a more detailed look at the structures and behavior of this portion of the back is required. First, typical dimensions for the lumbar vertebrae and associated structures of each motion segment will be described. This will be followed by a description of the limits of motion of each of the lumbar motion segments, including both translation and rotation, from an erect posture to maximum flexion. Finally,

typical forces seen I the lumbar spine will be described. It is only though understanding the shape and kinematics of the lumbar spine that a mechanism can be designed to successfully mimic and support it through the entire range of motion without risk of injury or loss of efficacy.

As mentioned above, the lumbar vertebrae bear the highest compressive stress of all vertebrae of the spine, and are thus the largest. As can be seen below, with some variation, the centra (a centrum is the largest portion of the vertebral body) of lumbar vertebrae generally increase in height from L-1 to L-5 for both men and women (van Bodegom, et al., 1998):

	Centrum Height (mm)	
Vertebra	Male	Female
L-1	27.14	26.54
L-2	28.43	28.35
L-3	29.41	29.21
L-4	29.14	29.68
L-5	29.21	30.3

The large range of motion exhibited by the human spine is a result of the contributions of each motion segment along its length. The lumbar spine, as a whole, can flex over 30 degrees from maximum flexion to maximum extension, however, each motion segment has a relatively small angular rotation range (typically less than 10° in flexion), as shown below (Panjabi, Oxland, Yamamoto, & Crisco, 1994; Ashton-Miller & Schultz, 1997):

Motion Segment	**Max. Flexion (degrees)**
L-1 / L-2	5
L-2 / L-3	7
L-3 / L-4	7
L-4 / L-5	9
L-5 / 10	9

The loading experienced by the lumbar spine in daily life has been estimated by many modeling and *in vitro* studies, but relatively few direct measurements have been made *in vivo*, due largely to concern over damage to the structures of the spine that might occur from implantation of

measurement devices. Using a pressure transducer implanted in an L-4/L-5 intervertebral disc, one such study by Wilke, Neef, Caimi, Hoogland, and Claes (1999) detailed the large range of compressive loading experienced by the lumbar spine of one test subject in performing normal daily activities, as shown below:

Activity	**Intervertebral Disc Pressure (MPa)**
Lying Prone	0.1
Standing Erect	0.5
Forward Flexion	1.1
Holding 20 kg Weight Close to the Body	1.1

It was also shown by Wilke *et al.* (1999) that in the evening when a person sleeps (in a supine position), which is when the intervertebral disc rehydrates, the nominal pressure increased from 0.1 MPa to 0.24 MPa. It must be emphasized again that this data came from one male test subject, limiting the applicability of the numbers given, but the data still give valuable insight into actual pressures and loads within the lumbar spine.

1.2 MUSCLES OF THE LOWER BACK

The muscles of the lower back can be divided into three primary groups, based on function: 1. Flexors, 2. Extensors, and 3. Lateral Flexors. All three of these groups are shown above in Figure 1.3. Put simply, flexors bend the spine and torso forward, extensors lean them back, and lateral flexors tilt them to the left or right. This study focuses primarily on the extensors, but due to the complicated overlapping functions of each group (and continuing controversy over what contributions each has to any particular motion), all three will be described here. This is by no means an all-inclusive list of every muscle of the lower back, or those that act on the spine. Muscles such as the abdominals and the lumbodorsal fascia will not be covered, except for positional reference. In this section, the word fascicle refers to a (usually named) bundle of muscle fibers.

1.2.1 Flexors

The primary flexor muscle directly attached to the lumbar spine is the psoas major, shown below in Figure 1.4. This muscle attaches laterally to each lumbar vertebra on the

transverse processes, as well as having intervertebral connections that span each intervertebral disc. The psoas major terminates at the trochanter minor of the femur after passing along the pelvis.

The psoas major, due to its function as a flexor of the spine, bends the spine and upper torso forward. Its exact roles in other motions of the spine remain controversial. Some studies have shown that the psoas major is active in maintaining an erect posture, while others have stated that it could act as another lateral flexor. Still others believe the psoas major is vital in balancing the spine during walking (Hansen, de Zee, Rasmussen, Anderson, Wong, & Simonsen, 2006).

1.2.2 Extensors

Erector spinae. The erector spinae is a large mass of muscle running nearly the length of the spine, as shown below in Figure 1.5. As it crosses into the lumbar region, the muscle is split into three main columns: the spinalis dorsi (the most medial, near the spinous processes), the longissimus (immediately lateral to the spinalis), and the iliocostalis lumborum (most lateral of the three). The medial two columns lie immediately over the grooves created by the processes of the vertebrae. The erector spinae, in general, crosses through the lumbar region of the back without directly attaching to the vertebrae, and some of its caudal constituent fascicles (iliocostalis lumborum pars lumborum and iliocostalis lumborum pars thoracis) attach directly to the iliac crest of the pelvis. In the lower lumbar region, the collective muscle groupings of the erector spinae are sometimes referred to as the sacrospinalis. The erector spinae are covered superficially by the thoraculumbar and lumbodorsal fascia.

When the muscles of the erector spinae act bilaterally, they have the effect of increasing the lordosis of the spine, and provide a counter balance to the forces of the abdominal muscles. The erector spinae works in concert with the multifidus (described below) to prevent excess rotation of the spine in flexion (Hansen, de Zee, Rasmussen, Anderson, Wong, & Simonsen, 2006).

Multifidus. Another group of extensors of the lumbar spine are the multifidus muscles, collectively called the multifidi. These muscles lie deep in the back (See the Figures 1.3, 1.5, and 1.6), under the erector spinae within the same grooves between the vertebral processes. As shown below in Figure 1.6, this group of muscles anchors each of the lumbar vertebrae to other vertebrae and the sacrum. The deepest of the multifidi are fascicles that connect the lower

surface of each vertebra to the superior processes of the vertebrae two places below it (see Figure 1.6,A). For L-5, the fascicles connect to the sacrum. The longer, larger fascicles of the multifidi (Figure 1.6, B-F) originate at the spinous process of each lumbar vertebrae, connecting first to the superior processes of the vertebra two places below and then to each subsequent vertebrae and the sacrum. The multifidi of L-1 to L-3 also connect to the iliac crests of the pelvis, each connection descending in height with the location of the associated vertebra.

The multifidi are not believed to be primary extensors of the lumbar spine; rather, they act to stabilize the position and orientation of each of each vertebra, preventing excessive segmental motion. As mentioned above, they are believed to provide resistance to flexion from the abdominal muscles along with the erector spinae (Hansen, de Zee, Rasmussen, Anderson, Wong, & Simonsen, 2006).

Intertransversarii and interspinales. The intertransversarii and interspinalis are small groupings of muscles that interconnect the processes of each of the vertebrae of the spine, similar to the small sub-groups of laminar fibers of the multifidi. The intertransversarii can be subdivided into two subgroups in the lumbar region: the mediales (most important for extension) and the laterales (described in the next section). The mediales connect the accessory process of each lumbar vertebra (at the posterior base of each transverse process of the lumbar vertebrae) to the mamillary process (located laterally on the dorsal margin of the superior articular processes of the lumbar vertebrae) of the vertebra below (Online Med. Dic.). The vertebral processes mentioned are shown below in Figure 12.

The interspinalis are similar to the intertransversarii in that they are paired sets of muscles connecting the spinous processes of adjacent vertebrae. The exact functions of the intertransversarii and interspinales are still being debated, but it is believed they are primarily devoted to stability and accurate positioning of the lumbar and sacral spine (Hansen, de Zee, Rasmussen, Anderson, Wong, & Simonsen, 2006).

1.2.3 Lateral Flexors

Quadratus lumborum. The quadratus lumborum is, as the name suggests, a muscle of the lumbar back roughly shaped like a quadrilateral that exists on either side of the spine. It attaches at its extremes to the twelfth rib and the iliac crest of the pelvis, and also to the transverse processes of the upper four lumbar vertebrae in between, as shown in blue in Figure

8. This muscle is primarily involved in lateral flexion, but it has also been suggested to aid in respiration (Hansen, de Zee, Rasmussen, Anderson, Wong, & Simonsen, 2006).

Lateral intertransversarii. The intertransversarii laterales are a subgroup of the intertransversarii, as mentioned above. The laterales can be further divided into the ventrales and dorsales. These muscles connect the transverse and accessory processes of a lumbar vertebra to the transverse processes of the next caudal vertebra (Hansen, de Zee, Rasmussen, Anderson, Wong, & Simonsen, 2006).

1.3 SPINAL OFFLOADING VIA A CORRECTIVE SUPPORT: A THEORETICAL MODEL

The compressive load on the spine can be offloaded by two interrelated support mechanisms: increasing intraabdominal pressure and reducing the activity of the postural muscles of the lower back (Örtengren, Andersson, & Nachemson, 1981; Ashton-Miller & Schultz, 1997), one or both of which can be provided through spinal orthoses (Lantz & Schultz, 1986; Bussel, Merritt, Fenwick, 1995). Intraabdominal pressure can be increased through the use of corset-style orthoses or belts. In order to be effective, however, these devices must be worn very tightly, which can create discomfort and impede mobility of the lumbar spine in movements such as flexion. Reduction in lower back muscle activity (erector spinae and multifidi, esp.) requires a reduction in the force required from these muscles to maintain a stable posture of the trunk. While increasing intraabdominal pressure can allow for a reduction in the force required of the lower muscles, another means of creating this effect is through the application of an external force to the trunk (hereafter referred to as a "corrective support). In particular, applying an extension moment to the thorax via a corrective support applied anteriorly to the spine can reduce the extension moment (and thus force and activity) required of the lower back muscles in order to balance the gravitational flexion moments of the thorax.

The effect of a corrective support on lower back muscle force required for postural stability can be illustrated in a two-dimensional model (sagittal plane) of the trunk and the forces acting upon it (Figure 1.8), including the external forces of a corrective support and the weight of an external mass carried by the trunk. For each section of the body, appropriate values for position, (x_i , z_i), and mass, m_i, are taken from the literature (Ashton-Miller & Schultz, 1997; Hall, 2007), and the total mass (78 kg) and height (1.8 m) of an average European male are taken from the AnyBody Modeling System™ (version 3.0.1; AnyBody Technology A/S, Aalborg, DEN). The z-component of the application point of the corrective support is approximately at

the base of the ribcage, also taken from the AnyBody model. It is assumed that the corrective support is applied at approximately the same x-position as the center of mass of the trunk. The example external mass used here is that of a typical lead vest (LB 16 Rev. D; BMS, Newport News, VA, USA; see Chapter 2), which is assumed to be evenly distributed around the trunk (i.e.no net moment is created) and supported at the shoulders. Here, all muscles of the lower back are assumed to concentrate their force application at the level of L-3, in the mid- lumbar spine. A summary of the mass (if applicable) and point of application of each force within the model is summarized here:

Component	**Mass**	**Point of Application**	
Head/Neck:	$m_H = 6.44$ kg	$x_H = 0.05$ m	$z_H = 0.646$ m
Arms (together):	$m_A = 9.0$ kg	$x_A = 0.0$ m	$z_A = 0.54$ m
Trunk:	$m_T = 36.54$ kg	$x_T = 0.01$ m	$z_T = 0.34$ m
External Mass:	$m_E = 3.70$ kg	$x_E = x_A$	$z_E = z_A$
Corrective Support:		$x_C = x_T$	$z_C = 0.13$ m
Back Muscles:		$x_M = -0.06$ m	z_M =0.07 m

The forces required of the lower back muscles are calculated by balancing the sum of the moments created by each component about the origin. In the erect posture, the moment arm for each component is its x-position. In the a flexed posture, the gravitational forces remain oriented in the same direction; for simplicity, we assume that the corrective support is always oriented vertically (i.e., applied as a distraction force) and that the points of application of the muscle force and corrective support do not move in flexion. In a flexed posture, the new moment arm of every component (excluding the muscles and corrective support) about the y axis must be calculated using the x and z positions and equation (1) below, where r_i is the length of the moment arm (in meters) and θ is the angle (in degrees) of flexion at the level of L-5/S-1 (the origin) from an erect posture (i.e., θ = 0°). Note that for all applied forces, $r_i(0) = x_i$:

$$r_i(\theta > 0) = \sqrt{{x_i}^2 + {z_i}^2}\sin\theta \qquad (1)$$

To calculate the weight of each component (in Newtons; where applicable), the external and body-component masses are multiplied by the gravitational constant (9.81 m/s^2). Finally, a

summation of moments about the origin is used to solve for the required back muscle force (F_M) as a function of the corrective support (F_c) and flexion angle (θ), shown below in equation (2):

$$F_M(Fc, \theta > 0) = \frac{g(m_H\sqrt{{x_H}^2+{z_H}^2}\sin\theta+(m_A+m_E)\sqrt{{x_A}^2+{z_A}^2}\sin\theta+m_T\sqrt{{x_T}^2+{z_T}^2}\sin\theta)-F_C|x_T|}{|x_M|} \quad (2)$$

The results for a variety of flexion angles (θ = 5°-25°, in 5° increments) and corrective support magnitudes (F_C = 0 N, 10 N, 50 N, and 100 N) are shown in Figure 1.9; the results for body gravitational forces only (m_E = 0 and F_C = 0 N) are also included as a reference. As the model results show, the application of an external mass not only increases the required back muscle force throughout the range of flexion angles, but also changes the shape of the resulting trend for F_M vs. θ. For the remaining results (all with m_E = 3.7 kg) , each corrective support magnitude results in a relatively constant reduction in the required back muscle force across the entire range of flexion. Looking at percent reductions in required back muscle force, the largest reductions all occur at the lowest flexion angle (5°) and range from 6.5% to 64.8% (for F_C = 10 N and 100 N, respectively); the smallest reductions occur at the largest flexion angle (25°) and range from 1.3% to 13.4% (for F_C = 10 N and 100 N, respectively). Even with this simple model and its assumptions, the results suggest that 1) an external mass applied to the trunk (with a weighted garment such as a lead vest) increases the required back muscle force to maintain flexed postures, and 2) the use of a corrective support applied to the trunk (and the resulting corrective moment it imparts to the trunk) should produce a reduction in required back muscle force (and thus back muscle activity) to maintain flexed postures. As discussed above, this effectively means that the use of a corrective support should partially unload the compressive forces acting on the spine, thus potentially reducing the likelihood of not only muscle fatigue, but also damage to the spine.

1.4 WORKING HYPOTHESIS AND THESIS OVERVIEW

The purpose of this thesis, as described in the following chapters, is to test the hypothesis that the activity of the postural muscles of the lower back in erect and flexed postures, both with and without the wearing of a weighted garment, can be reduced through the wearing of a novel thoracolumbosacral orthosis (the Exoskeletal Spinal Support, or ESS) that generates a sustained corrective moment on the thorax over a range of postures. Chapter 2 describes a study which recreated the working postures of a population which regularly wears weighted garments as part of their occupation (interventionalists), and discusses which factors (of several studied) have a significant effect on lower back postural muscle activity. Chapter 3

details an exploratory study of the normal contact stress developed as a consequence of two potential mechanisms of offloading compressive forces on the spine: distraction forces and moments applied to an orthosis. Chapter 4 details the design and initial validation of a novel prototype orthosis for use by interventionalists (and others) which is meant to offload the spine through the application of corrective moments over a range of motion. Chapter 5 discusses the work of each individual experiment (from Chapters 2-4) individually and in aggregate, and Chapter 6 summarizes the overall conclusions of this thesis. Finally, Chapter 7 details suggestions for future work in the design and validation of the prototype orthosis (and the technological architecture it represents).

1.5 REFERENCES

Adams, M., McMillan, D., Green, T., & Dolan, P. (1996). Sustained loading generates stress concentrations in lumbar intervertebral discs**.** *Spine*, 21(4), 434-438.

Ashton-Miller, J. & Schultz, A. (1997). Biomechanics of the human spine. In *Basic Orthopedic Biomechanics* (2nd ed.)(pp. 353-392). Philadelphia: Lippincott-Raven Publishers.

Bogduk, N., Macintosh, J., & Pearcy, M. (1992). A universal model of the lumbar back muscles in the upright position**.** *Spine*, 17, 897-913.

Bogduk, N. (1997). *Clinical Anatomy of the Lumbar Spine and Sacrum* (3rd ed.). London, UK: Churchill Livingstone.

Bussel, M., Merritt, J., & Fenwick, L. (1995). Spinal Orthoses. In J. B. Redford, J. V. Basmajian, & P. Trautman (Eds.), *Orthotics: Clinical Practice and Rehabilitation Technology* (pp. 71-101). Philadelphia, PA: Churchill Livingstone.

Dept. of Medical Oncology, University of Newcastle upon Tyne. *Online Medical Dictionary*. Retrieved from: http://cancerweb.ncl.ac.uk/cgibin/omd?action=Search+OMD& query=mamillary+process.

Gray, H. (1918). Anatomy of the human body (20th ed.). W. H. Lewis (Ed.). Philadelphia: Lea & Febiger.

Hall, S. J. (2007) *Basic Biomechanics* (5th ed.). New York: McGraw-Hill.

Hansen, L., de Zee, M., Rasmussen, J., Anderson, T., Wong, C., & Simonsen, E. (2006). Anatomy and biomechanics of the back muscles in the lumbar spine with reference to biomechanical modeling. *Spine*, 31(17), 1888-1899.

Lantz, S. A., & Schultz A. B. (1986). Lumbar spine orthosis wearing. II. Effect on trunk muscle myoelectric activity. *Spine*, 11(8), 838-842.

Örtengren, R., Andersson, G. & Nachemson, A. (1981). Studies of relationships between lumbar disc pressure, myoelectric back muscle activity, and intra-abdominal (intragastric) pressure. *Spine*, 6(1), 98-103.

Panjabi, M., Oxland, T., Yamamoto, I., & Crisco, J. (1994). Mechanical behavior of the human lumbar and lumbosacral spine as shown by three-dimensional load-displacement curves. *The Journal of Bone and Joint* Surgery, 76-A(3), 413-424.

van Bodegom, J., Kuiper, J., Rijn, R., Kuijk, C., Zwamborn, A., & Grashuis, J. (1998). Vertebral dimensions: Influence of x-ray technique and patient size on measurements. *Calcified Tissue Int.,* 62, 214-218.

Wassell, J. T., Gardner, L. I., Landsittel, D. P., Johnston, J. J., & Johnston, J. M. (2000). A prospective study of back belts for prevention of back pain and injury. *The Journal of the American Medical Association*, 284(21).

Wilke, H., Neef, P., Caimi, M., Hoogland, T., & Claes, L. (1999). New *in vivo* measurements of pressures in the intervertebral disc in daily life. *Spine*, 24(8), 755-762.

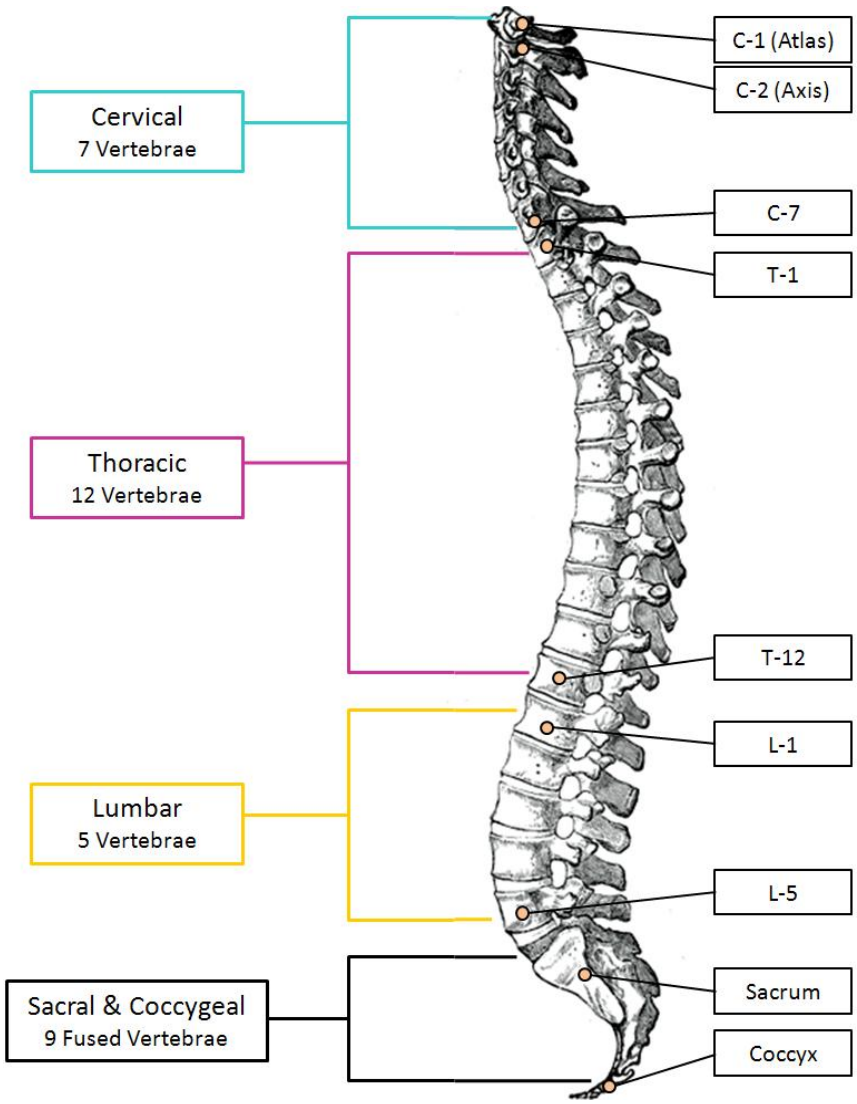

Figure 1.1: The divisions of vertebrae in the human spine, left lateral view. Adapted from Gray (1918); Wassell, Gardner, Landsittel, Johnston, & Johnston (2000).

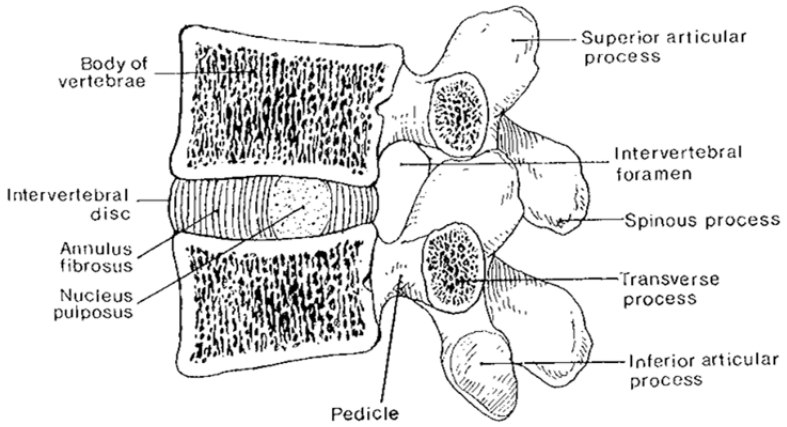

Figure 1.2: A typical motion segment, posterior to the right (Ashton-Miller & Schultz, 1997).

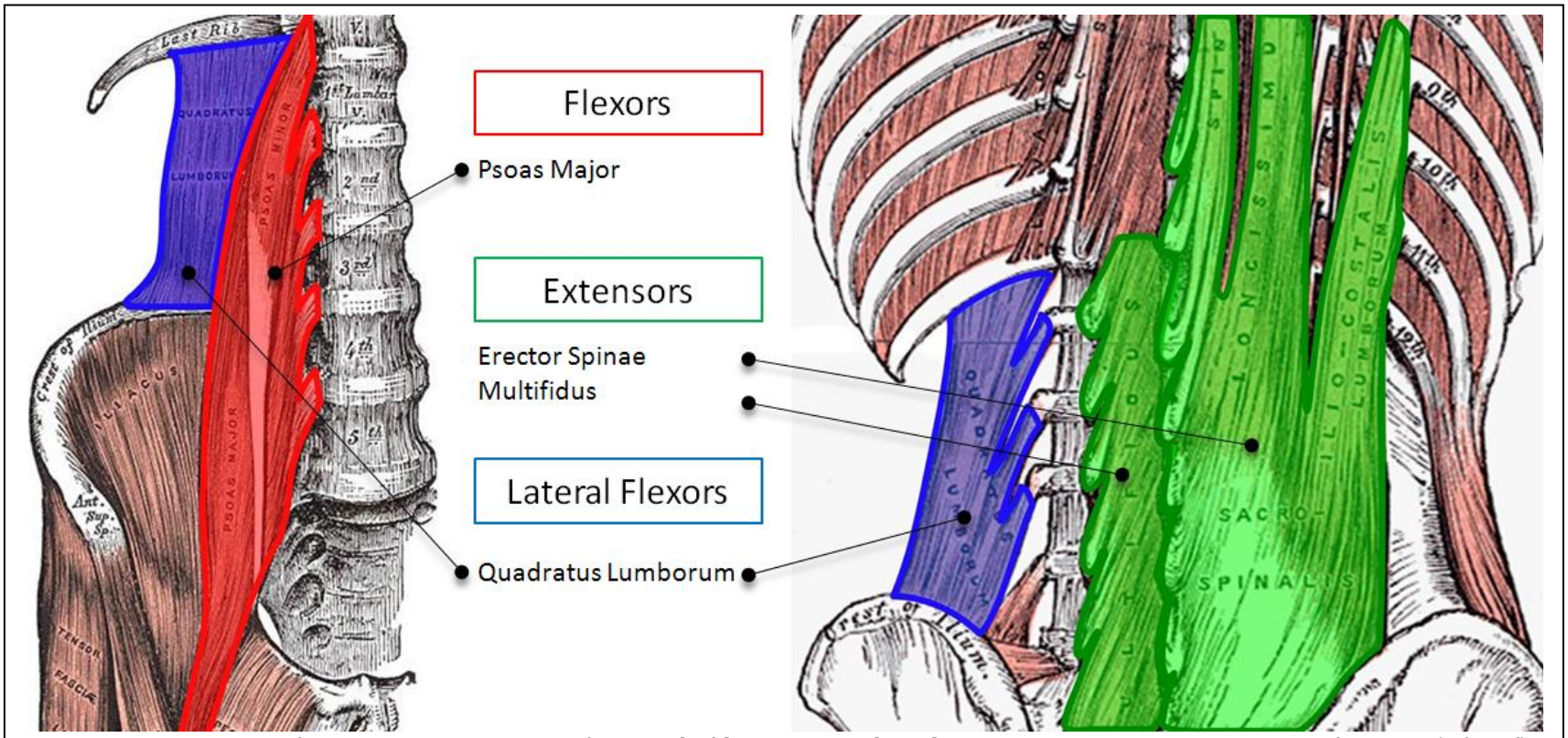

Figure 1.3: Some muscles of the lower back, grouped by function. [Left] Ventral view. [Right] Dorsal view, showing deeper muscles of the back (left half) and shallower muscle layers (right half). Adapted from Gray (1918).

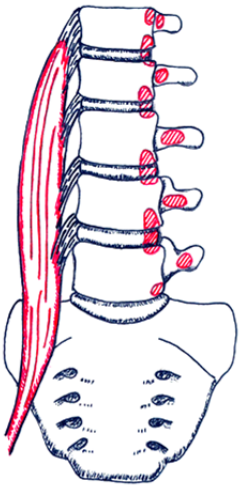

Figure 1.4: The psoas major and the lumbar spine (anterior view), showing muscle (left) and main attachment points (right). Adapted from Gray (1918); Bogduk, Macintosh, & Pearcy (1992).

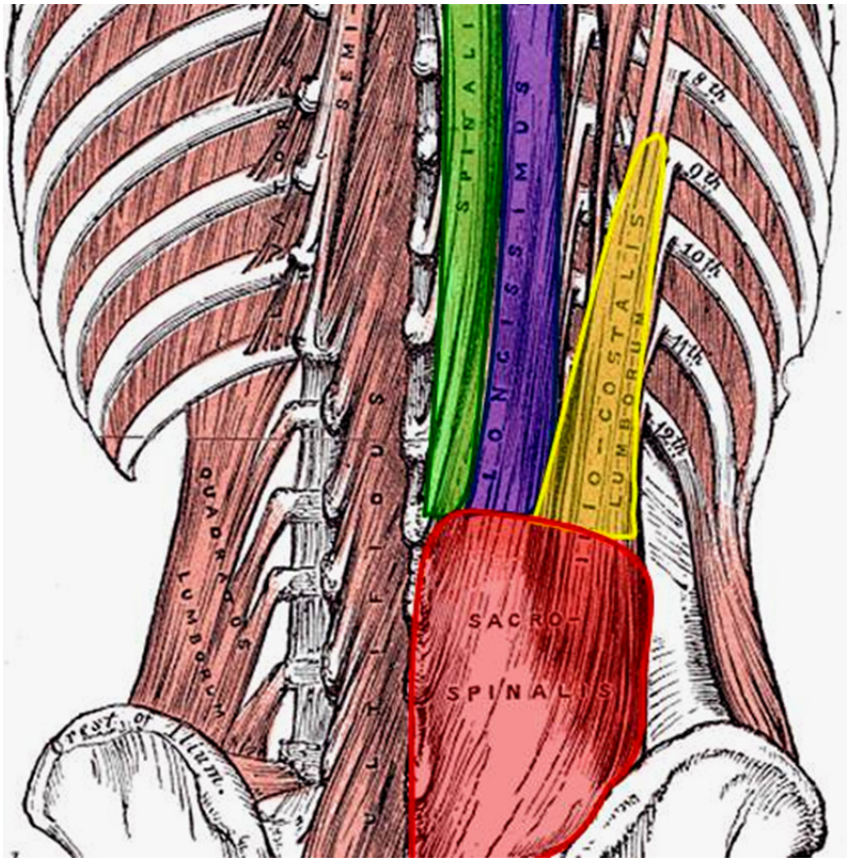

Figure 1.5: The major sub-groups of the erector spinae near the lumbar spine: spinalis dorsi (green), longissimus dorsi (blue), iliocostalis lumborum (yellow), and sacrospinalis (red). The left half of the figure shows deeper muscle layers, including the multifidus (immediately left of midline) and the quadratus lumborum (far left). Adapted from Gray (1918).

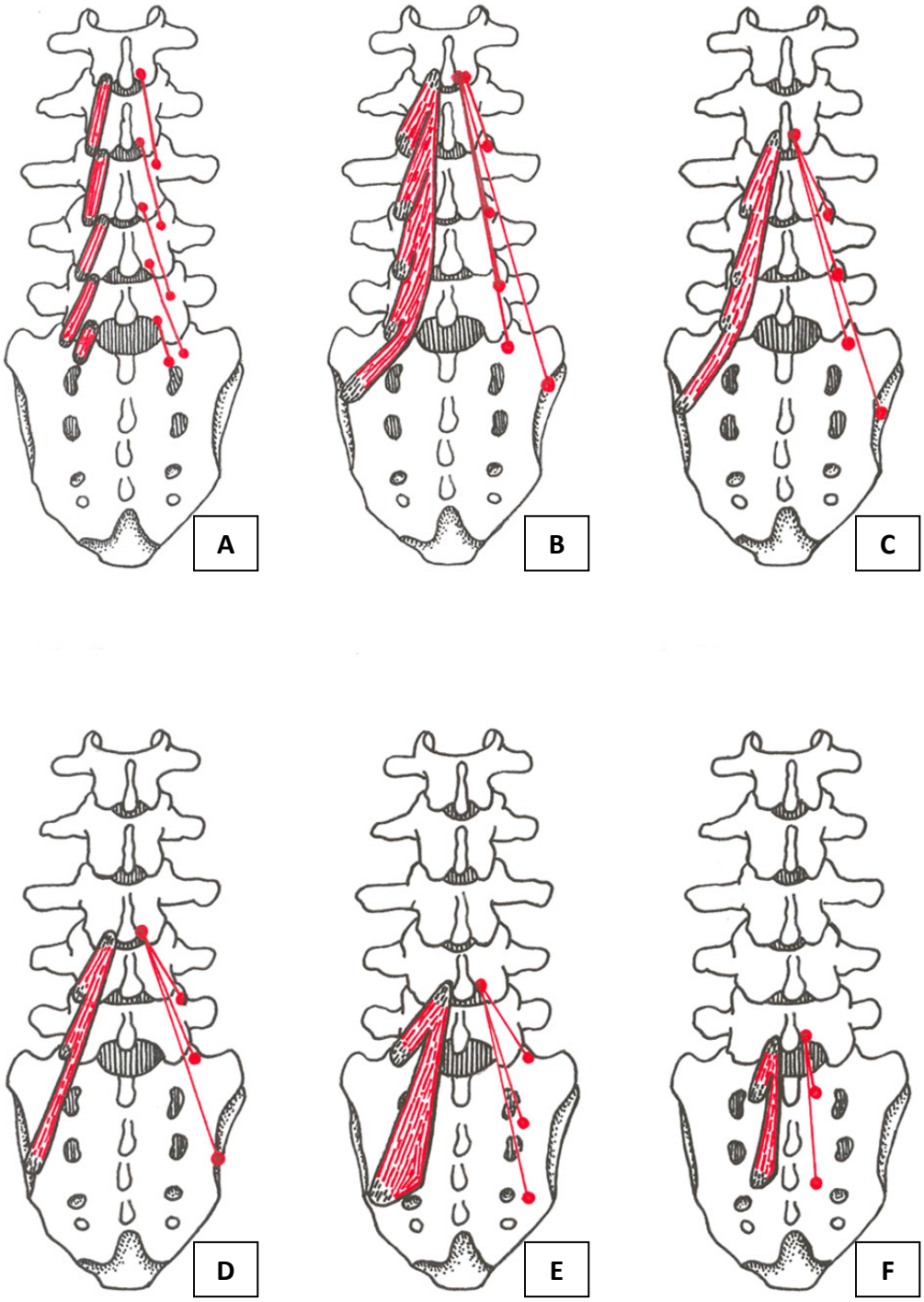

Figure 1.6: The multifidi of the lumbar spine. [A] Laminar Fibers, [B–F] fascicles originating from the spinous processes of L-1 to L-5, respectively. Muscles (left) and attachment points with lines of action (right) are shown in each. Adapted from Gray (1918); Bogduk, (1997).

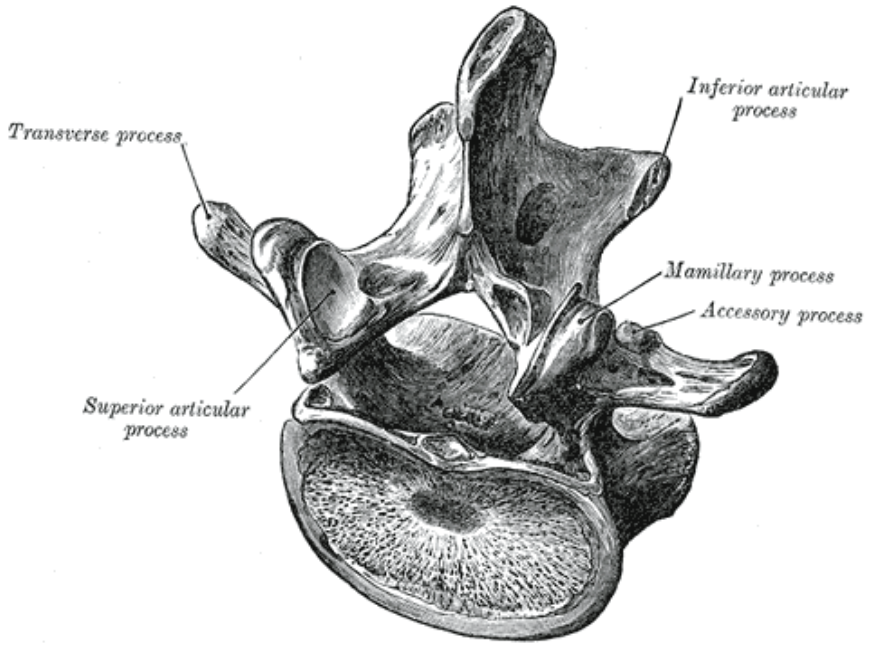

Figure 1.7: A lumbar vertebra, with processes labeled. (Gray, 1918).

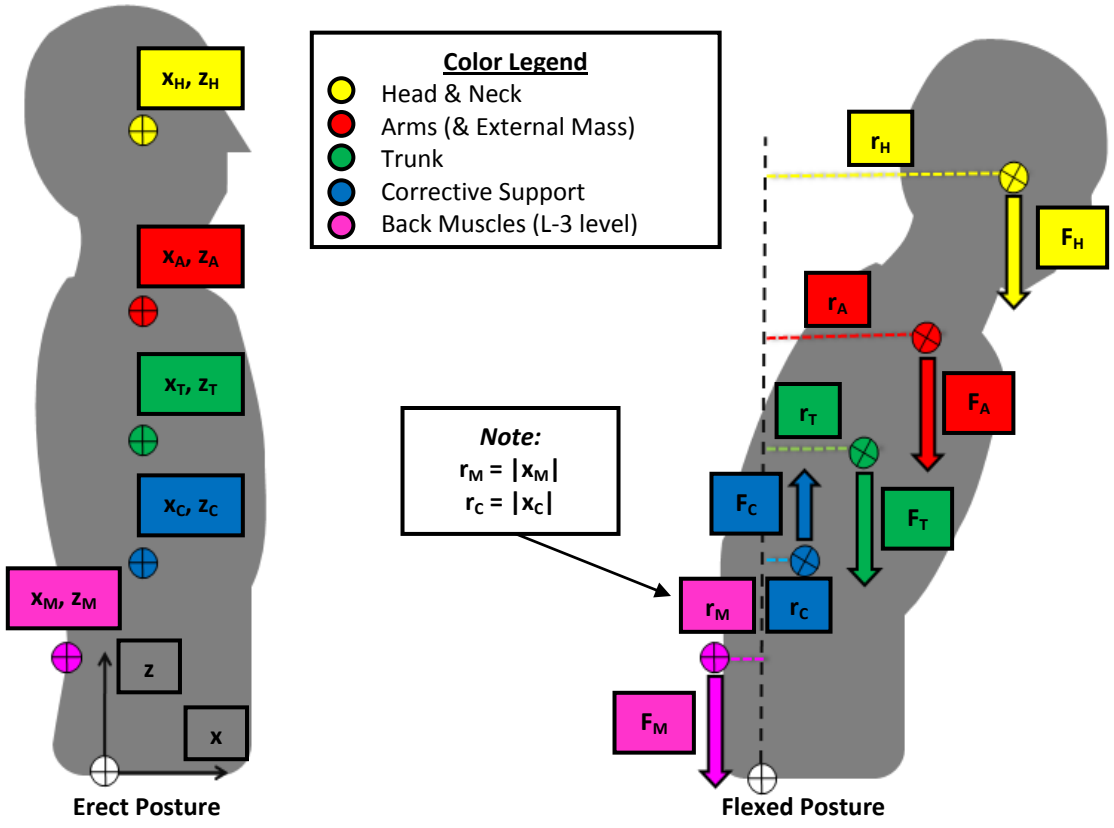

Figure 1.8: 2-D model of forces on the trunk in both erect and flexed postures. Forces are shown as arrows, moments arms as dashed lines, and force application sites as circles. The origin is at the L-5 / S-1 level. Forces and moment arms are not shown in the erect posture for clarity.

Figure 1.9: 2-D model results of lower back postural muscle force required for postural stability for various flexion angles and corrective force magnitudes. The model results for no external mass or corrective force (i.e., body gravitational forces only) are included as a reference.

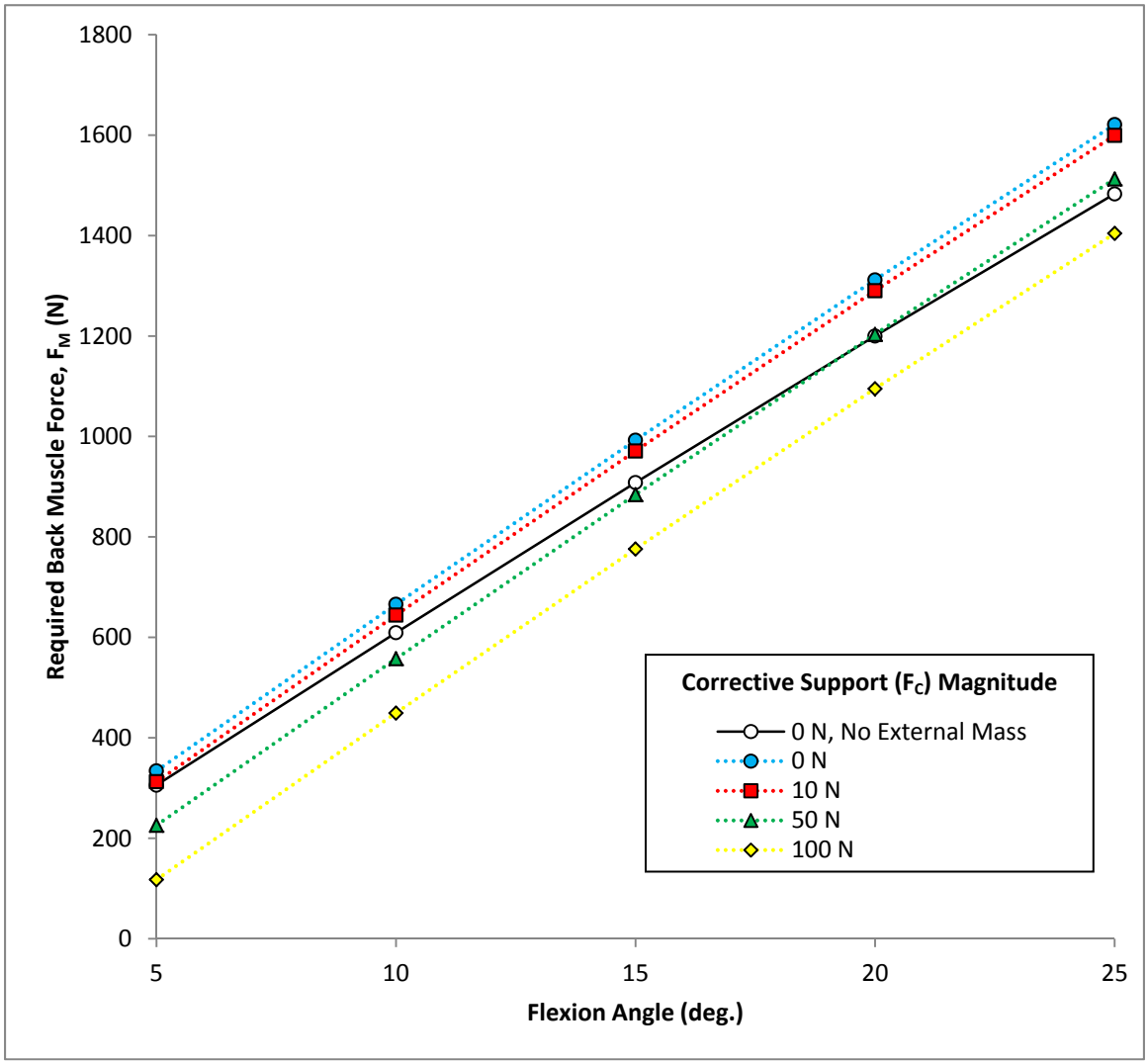

Chapter 2

Effect of Lead Use on Back and Shoulder Postural Muscle Activity in Healthy Young Adults

2.1 INTRODUCTION

Back pain, a common occupational injury in the United States, leads to lost productivity and a significant expenditure of medical resources annually (Katz, 2006; Martin et al., 2008; Murphy & Volinn, 1999). Back pain is often associated with occupations requiring frequent bending and lifting maneuvers, which can impose considerable loads on the spine (Bonato et al., 2003; Pope, Goh, & Magnusson, 2002; Sullivan, 1989). While large loads increase the risk for injury, sustained static flexion of the spine can also lead to back pain as the extensor muscles of the lower back become fatigued (Shin, D'Souza, & Liu, 2009). Similarly, prolonged awkward postures of the head and neck can produce discomfort (Aarås, 1994; Aarås & Ro, 1997).

The performance of physicians in the operating room can be adversely affected by postural fatigue and discomfort, which are aggravated by the static postures frequently required during procedures. General surgeons, for example, spend 65% of their operating time in static postures of the head and neck, with 14% of those in a flexed (forward bent) position (Kant, de Jong, van Rijssen-Moll, & Borm, 1992). The same study concluded this group of physicians to be at a "higher risk for back and neck/shoulder disorders". Physicians who perform minimally-invasive (laparoscopic, endoscopic) surgical procedures also experience long periods of static postures (Berguer, Rab, Abu-Ghaida, Alarcon, & Chung, 1997; Supe, Kulkami, & Supe, 2010). The term "Surgical Fatigue Syndrome" has even been created to describe what these physicians can experience during minimally-invasive procedures (Cuschieri, 1995).

One subgroup of operating physicians that is believed to experience a higher-than-average incidence of back pain is interventionalists. These include the neurosurgeons, radiologists and cardiologists, for example, who operate using real-time radiography. The radiation levels in the operating room require the use of shielding garments (called "leads") for the full duration of procedures. It has been suggested anecdotally that the added weight

of these garments on the trunk increases the risk for neck, shoulder, and/or back pain (Pelz, 2000), but an initial quantitative study failed to establish an association (Moore & Novelline, 1992). In a later study, Ross, Segal, Borenstein, Jenkins, and Cho (1997) were able to show that physicians who used leads regularly (in this case, cardiologists who wore leads up to 8.5 hours per day) had the highest incidence of missed work days due to neck/back pain (21.3%) and required more treatment than other, non-lead-using physicians. The same study also showed a higher incidence of multiple-disc herniations of the cervical and lumbar spine among interventionalists, a condition that has been termed "Interventionalist's Disc Disease".

While the work of Ross et al. suggests an association between lead use and neck/back pain, there is a lack of studies of how much back muscle activity is required to equilibrate the gravitational effect of wearing the lead vest in various torso postures. One study by Cholewicki, Panjabi, and Khachatryan (1997) does show that trunk extensor muscle activity increases more rapidly with flexion when an external mass is applied to the trunk, but the singular mass used in those experiments (32 kg) was nearly an order of magnitude larger than that of a typical lead vest. Understanding any such changes in muscle activity is relevant because the activity of the lower back muscles is known to directly correlate with lumbar intervertebral disc pressure (Örtengren, Andersson, & Nachemson, 1981), and prolonged exposure to high intervertebral pressures can lead to discomfort, as well as permanent structural damage of the intervertebral discs (Adams, McMillan, Green, & Dolan, 1996).

Thus, the purpose of this study was to test the primary hypothesis that wearing a lead vest does significantly affect lower-back and/or trapezius muscle activity, and the secondary hypotheses that neither gender nor a forward-flexed trunk posture affect these muscle activities in the presence or absence of the lead. If any of these three factors (or a combination) was found to increase back muscle activity, the results may inform future interventions aimed at reducing this potential source of musculoskeletal stress in interventionalists.

2.2 METHODS

2.2.1 Study Design

The primary outcome was the recorded muscle activity of three muscle groups. For each muscle group, a two-group (by gender), repeated-measures study with two within-subject factors (erect or forward-flexed posture, presence or absence of the vest) was performed.

2.2.2 Subjects

Nineteen healthy young adults were recruited (ten males, nine females), between 21 and 30 years of age, and between 1.65 m and 1.83 m tall. The inclusion criteria also required no history of medical treatment for: vertebral fractures, spondylolysis, spondylolithesis, congenital abnormalities of the spine, scoliosis, kyphosis, osteoporosis, recurrent back pain, or disc herniation. Women also had to be non-pregnant.

All subjects gave written, informed consent and all procedures were approved by an institutional review board (IRB).

2.2.3 Data Acquisition

Setup. Each subject was fitted with 6 pairs of bipolar (2 cm spacing) surface electromyography (SEMG) electrodes (N00-S-25, Ambu®, Ballerup, DNK) over the muscles of the shoulders, lower back, and hips (Figure 2.1). A single electrode placed on an iliac crest served as a reference/ground for the system. Four pairs of electrodes were attached bilaterally *ad modum* De Nooij, Kallenburg, and Hermens (2009) at the L3 level, approximately 3 cm (the "back - medial" group) and 6 cm (the "back - lateral" group) from the midline. The remaining two pairs of electrodes were attached bilaterally over the midpoint of each trapezius (the "trapezius" group). Each electrode pair was then connected to one of six differential-input amplifiers (MyoSystem 2000, Noraxon, Inc., Scottsdale, AZ, USA) and then sampled at 2 kHz via a 16-bit DAQCard-6024E (National Instruments, Inc., Austin, TX, USA) analog-to-digital converter board and notebook PC running LabVIEW™ (version 8.20, National Instruments, Inc., Austin, TX, USA). Subjects then performed a standardized series of test procedures:

Calibration 1 – lateral and medial back groups, isometric maximum voluntary contraction (MVC). To measure this, subjects were asked to stand erect in front of a wall-mounted padded stand against which they placed their anterior iliac spines. A lightly padded seatbelt strap was then passed around the subject just under the armpits. Subjects were then instructed to extend their backs against the strap building to a maximum effort over 3 seconds and holding it for no more than 2 seconds while the SEMG data were recorded. The strap and padded stand constrained the thorax and pelvis (respectively) of the subjects, thus forcing them to maintain a nearly erect posture during the test.

Calibration 2 - trapezius group, isometric MVC. This was measured by having the subjects sit erect in a chair and grab the bottom edge of their seat while keeping their arms as

straight as possible. Subjects were instructed to pull straight up with both arms with maximum effort while data was recorded, again for 5 seconds.

Baseline muscle resting activity 1. This was an initial measurement of baseline muscle activity with subjects having relaxed all the muscle groups as much as possible while they lay in a supine posture on a mattress for approximately 3 minutes taking slow, deep breaths. EMG data were recorded at the end of this period for 10 seconds.

Test 1 - erect posture, no lead vest. Subjects were instructed to assume and maintain a normal, erect posture, with the arms held loosely at the sides. Data were recorded for 10 seconds once subjects were erect and stationary.

Test 2 - forward flexed posture, no lead vest. Subjects were fitted laterally with two optoelectronic markers mounted to Velcro™ straps at approximately the levels of T12 and L5/S1 (Figure 2.2). Two more markers were affixed to a vertical reference structure behind the test subjects. The markers were tracked at 100 Hz using a three-camera, optical-measurement system (Optotrak® 3020, Northern Digital Inc., Waterloo, ONT, CAN). Both the markers and camera unit were controlled by a desktop PC running NDI ToolBench™ (version 3.00.39, Northern Digital Inc., Waterloo, ONT, Canada). A real-time numerical readout from the software reported the absolute angle between the lines connecting the fixed and torso pairs of markers on a computer monitor fixed approximately 1.1 m off of the floor in front of the subject (with the viewing angle adjusted for each subject). These angle measurements were not recorded but only used as a visual aid for assisting test subjects in reaching and maintaining the proper torso flexion angle for the test duration. Subjects were asked to maintain a posture of 25° of forward flexion of the trunk, with the arms relaxed and hanging vertically. Once the subjects reached and held the correct posture, data were recorded for 10 seconds.

Test 3 – erect posture, wearing lead vest. The optical markers of Test 2 were removed from the test subjects, and they were then assisted in donning the vest portion of a typical lead (mass: 3.70 +/- 0.05 kg; LB 16 Rev. D, BMS, Newport News, VA, USA). After the lead's torso straps were comfortably tightened subjects were asked to assume a normal, erect posture with arms held loosely at the sides. Data were recorded for 10 seconds.

Test 4 – forward flexed posture, wearing lead vest. While still wearing the lead vest, the optical markers from Test 2 were again placed on the subject, this time over the vest. As in Test 2, subjects were asked to assume a posture of 25° of flexion of the trunk, with the arms relaxed

and hanging vertically. Once subjects were stationary and in the correct posture, data were recorded for 10 seconds.

Test 5 – forward flexed posture, wearing lead vest, long duration. Subjects were asked to maintain 25° of trunk flexion while wearing the vest for a period of up to 30 minutes. During this time they were allowed to use a computer, which also monitored their posture, for normal activities such internet browsing and email. The keyboard and mouse of the computer were placed at approximately hip-level on an adjustable pedestal, directly in front of the monitor. Subjects were instructed not to place any weight on the keyboard pedestal and to keep their posture within +/- 2° of the target 25° of flexion. At the conclusion of the 30-minute period (or if the subject experienced pain/fatigue and wished to stop at any point), data were recorded for 10 seconds. During the data recording interval, the subjects were instructed maintain their posture and to let their arms hang relaxed and vertical, as in previous flexion tests.

Baseline resting muscle activity 2. Test 3 procedures were repeated with the subjects lying supine on the mattress for approximately 3 minutes. Data were once again recorded for 10 seconds at the conclusion of that period.

Questionnaires. After concluding Tests 3-5 subjects were asked to fill out a brief questionnaire on which they described their perceived level of effort and discomfort in postures with and without the lead using graphic rating scales (GRSs) (Mannion, Balagué, Pellisé, & Cedraschi, 2007): Subjects were asked to compare Tests 3 and 4 with Tests 1 and 2, respectively. For Test 4, subjects were also asked to describe the effort and discomfort experienced in attaining the test posture. Both effort and discomfort levels were rated on a GRS from -2 (*much less*) to 2 (*much more*), with 0 indicating no noticeable change. After Test 5, subjects were asked to quantify the maximum level of discomfort they experienced during the test, on a GRS from 0 (*none*) to 4 (*severe*). Finally, subjects were asked how any discomfort they experienced during Test 5 changed with time, as indicated on a GRS from -2 (*decreased*) to 2 (*increased*), with 0 indicating that the level of discomfort remained constant over the duration of the test.

2.2.4 Data Analysis

All data files were post-processed by subject using MATLAB® (version 7.0.0.19920 with Signal Processing Toolbox installed, The Mathworks, Inc., Natick, MA, USA). The recorded signals were assumed to be stationary over the duration they were recorded. All SEMG data had the initial 0.25 seconds removed in order to eliminate any startup transients, as well as any constant

offset voltage. The data were then filtered through a bandpass third-order Butterworth filter with break points at 30 and 1000 Hz, and a similar bandstop filter centred at 60 Hz. The filtered data on each channel were then analyzed via a moving root-mean-square (RMS) window *ad modum* Burden and Bartlett (1999), with the RMS value found for every 100 points of data (approximately 50 ms). The minimum RMS value was chosen for the two Baseline tests, the maximum RMS value was chosen for the two MVC tests, and the mean RMS values were used for Tests 1-5. The data for Tests 1-5 were then normalized to values from 0 - 100% of MVC (%MVC) using a method similar to the second of two described by Mirka (1991), shown as Equation (1) below:

$$\%MVC = \frac{(Test\ RMS\ Value - Baseline\ RMS\ Value)}{(MVC\ RMS\ Value - Baseline\ RMS\ Value)} \times 100 \qquad (1)$$

Finally, corresponding left and right muscle data (tests 1 and 4, 2 and 3, 5 and 6, respectively) were averaged to remove any left/right bias. The entire MATLAB script written for the post-processing described above is included in Appendix A.

The hypotheses were tested by subjecting the post-processed data to statistical analysis using PASW Statistics (version 18.0.3, SPSS Inc., Chicago, IL, USA). Each muscle group was analyzed individually using a general linear model (for repeated measures) with the normalized SEMG value chosen as the single dependent variable. Each model used subject gender as the single, two-level, between-subject independent variable. Subject posture (erect/flexed) and use of the lead vest (with/without) were specified as the two, two-level, within-subject independent variables. ANOVA, using a 95% confidence interval and linear contrast tests, was conducted to determine the significance of each factor in the models. A p value less than 0.05 was considered significant in testing the primary hypothesis (effect of lead vest). A Bonferroni-adjusted p value of p less than 0.008 was used when testing the secondary hypotheses relating to posture and gender. Each single factor found to be significant had the magnitude and direction of its effect on the dependent variable quantified via pairwise comparisons of the difference in marginal means.

Test questionnaires were collected and the frequency of each response and question were tabulated. For the questions concerning Tests 3 and 4, a Wilcoxon matched pairs signed rank test (two-tailed) was performed on each set of responses to test for the significance (α = 0.05) of any differences from Tests 1 and 2, respectively.

2.3 RESULTS

2.3.1 Mean RMS SEMG Amplitude and ANOVA, Tests 1 through 4

The mean RMS SEMG amplitude data are shown for each muscle group and posture across all subjects in (Figure 2.3), and the results of the ANOVA of Tests 1-4 are shown in (Table 2.1). Of the tests on 19 subjects, 18 resulted in useful data for the medial back muscle group and 17 resulted in useful data for the trapezius group due to technical problems. If one SEMG channel was deemed faulty, data from both sides were dropped from the analysis since the effects of any left/right bias could not be mitigated by averaging.

Based on the ANOVA results (the mean RMS SEMG amplitude data alone is inconclusive), the primary hypothesis (use of the lead vest significantly increases back and shoulder muscle activity) was rejected for all muscle groups. The mean RMS SEMG data show that, for each posture, use of the lead decreases the activity of the medial back muscle group with a 2.3 %MVC decrease between Tests 1 and 3, and a 1.2 %MVC decrease between Tests 2 and 4. The mean RMS SEMG data also show the trapezius group had the lowest %MVC values (3.7 - 5.0 %MVC) as well as the smallest range (1.3 %MVC, which occurred between Tests 1 and 4). The ANOVA results show that use of the lead vest was a significant factor affecting the activity of the medial back and trapezius muscles. However, the pairwise comparison of the marginal means show that use of the lead vest resulted in slight decreases in muscle activity (-1.738 %MVC and -0.611 %MVC, respectively). In the lateral back muscle group, no trends were associated with lead use.

As strongly suggested by the mean RMS SEMG amplitude data and shown in the ANOVA results, posture was a significant factor affecting muscle activity in all three muscle groups. The largest variation in mean RMS SEMG amplitude was observed in the medial back muscle group between the erect and flexed posture tests, both with and without the lead vest: a 10.3 %MVC increase from Test 1 to Test 2, and an 11.4 %MVC increase from Test 3 to Test 4. The separation between these values is such that, in both instances, the data lie outside the bounds of standard error of each other. The ANOVA results also show that posture was the most significant factor for the lateral and medial back muscle groups. Pairwise marginal means comparison shows that the lateral and medial back muscle groups increased their activity levels in the flexed posture (+4.374 %MVC and +10.858 %MVC, respectively). In the trapezius muscle group, there was a trend for posture to be a significant factor. Pairwise marginal means comparison shows that the trapezius group experienced slightly decreased activity in the flexed posture (-0.668 %MVC).

Finally, the ANOVA results show that the effect of gender did not prove to be significant for any of the muscle groups, but a trend was observed in the lateral back muscle group. It should be noted that the statistical power for this last analysis was reduced by the nearly-even split of males and females in the subject pool.

Apart from considering the effects of lead use, posture and gender, we also examined the possibility of interaction effects in the general linear models for each muscle group. The ANOVA results show that the only significant interaction effect occurred between gender and lead use in the lateral back muscle group.

2.3.2 Mean RMS SEMG Amplitude, Test 5

The results from the exploratory Test 5 (shown in Figure 2.4) could not be analyzed in the same detail as Tests 1-4 because eight of the test subjects had to terminate the test early due to discomfort, resulting in a wide range of times (approximately 8 to 17 minutes) of sustained flexion for those who stopped the test early. Also, having only one test with a significant time element (and only 11 subjects lasting for the full duration) would not provide a useful point of comparison for the full ANOVA performed on the other (acute loading) test conditions. As shown in Figure2. 4, however, some conclusions can be drawn just from the %MVC results of each subgroup. Those subjects who completed Test 5 showed the highest %MVC readings recorded for both the lateral and medial back groups (29.4 %MVC and 23.6 %MVC, respectively). Those same subjects, however, showed the lowest recorded value (2.9 %MVC) for the trapezius group. The subjects who terminated Test 5 exhibited average values below the maximum values recorded in Tests 1-4 for all three muscle groups.

2.3.3 Questionnaire Results

The frequency of each response to the questions asked after Tests 3-5 are shown in Table 2.2, with the highest frequency responses to each question in bold. The Wilcoxon matched pairs signed rank tests performed on the questions concerning Tests 3 and 4 show significant changes in each category except for the effort to maintain the (erect) posture of Test 3 (z = -1.461). The test for the change in discomfort while maintaining the Test 3 posture was only slightly beyond the threshold for significance (z = -1.992). The remaining tests were well beyond the threshold value (with z values between -2.197 and -3.110). Thus, in the erect posture, the

subjects likely perceived an increase in discomfort wearing the lead vest. In the flexed posture, subjects perceived increases in effort and discomfort to achieve and maintain the posture.

2.4 DISCUSSION

This study shows that acute use of a lead vest does not appear to significantly increase the muscle activity of the lower back and shoulders. Rather, use of the lead vest was shown to produce statistically significant, but likely clinically insignificant, reductions in the activity of these muscle groups.

Cholewicki *et al.* (*op cit.*) showed that, in order to maintain spinal stability, the flexor-extensor muscles of the trunk demonstrate increased activity when an external mass is placed on the trunk, an effect which is amplified as the trunk tilts further from a neutral posture. In this study, the imposition of the lead resulted in a slight reduction (< 2% MVC) in observed muscle activity of the medial back muscle. For the lateral back muscle group, it was expected that any differences in muscle activity due to the lead would be smaller than those observed in the medial group (due to the latter encompassing more of the trunk extensor muscles), and the signal-to-noise level seemed to be sufficiently low that we were not able to observe differences in recorded values.

While the lead vest did not significantly increase the activity of any muscle group in the short-term, it is possible that significant differences would be observed with more chronic loading. Loading of the trapezius (especially over prolonged periods) has been shown to produce fatigue and pain in the neck and shoulder region (Aarås, 1994), so further study involving prolonged use of the lead vest could still be relevant to interventionalists. It was thus disappointing not to obtain a complete set of results for the Test 5 experiment in this study.

The fact that a flexed posture significantly increased the muscle activity at both lower back measurement sites corroborates earlier studies showing a forward flexed posture is a potent stimulus to increasing back and shoulder muscle activity (Andersson, Örtengren, & Herberts, 1977; Schultz, Haderspeck-Grib, Sinkora, & Warwick, 1985; Andersson, Oddsson, Grundström, Nilsson, & Thorstensson, 1996).

While both back muscle groups show a large increase in activity in the flexed posture, the trapezius group showed a slight reduction. While Figure 2.3 suggests that this reduction is within the bounds of the standard error, the statistical analysis shows that the flexion did significantly affect trapezius activity (albeit with a < 1 %MVC change). The trapezius is the

primary soft tissue structure loaded by the weight of the lead in the erect posture, primarily by its action of depressing the shoulders. In a flexed posture, the gravitational loading applied by the vest shifts posteriorly to load portions of the middle and lower back, which could explain why this muscle group showed a reduction in activity in that posture.

The medial back electrodes recorded activity primarily from the erector spinae (sacrospinalis, spinalis dorsi, longissimus dorsi) and multifidi. The lateral electrodes recorded parts of the erector spinae and quadratus lumborum, but were probably positioned too far laterally to capture multifidus activity. The anatomical differences in the muscle groups recorded by the lateral and medial electrodes may underlie the differing results. Biomechanically, the multifidi are believed to work in concert with the erector spinae to prevent excess rotation of the lumbar spine during flexion; without their stabilizing effect, the lumbar spine would experience excessive lordosis (Hansen et al., 2006). Thus, the greater sensitivity of the medial electrode group to postural changes could reflect increased multifidus and longissimus activity during flexion.

The results of Test 5, while incomplete, suggest at least one outcome that is expected based on previous work. It has been shown that in sustained flexion, the amplitude of the EMG output of the extensor muscles (erector spinae and multifidi) of the lower back increases with time, a response which has been attributed to the shifting of restoring moment generation from passive tissues to the muscles (Shin & Mirka, 2007). The increase in recorded %MVC values from Test 4 (the acute loading condition) to Test 5 in the lateral and medial electrode groups of those subjects who completed Test 5 could be a result of this restoring moment transfer, but the error associated with the %MVC values makes the magnitude of any differences between Tests 4 and 5 uncertain.

There are several limitations to this study. First, the primary measurements were only made over the short term; measurements of myoelectric activity are needed over an eight-hour work day to study the effects of time on the muscle groups. Second, the measurements were made in healthy young subjects, not interventionalists who are used to wearing the vests; postural adaptations may occur with practice. Third, the use of surface electrodes, while practical, does not allow individual muscle contributions to be parsed from the averaged activity recorded from the measurement volume. Fourth, while orienting surface electrodes parallel to the muscle fibers under study is desired, the muscles under study here make such an arrangement impractical. The most superficial layer of the erector spinae is inclined

approximately 10° from the vertical (the sagittal plane), the next deepest layer is inclined approximately 20°, and the multifidi have the opposite inclination (Sobotta, 1974). Fifth, this study did not include any of the abdominal muscles, some of which are active spinal stabilizers (see Cholewicki et al.). Sixth, moderate group sizes meant limited statistical power; a post-hoc analysis of the observed power for the lead use factor reported values between 0.215 (lateral back) and 0.610 (trapezius). Thus, it is possible that some/all of the gender and interaction effects would indeed become significant with larger group sizes. The gender effect, especially, seems reasonable given that men and women used the same lead size and weight in this study. Had the weight of the lead been scaled to body weight, for example, then gender probably would play less of a role. Thus, more definitive conclusions about the effects of acute use of the lead vest could be drawn with greater statistical power; for example, to achieve a power of 0.90 for all three muscle groups, an approximate *a priori* power analysis (using size effects observed in this study) suggested at least 22 subjects would be needed. Seventh, some psychological effect may have influenced the results of Test 5. A majority of the participants who completed Test 5 were female (7 of 11), a result which may have been in part due to a desire to please the male principal investigator. Had the principal investigator been female, the gender balance of those who completed Test 5 may have been reversed. Eighth, the lead vest used in this study is likely to be less massive than older models, which also were not secured tightly around the trunk (thus exerting a greater flexion moment on the trunk). Had an older model of lead vest been used in this study, it may have produced a significant increase in the activity of the muscles studied here, since those designs were anecdotally associated with higher incidence of back fatigue. Lastly, the test-retest reliability of our SEMG measurements is not presently known and could be influenced by several common factors, including unfiltered ambient electrical signals, cross-talk, and variation in the stability and quality of the electrode-skin contact sites (Tassinary & Cacioppo, 2000).

2.4.1 Conclusions

Despite producing perceived increases in effort and discomfort levels (as reported in the questionnaires), use of the lead vest did not result in a significant increase in muscle activity in any of the three muscle groups studied; in fact, it led to slight decreases in the medial back and trapezius groups, perhaps due to an increase in lumbar lordosis. Posture had, by far, the greatest effect on muscle activity, particularly in the medial back group (which encompassed the

erector spinae/quadratus lumborum). Subject gender did not significantly affect muscle activity. The only significant interaction effect from combining lead use with one or both of the other two factors occurred in the lateral back muscle group with lead use and gender. Thus, while the use of a lead does not necessarily contribute to increased loading of the neck and back muscles, avoiding sustained flexed postures would be a way for interventionalists to significantly reduce muscle activity in the back. This could result in corresponding declines in fatigue and pain/injury in the back.

2.5 REFERENCES

Aarås, A. (1994). Relationship between trapezius load and the incidence of musculoskeletal illness in the neck and shoulder. *The International Journal of Industrial Ergonomics*, 14 (4), 341-348.

Aarås, A. & Ro, O. (1997). Electromyography (EMG) - methodology and application in occupational health. *The International Journal of Industrial Ergonomics*, 20 (3), 207-214.

Adams, M., McMillan, D., Green, T. & Dolan, P. (1996). Sustained loading generates stress concentrations in lumbar intervertebral discs. *Spine*, 21(4), 434-438.

Andersson, E. A., Oddsson, L. I. E., Grundström, H., Nilsson, J. & Thorstensson, A. (1996). EMG activities of the quadratus lumborum and erector spinae muscles during flexion-relaxation and other motor tasks. *Clinical Biomechanics*, 11(7), 392-400.

Andersson, G.B., Örtengren, R. & Herberts, P. (1977). Quantitative electromyographic studies of back muscle activity related to posture and loading. *Orthopedic Clinics of North America*, 8(1), 85-96.

Berguer, R., Rab, G. T., Abu-Ghaida, H., Alarcon, A. & Chung, J. (1997). A comparison of surgeons' posture during laparoscopic and open surgical procedures. *Surgical Endoscopy*, 11, 139-142.

Bonato, P., Ebenbichler, G.R., Roy, S.H., Lehr, S., Posch, M., Kollmitzer, J. & Croce, U.D. (2003). Muscle fatigue and fatigue-related biomechanical changes during a cyclic lifting task. *Spine,* 28 (16), 1810-1820.

Burden, A. & Bartlett, R. (1999). Normalisation of EMG amplitude: an evaluation and comparison of old and new methods. *Medical Engineering & Physics*, 21, 247-257.

Cholewicki, J., Panjabi, M., & Khachatryan, A. (1997). Stabilization Function of Trunk Flexor-Extensor Muscles Around a Neutral Spine Posture. *Spine*. 22(19), 2207-2212.

Cuschieri, A. (1995). Whither minimal access surgery: tribulations and expectations. *The American Journal of Surgery*, 169, 9-19.

De Nooij, R., Kallenberg, L. A. C., & Hermens, H.J. (2009). Evaluating the effect of electrode location on surface EMG amplitude of the m. erector spinae p. longissimus dorsi. *Journal of Electromyography and Kinesiology.* 19, 257-266.

Hansen, L., de Zee, M., Rasmussen, J., Anderson, T., Wong, C. & Simonsen, E. (2006). Anatomy and biomechanics of the back muscles in the lumbar spine with reference to biomechanical modeling. *Spine*, 31(17), 1888-1899.

Kant, I. J., de Jong, L. C. G. M., van Rijssen-Moll, M. & Borm, P. J. A. (1992). A survey of static and dynamic work postures of operating room staff. *International Archives of Occupational and Environmental Health*, 63, 423-428.

Katz, J. N. (2006). Lumbar Disc Disorders and Low-Back Pain: Socioeconomic Factors and Consequences. *The Journal of Bone & Joint Surgery.* 88, 21-24.

Mannion, A. F., Balagué, F., Pellisé, F., & Cedraschi, C. (2007). Pain measurement in patients with low back pain. *Nature Clinical Practice Rheumatology.* 3(11), 610-618.

Martin, B. I., Deyo, R. A., Mirza, S. K., Turner, J. A., Comstock, B. A., Hollingworth, W., & Sullivan, S. D. (2008). Expenditures and Health Status Among Adults With Back and Neck Problems. *The Journal of the American Medical Association.* 299(6), 656-664.

Mirka, G. A. (1991). The quantification of EMG normalization error. *Ergonomics.* 34(3), 343-352.

Moore, B. & Novelline, R. A. (1992). The relationship between back pain and lead use in radiologists. *American Journal of Roentgenology*, 158(1), 191-193.

Murphy, P.L. & Volinn, E. (1999). Is occupational low back pain on the rise? *Spine*, 24(7), 691-697.

Örtengren, R., Andersson, G. & Nachemson, A. (1981). Studies of relationships between lumbar disc pressure, myoelectric back muscle activity, and intra-abdominal (intragastric) pressure. *Spine*, 6(1), 98-103.

Pelz, D. M. (2000). Low back pain, lead aprons, and the angiographer [letter]. *American Journal of Neuroradiology*, 21(7), 1364.

Pope, M.H., Goh, K.L. & Magnusson, M.L. (2002). Spine ergonomics. *Annual Review of Biomedical Engineering*, 4, 49-68.

Ross, A. M., Segal, J., Borenstein, D., Jenkins, E. & Cho, S. (1997). Prevalence of spinal disc disease among interventional cardiologists. *American Journal of Cardiology*, 79(1), 68-70.

Schultz, A. B., Haderspeck-Grib, K., Sinkora, G. & Warwick, D. N. (1985). Quantitative studies of the flexion-relaxation phenomenon in the back muscles. *Journal of Orthopaedic Research*, 3, 189-197.

Shin, G. & Mirka, G. (2007). An in vivo assessment of the low back response to prolonged flexion: Interplay between active and passive tissues. *Clinical Biomechanics*, 22(9), 965-971.

Shin, G., D'Souza, C. & Liu, Y. H. (2009). Creep and fatigue development in the low back in static flexion. *Spine*, 34(17), 1873-1878.

Sobotta, J. (1974). *Atlas of Human Anatomy* (Vol. 1). F. H. J. Figge, (Ed.). New York, NY: Hafner Press.

Sullivan, M.S. (1989). Back support mechanisms during manual lifting. *Physical Therapy*, 69 (1), 38-46.

Supe, A., Kulkami, G. & Supe, P. (2010). Ergonomics in laparoscopic surgery. *Journal of Minimal Access Surgery*, 6(2), 31-36.

Tassinary, L. G. & Cacioppo, J. T. (2000). The skeletomuscular system: surface electromyography. In J. T. Cacioppo, L. G. Tassinary and G. G. Berntson (Eds.), *Handbook of psychophysiology* (2nd ed.) (pp. 163-199). New York: Cambridge University Press.

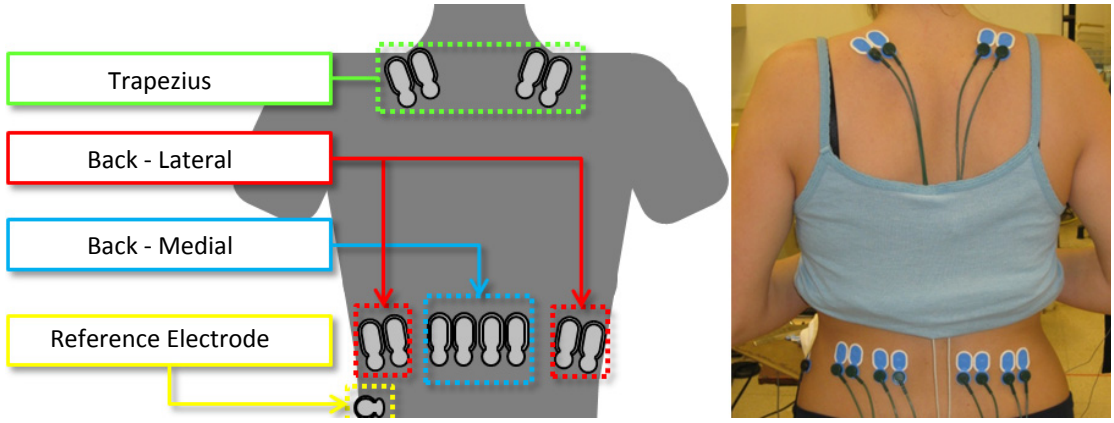

Figure 2.1: SEMG electrode groups and placement.

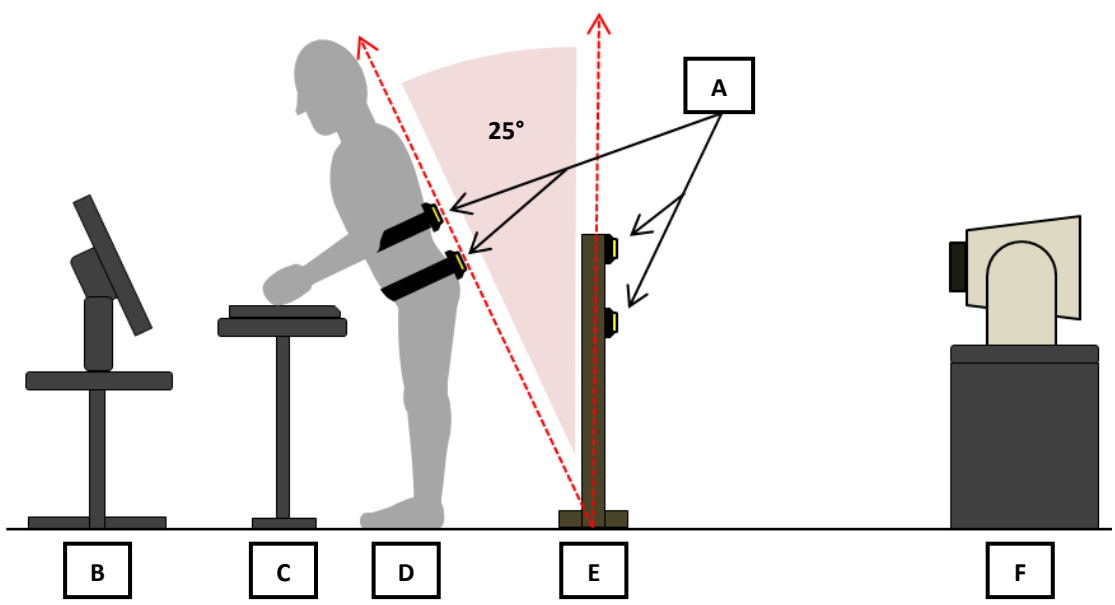

Figure 2.2: Optical posture measurement system setup for Tests 3 and 5.
A - optoelectronic markers, B - computer monitor stand, C - keyboard/mouse pedestal, D - test subject, E - vertical reference, F - optical measurement system camera unit.

Figure 2.3: Mean (bars denote S.E.) normalized muscle activity by test and muscle group (both genders).

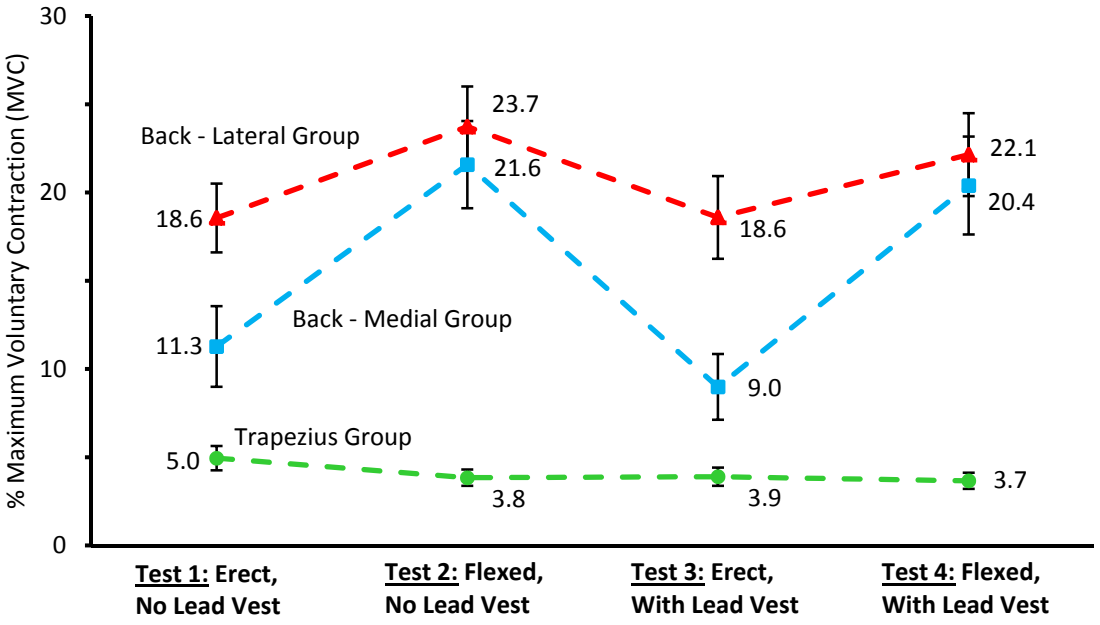

Figure 2.4: Mean (bars denote S.E.) normalized muscle activity in Test 5, by sub-group and muscle group.

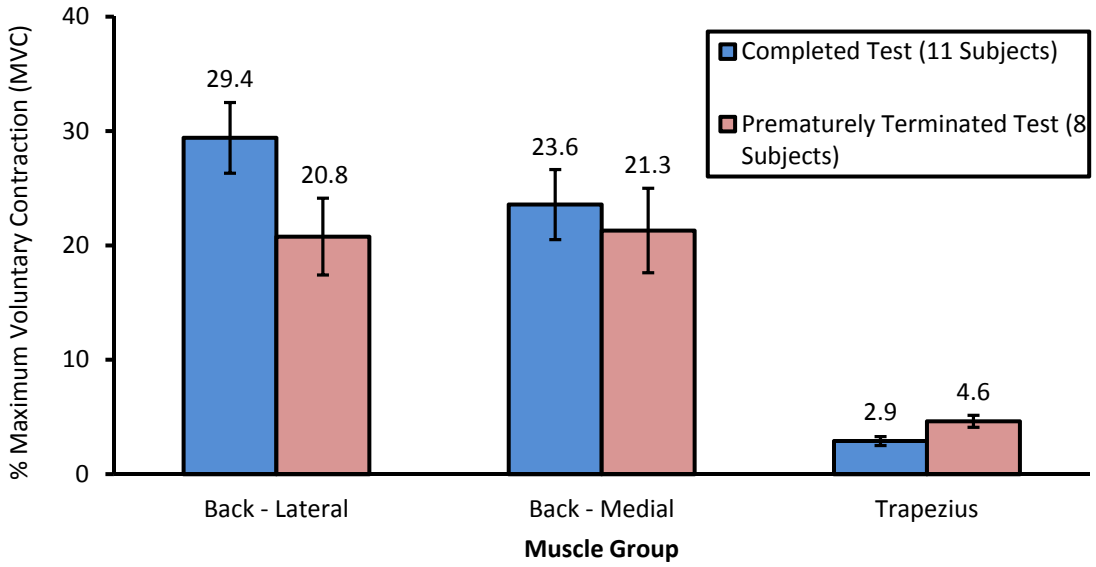

Table 2.1: ANOVA of repeated-measures GLM, Tests 1-4 by muscle group.

Back - Lateral (Hypothesis *df* = 1, Error *df* = 17)		
Factor	***F***	***p***
Lead Use	1.534	0.232
Posture	14.271	0.000*
Gender	4.152	0.010
Lead Use & Gender	5.335	0.006
Posture & Gender	0.027	0.145
Lead Use & Posture	1.760	0.034
Lead Use & Posture & Gender	0.004	0.158
Back - Medial (Hypothesis *df* = 1, Error *df* = 16)		
Factor	***F***	***p***
Lead Use	5.441	0.033
Posture	2121.965	0.000*
Gender	0.648	0.072
Lead Use & Gender	1.000	0.055
Posture & Gender	2.992	0.017
Lead Use & Posture	0.274	0.101
Lead Use & Posture & Gender	0.178	0.113
Trapezius (Hypothesis *df* = 1, Error *df* = 15)		
Factor	***F***	***p***
Lead Use	5.729	0.030
Posture	4.744	0.008
Gender	1.592	0.038
Lead Use & Gender	0.002	0.162
Posture & Gender	0.000	0.165
Lead Use & Posture	3.994	0.011
Lead Use & Posture & Gender	0.004	0.158
Notes:		
*rounded non-zero value.		
Significant at the p < 0.050 level.		
Significant at the p < 0.008 level (Bonferroni correction).		

Table 2.2: Questionnaire response tally.

Test and Question	Graphic Rating Scale				
	Much Less		*No Change*		*Much More*
	-2	*-1*	*0*	*1*	*2*
Test 3: Effort to Maintain	0	1	**15**	3	0
Test 3: Discomfort to Maintain	0	1	**13**	5	0
Test 4: Effort to Achieve	0	1	**9**	8	1
Test 4: Discomfort to Achieve	0	1	**12**	6	0
Test 4: Effort to Maintain	0	1	6	**10**	2
Test 4: Discomfort to Maintain	0	1	**9**	8	1
	None		*Moderate*		*Severe*
	0	*1*	*2*	*3*	*4*
Test 5: Max Level of Discomfort	0	1	4	**12**	2
	Decreased		*Constant*		*Increased*
	-2	*-1*	*0*	*1*	*2*
Test 5: Discomfort Change with Time	0	0	0	5	**14**

Note: Most frequent responses are in bold. (N = 19)

Chapter 3

Contact Stress Distribution under a Lower Thorax Partial Orthosis Worn by Healthy Young Men: Effects of Distraction Force, Sagittal Plane Moment, Respiration Phase, and Thoracic Cross-sectional Shape

3.1 INTRODUCTION

Patients with stable spinal fractures or deformities such as idiopathic scoliosis often have to wear orthoses as part of their treatment. Such orthoses typically apply sustained forces to the trunk and pelvis in order to immobilize one or more motion segments of the spine (Flanagan, Gavin, Gavin, & Patwardhan, 2000) or apply corrective bending and/or torsional moments (Chase, Bader, & Houghton, 1989). In the field of orthotics, braces exert their corrective actions by applying what is termed "pressure" to the skin over bony landmarks or regions. But in terms of tissue mechanics that interface pressure may be decomposed into a contact stress oriented normal to the skin surface (henceforth termed 'contact stress'), and two orthogonal interface shear contact stresses in the plane of the skin. When orthoses are custom-made for each patient (Bernardoni & Gavin, 2006), orthotists generally seek to reduce the normal and shear contact stresses over pressure points by redistributing the stress over a larger area, and/or using univalve (for plaster) or bivalve (for fiberglass) designs (Remaley & Jaeblon, 2010). Sustained or abnormally large contact stress is one of many factors in the etiology of skin abrasion, blisters, and pressure ulcers (Sanders, Goldstein, & Leotta, 1995), a serious injury entailing the breakdown of the skin and underlying tissues (Leigh & Bennett, 1994). Even though it is not the sole predictor of the risk of pressure ulcers (Reenalda, Jannink, Nederhand, & IJzerman, 2009) a better understanding the magnitude of the mechanical load, whether in the form of a normal or a shear stress, or both, that is applied to a unit area of skin by such an orthosis can still be useful in trying to predict and prevent skin complications in current and future orthosis designs.

The contact stress distribution under a thoracolumbosacral orthosis (TLSO) has been measured in patients being treated for idiopathic scoliosis in several studies using a variety of

sensor technologies (Chase, Bader, & Houghton, 1989; van den Hout, van Rhijn, van den Munckhof, & van Ooy, 2002; Périé, Aubin, Lacroix, Lafon, & Labelle, 2004; Pham *et al.*, 2008; Lou, Hill, & Raso, 2010). The recorded stress values showed a wide variation between each study. For example, van den Hout *et al.* (2002) observed mean magnitudes varying between 12 and 55 kPa depending on the posture of the patient (supine, prone, sitting, standing, etc.) and location (lumbar padding produced the highest, thoracic the least), while Pham *et al.* (2008) observed mean stress magnitudes of 7 - 10 kPa under similar testing conditions. Whether this variation is due to the technology used to make the measurement, the implementation of the orthosis, or subject selection is not known.

Breakdown of the skin and even subcutaneous tissues under an orthosis is a continual source of concern for the patient and clinician. One mechanism under mechanical stress is ischemia or restriction of the blood supply at the site of loading. This can particularly occur over boney prominences (Black *et al.*, 2007), which include the iliac crests, spinous processes, and the ribs. Ischemia is thought to be due to inadequate perfusion of nutrients and removal of waste products. This is a process that is regulated through a complex series of electrochemical channels which control the relative dilation and thus flow rate of capillaries and other adjacent vessels (Wywialowski, 1999). The capillaries near the skin surface in most healthy persons have an average internal pressure of approximately 25-32 mmHg (3.33-4.27 kPa), and any applied contact stress exceeding this may eventually occlude these vessels (Remaley & Jaeblon, 2010; Leigh & Bennett, 1994), creating localized ischemia. The skin is able to tolerate higher contact stresses for brief periods of time without any permanent damage; when pressure is removed, tissues that had been under contact stress experience a period of hyperemia, in which the body dilates the blood vessels in the affected area in order to flush out the accumulated metabolites and restore adequate oxygenation. The time required to fully recover from a sustained applied contact stress varies according to the magnitude and duration of loading (Remaley & Jaeblon, 2010). Husain (1953) showed that, in general, the time that skin and muscle tissue can tolerate sustained contact stress has an inverse relationship to the magnitude of the contact stress. The same study also showed that skin and muscle tissue can tolerate contact stresses upwards of 100 mmHg (13.3 kPa) for periods of up to 2 hours. While there have been some attempts to better model damage from sustained contact stress in concert with other factors (Gefen, 2007), standard prevention still focuses on the temporal threshold (2 hours of sustained immobility for

a patient) and being watchful for risk factors other than contact stress magnitude (Leigh & Bennett, 1994).

Knowledge gaps that will be addressed in the present study include documenting the magnitude of the contact stress at the skin-orthosis interface at several locations around the lower thorax under various external loads, including the "damage" thresholds of 32 mmHg and 100 mmHg. This study will also address how the contact stress depends on the distraction force and bending moments applied to the orthosis, the phase of respiration (full inhalation and full exhalation) and, for a given modular orthosis component, and the eccentricity (out-of-roundness of the lower thorax. We tested the null hypothesis that the distribution of the contact stress at the skin-orthosis interface would not be affected by distraction force, sagittal plane bending moment, respiration phase or the geometry of the lower thorax in healthy young men.

3.2 METHODS

3.2.1 Subjects

Twenty healthy young male adults were recruited, between 20 and 30 years of age and with body mass indices (BMI) between 19.47 and 28.41 kg/m^2. The exclusion criteria included history of medical treatment for vertebral fractures, spondylolysis, spondylolithesis, congenital abnormalities of the spine, scoliosis, kyphosis, osteoporosis, recurrent back pain, or disc herniation. All subjects gave written, informed consent and all procedures were approved by an institutional review board (IRB).

3.2.2 Data Acquisition

Contact Stress Sensor Description & Calibration. The design of a thin and flexible transducer suited to measuring the normal contact stress at the skin-orthosis interface over the lower rib cage was developed by modifying a force-sensitive resistor described by Perner-Wilson (2010). Two linear arrays of seven piezoresistive sensors each were created (see Figures 3.1 and 3.3). Each sensor consisted of a core of conductive polymer (Velostat ®; 3M, St. Paul, MN, USA) sandwiched between two layers of conductive fabric (ArgenMesh™; Less EMF, Inc., Albany, NY, USA), all of which was sewn and glued together in a polyester sleeve. Two standard size 16 snap fasteners were used for electrical connections.

The electrical resistance of each sensor decreased as the contact stress applied to the active sensor area (where the Velostat® and ArgenMesh™ layers overlapped entirely, approximately 38.1 mm x 19.1 mm) increased. In order to measure the change in resistance, each sensor was placed in series with a 10 kΩ resistor as part of a voltage divider circuit (see Figure 3.2). Each array of seven sensors (and their corresponding voltage divider circuits) shared a single driving voltage input of +5V DC and a single local ground (shown in red and green in Figure 3.2, respectively). Each sensor/circuit signal was sampled by an analog input channel (shown in yellow in Figure 3.2) at 1 kHz via a 16-bit DAQCard-6024E (National Instruments, Inc., Austin, TX, USA) analog-to-digital converter board and notebook PC running LabVIEW™ (version 9.0, National Instruments, Inc., Austin, TX, USA). Note that each sensor was numbered according to its corresponding analog input channel on the DAQ (channels 2-15).

Prior to each session with a subject, each sensor array was laid on a flat surface and each sensor was calibrated individually using a sequence of non-ordinal applied loads *ad modum* Brimacombe, Wilson, Hodgson, Ho, and Anglin (2009). First, an aluminium plate of 12.54 g sized to fit the active sensor area (called the "base plate") was applied to the sensor. Next, a known reference mass was applied on top of the base plate. After a few seconds, data were recorded for 5 seconds; the mean of the recorded voltage readings was stored as the calibration point for that load. After a reading was taken, the sensor was offloaded except for the base plate and then loaded with the next mass in the sequence. A total of six masses were used to calibrate each sensor in this manner, in the following sequence: 1000 g, 700 g, 1500 g, 900 g, 1700 g and 1200 g.

In order to accurately measure the external forces that were imposed on each test subject, two load cells (TLL-500, Transducer Techniques, Inc., Temecula, CA, USA) were used in tension as part of the apparatus (see below). Each load cell was connected to a digital signal conditioner (DPM-3, Transducer Techniques), which then output a DC voltage updated at a frequency of approximately 60 Hz that varied in proportion to the applied tensile force. As with the contact stress sensors, the load cells were calibrated prior to each session with a test subject using a series of known applied loads, with data recorded for 5 seconds at each load and the mean of the readings used as the calibration value (as for the contact stress sensors). First, the digital signal conditioner was balanced to discount the mass of the load cell, attachments, and cabling from any subsequent readings. The load cells were then calibrated by loading them in sequence with masses of 0.5387 kg, 5.537 kg, 4.538 kg and 9.5369 kg.

Subject Anthropometry. Once each subject arrived, he was first asked to remove any shirts, jewelry, etc. from the upper body, and was then fitted with a shirt made from a section of tubular stockinette (tg® Tubular, Lohmann & Rauscher, Inc., Topeka, KS, USA). Subject height and mass were then measured using a medical scale. Next, the lower edge of the ribcage (encompassing the eleventh and twelfth, or "floating", ribs) was located by palpation while the subject held a full inhalation. Using a flexible measuring tape, the circumference of the lower edge of the ribcage was then taken at both a full inhalation (maximum lung volume) and full exhalation (minimum lung volume). Next, calipers were used to measure the lateral and mid-sagittal diameters of the lower edge of the ribcage, also at both full inhalation and full exhalation.

Test Setup. Each subject was assisted in donning the testing apparatus (see Figures 3.3 and 3.4), which consisted adjustable harness (the "test orthosis") lined with the two arrays of contact stress sensors and attached at two points (anterior and posterior midline) to wire rope cables anchored in an overhead gantry. Loads were applied via two cables (the "load lines" shown in green in Figure 3.4), each of which contained an in-line load cell. Two additional cables (the "safety lines" shown in red in Figure 3.4) were also attached to the test orthosis which could catch and hold the subject upright above the floor in case he fainted or the load lines failed. Each load line could be attached to a combination of up to four constant force springs mounted in the overhead gantry: three springs were rated at approximately 44 N and one at approximately 22 N.

The test orthosis (shown with subcomponents labeled in Figure 3.3) consisted of four flexible plastic segments: two flat, padded plates over the sternum and spine (each with an attachment point for cabling), and two semi-circular segments, each of which encircled one side of the ribcage. The segments were connected by nylon webbing and buckles, which allowed the separation between the segments to be adjusted. The test orthosis was adjusted for each subject such that the semi-circular segments were positioned over the lower edge of the ribcage (centered on each side) and each plate was centered on the midline.

Test Battery 1 – Thoracic Distraction Forces. For the first group of tests, approximately equal forces were applied to the two load attachment points of the test orthosis in order to apply a cranial distraction force to the thorax. Corresponding front and back loads were varied by changing which of the constant force springs were connected to each load line, with increasing loads from 22 N to 154 N in 22 N increments. At each applied load, each subject was

asked to fully inhale and hold his breath for 5 seconds while data were recorded. After taking several normal breaths, each subject was asked to fully exhale and hold his breath, again for 5 seconds as data was recorded.

Test Battery 2 – Thoracic Moments. The second battery of tests consisted of applying two sequences of increasing moments to each test subject at the mid-sagittal plane. To produce each sequence of moments, one load line remained connected to the lowest-rated coil spring (22 N) as the load on the other load line was increased from 44 N to 154 N. As in the distraction tests, data were recorded in 5 second intervals as subjects held a full inhalation followed by a full exhalation. Once the first moment sequence was complete, the sequence was repeated for the other load line.

3.2.3 Data Analysis

All data were initially processed initially using Excel (version 2007, Microsoft Corp., Redmond, WA, USA). First, the height and mass of each subject were used to calculate his Body Mass Index (BMI). Next, the eccentricity of the ribcage of each subject (approximated as an ellipse for the purposes of this study) was calculated by specifying the frontal plane and mid-sagittal diameters of the lower thorax as the major and minor axes of the ellipse. The eccentricity was calculated at both the full inhalation and exhalation and then averaged to produce a single, average thorax eccentricity value for each subject (used as a factor in the statistical analysis, below). Finally, the calibration data (applied contact stress vs. measured voltage) for each sensor was fitted to its own linear function. The data for each sensor was then converted from a measured voltage into a contact stress value (in kPa).

Statistical Analysis. The post-processed data were subjected to statistical analysis using IBM SPSS Statistics (version 19.0.0, International Business Machine Corp., Armonk, NY, USA). Each sensor was analyzed individually using a mixed linear model (for repeated measures), with the recorded contact stress chosen as the single dependent variable. Subject breath status (fully-inhaled or fully-exhaled), average thorax eccentricity, normalized distraction force, and normalized moment were chosen as the dependent factors to be analyzed for significance, using a 95% confidence interval. A p value less than 0.05 was considered significant for the test of each hypothesis.

3.3 RESULTS

The mean quasi-static contact stress magnitude data for each pair of corresponding left/right sensors from the distraction and moment test batteries are shown in Figures 3.5 and 3.6, respectively. The results of the F-tests for statistical significance of all factors in the mixed linear model constructed for each sensor are shown in Table 3.1. Individual data points were only excluded if the calculated contact stress reading (produced from the measured voltage reading and linear calibration function) was negative.

3.3.1 Normalized Applied Distraction Force

The distraction and moment tests produced different ranges of observed contact stresses. In the distraction test battery, the recorded contact stress varied from a minimum of 8.2 kPa (sensors 8 & 9, 22 N/22 N front/back loading, exhaled; Figure 3.5-G) to a maximum of 26.5 kPa (sensors 7 & 10, 154 N/154 N front/back loading, inhaled; Figure 3.5-F), which corresponds to a range of approximately 61.7-198.3 mmHg. In the moment test batteries, the recorded contact stress varied from a minimum of 13.0 kPa (sensors 2 & 15, 22 N/44 N front/back loading, exhaled; Figure 3.6-A) to a maximum of 27.8 kPa (sensors 7 & 10, 154 N/22 N front/back loading, inhaled; Figure 3.6-F), which corresponds to a range of approximately 97.7-208.7 mmHg.

The normalized applied distraction force was a significant factor affecting the recorded contact stress for every sensor except sensor 15 (Table 1). Among every other sensor, the largest fixed effect was observed at sensor 7 (+34.6 kPa/unit of normalized distraction force), while the smallest was observed at sensor 12 (+14.1 kPa/unit of normalized distraction force). All sensors exhibited a positive proportional relationship between normalized applied distraction force and recorded contact stress.

3.3.2 Normalized Applied Moment

Normalized applied moment was also found to be a significant factor affecting the contact stress recorded at most sensors, with some exceptions (see Table 1): sensor 4 ($p = 0.083$), sensor 13 ($p = 0.304$), sensor 14 ($p = 0.083$), and sensor 15 ($p = 0.392$). Among those sensors where the normalized applied moment was found to be significant, the largest effect for a positive moment (flexion) was observed at sensor 2 (+448.9 kPa/unit of normalized moment), while the largest effect for a negative moment (extension) was observed at sensor 7 (-444.3

kPa/unit of normalized moment). The smallest magnitude estimated effect from the normalized applied moment was observed in sensor 12 (-49.1 kPa/unit of normalized moment). It should also be noted that the sign of the estimated effect from normalized applied moment reversed at one location in each sensor array: between sensors 4 and 5 (attached to subject right) and between sensors 12 and 13 (attached to subject left).

3.3.3 Respiration Phase

The averaged recorded contact stresses show that for nearly each pair of sensors at every test point, the stresses recorded when the subjects held a full inhalation were higher than those when they held a full exhalation (Figures 3.5 and 3.6). The most obvious exception to this occurred in sensors 2 and 15 in the moment tests, which shows the full-exhalation contact stress to become greater than the full-inhalation contact stress for small negative (extension) normalized moments (Figure 3.6-A). It should also be noted that many readings overlap within the bounds of standard error.

When the output of each sensor is examined individually via the mixed linear model analysis, subject respiration phase (full inhalation or full exhalation) was found to have a significant effect on the recorded contact stress for nearly every sensor except sensors 14 and 15 ($p = 0.738$ and $p = 0.489$, respectively). The effect of switching between the two states was calculated using a full exhalation as the default state for the mixed linear model of each sensor; thus, the effect estimates listed in Table 1 are the estimated changes in contact stress in each sensor as the subject fully inhales. For each sensor where respiration phase was found to be significant, the recorded contact stress was found to increase when the subject fully inhaled; the largest estimated effect was found to occur in sensor 2 (+5.0 kPa) and the smallest was found to occur in sensor 5 (+1.5 kPa).

3.3.4 Average Thorax Eccentricity

Average thorax eccentricity was found to vary between 0.405 and 0.787. Using the mixed linear models for each sensor, it was found to be a significant factor affecting recorded contact stress for only sensors 10, 12, and 13 ($p = 0.022$, 0.046, and 0.023, respectively), which were all on the sensor array attached to subject left. The estimated effect average thorax eccentricity produced on skin contact stress was similar in magnitude (but not necessarily sign) for each of the three sensors: -9.0 kPa (sensor 10), +6.2 kPa (sensor 12), and +7.8 kPa (sensor

13) (Table 1). For the other sensor array (sensors 2-8), slight positive trends were observed for three sensors (2, 3, and 6, with p = 0.089, 0.087, and 0.074, respectively), but thorax eccentricity did not approach significance for any other sensor on either array.

3.4 DISCUSSION

This is the first study that describes the contact stress distribution developed between the skin and a partial thoracic orthosis for a given applied external distraction force and moment, as well as other contributing factors. The results show that the contact stress was significantly affected by applied external distraction force, applied external moment and respiration phase at nearly every location tested. The effect of the eccentricity of the lower thorax was not significant for all but a small minority of measurement sites. For all test conditions, recorded contact stresses exceeded 32 mmHg (4.27 kPa), the average contact stress required to occlude the capillaries near the surface skin. In nearly all testing conditions, the contact stresses exceeded the 100 mmHg (13.3 kPa) threshold for eventual damage first suggested by Husain (1953). The range of contact stresses observed is similar to that observed by van den Hout *et al.* (2002) in their study, which also featured an orthosis applying sustained forces (for correction of scoliosis), albeit at different load application sites from this study.

The mean recorded contact stress values for every sensor increased with applied normalized distraction load across the entire testing range, generally outside the bounds of standard error (as shown in Figure 3.5). Any external load imposed on the test orthosis was ultimately counterbalanced by contact stress distribution applied to the thorax of each subject. The lack of any noticeable decrease in the mean contact stress at all sites suggests that there are no secondary loading mechanisms which arise at any loading threshold within the testing range. This is reasonable given that the modular orthosis essentially acted as a ring half way up the lower torso (shaped like an inverted truncated cone) so as to lift it. The shape of the loading curve likely depends on the shape of the thorax, the compliance of the boney thorax, the thickness of subcutaneous fat and muscle over the ribs, the muscle tone in the intercostals muscles, and the mechanical behavior of the tissues being loaded. Apart from perfusion away from the site of application (blood, lymph, interstitial fluid), skin undergoes several structural changes when subjected to contact stress, including a re-orientation of the collagen fiber bundles constituting much of the intercellular support structure along with elastin fibers (Edsburg, Natiella, Baier, & Earle, 2001; Sanders, Goldstein, & Leotta, 1995). Such time-

dependent changes in the tissue produce creep effects in the load/displacement behavior of skin under load (Remaley & Jaeblon, 2010). Finally, skin and other tissues require time to regain full integrity after the contact stress is removed, with the time required increasing with both the magnitude and duration of the applied contact stress (Husain, 1953).

For the moment tests, it was expected that a more pronounced difference between the contact stresses recorded at corresponding positive and negative moments would appear in sensors further from the midline (sensors 5 and 12), the approximate center of rotation. Sensors at the posterior of the orthosis (such as sensors 8 and 9) would be expected to record much higher average mean contact stresses when a positive (flexion) moment was applied to the orthosis than when a negative (extension) moment was applied, and vice versa. These large expected differences did not appear in the data; in fact, a slight trend to the opposite appears at those sensors near the anterior and posterior of the test orthosis. This is most likely due to how moments were generated in the moment test batteries. All of the tests in this study used combinations of vertical distraction loads applied at the anterior and posterior of the test orthosis. Thus, the tests involving an applied moment also included a large distraction force applied simultaneously. Any large differences in recorded contact stress between positive and negative moments from the moment alone may have been masked by the balanced contribution of the distraction force component of the loading. As for the slight reverse trend in observed loading differences, this may have arisen from subjects not remaining in an entirely erect posture, especially at the higher load configurations. The subject may have partially shifted towards the opposite surface for comfort/balance, thus redistributing more contact stress to the sensors opposite the point of load application (i.e., for a large negative moment, subjects may have assumed a partially extended posture and shifted some of their weight to the posterior of the test orthosis).

Respiration phase (full inhalation or full exhalation) was expected to have a pronounced effect on the recorded contact stress levels, and this result is clearly seen in the relatively large separation in readings produced by the subjects at each breathing phase for corresponding loading configurations. The effect is especially pronounced at lower load configurations: approximately less than 0.20 normalized distraction force and between +/-0.002 normalized applied moment. As notes above, the highest recorded contact stresses were observed in tests where the subjects were at maximal inhalation, while the lowest contact stresses were recorded when subjects were at maximal exhalation. This compares with the study by Pham *et al.* (2008)

of an orthosis worn to treat idiopathic scoliosis; respiration was found to be significant in contributing to recorded contact stress at the orthosis-skin interface, but the effect produced smaller changes in contact stress (approximately 1.3 kPa at most) than those observed here. It should be noted that the range in contact stress values recorded between inhalation/exhalation was not constant across all loading configurations. In general, as the overall external applied loads increased in magnitude, the difference between inhalation/exhalation contact stresses shrank: for the distraction tests the range varied between approximately 9.2 kPa (Sensors 8 & 9, 22 N front/back loading; Figure 3.5-G) and 0.4 kPa (Sensors 7 & 10, 154 N front/back loading; Figure 3.5-F). As suggested above, the shape of the loading curves (and specifically, the separation between those at maximal inhalation/exhalation) may be influenced by creep effects that appear in the tissue under sustained loading. Had all imposed external loading been removed for some period of time between each test, giving the loaded tissues' time to recover full integrity (and elastic response), the separation in recorded contact stresses at full inhalation and exhalation might have remained more constant.

There are several limitations to this study. Firstly, perhaps the greatest factor influencing the accuracy and precision of the data is the reliability of the contact stress sensors used in this study. Each sensor array was constructed by hand for this study, and there are likely to have been many inconsistencies in the dimensioning and performance of each individual sensor because of this. These sensors also share many of the same limitations as other so-called "force-sensitive resistors" (FSRs): hysteresis, drift, and requiring a "break-in" period before behavior becomes stable enough to be consistent (Hall, Desmoulin, & Milner, 2008). Certain countermeasures taken in this study were suggested by Brimacombe *et al.*, 2009 and can help mitigate these effects, but an even more thorough construction methodology might improve the validity and reliability of the contact stress measurements, including 1) adding an extra calibration period after each subject completes all of the test batteries (which would capture any effect of drift over the testing period), 2) completely offloading the orthosis in between each test (as in the calibration phase), and 3) randomizing the testing configuration (rather than conducting the test batteries in the same sequence). Secondly, the fit of the orthosis most likely greatly influenced the results from each subject, and may throw any analysis of the effect of the average thoracic eccentricity into doubt. The test orthosis, while made of a soft polystyrene and broken into segments to improve its ability to conform to varying geometries, still developed some resistance to bending in the lateral strips where each sensor array was mounted. This may

have made sensor readings near the anterior and posterior poles of those with more elliptical thorax geometries appear much lower than would appear in a well-fitted orthosis. Any lack of proper fit may also have lead to the appearance of contact stress concentrations at specific points which may have artificially elevated other readings. The ideal testing scenario would employ a custom test orthosis for each subject, a scenario which was cost-prohibitive for this feasibility study. Thirdly, this study does not take into account the element of time. Both the tissues being loaded and the sensors used in this study are known to exhibit some degree of variation in their responses to load with time (i.e., creep effects). While each testing period was short (5 sec per test configuration, and total subject time in-harness limited to approximately 45 min), those tests conducted last might have demonstrated pronounced creep effects and that this statistical analysis would be unable to separate from other factors. Future work may require set recovery time periods between each loading configuration, in order to assure full tissue recovery between testing, as well as tracking loads with time for each sensor (rather than averaging, as was done here). Fourthly, the loading protocol required the use of "impure" moments, which was largely determined by the nature of the test orthosis: constant distraction forces were required to maintain contact with each subject. In order to more effectively analyze the effect of imposed moments, a more-rigid test orthosis would have to be subjected to torque without any distraction forces. Fifthly, more-precise anthropometry could be provided by optical scanning systems to trace the thoracic contours and geometries (Fourie, Damstra, Gerrits, & Ren, 2011; Susato, 2011) . Finally, this study only examined the brace effects in a modest population of young, healthy males. The results cannot be extrapolated to females, the obese, the elderly or those with musculoskeletal impairments without further research.

3.4.1 Conclusions

There is no single threshold of maximum "safe" contact stress which can be applied indefinitely to the skin of a specific person, with the possible exception of dermal capillary pressure. Thus, knowing the precise magnitude of the applied contact stress at any moment may not be as important as awareness of other risk factors for contact stress -related injury, such as duration of loading. Contact stress monitoring can be used in existing orthoses as a means of reminding the patient/caregiver that the patient needs to be repositioned (i.e., have the contact stress load on their skin redistributed) at regular intervals to prevent damage. Monitoring the levels of contact stress applied to the skin by various orthoses is also a useful

design tool when it is used to assess the relative contact stress magnitudes created by various orthosis configurations. In general, it can be said that applying lower contact stress magnitudes at the skin is an improvement, as long as the required clinical effects (immobilization, corrective forces/moments) are still satisfactory.

As a final note, it should be remembered that this study did not include measurements of the two orthogonal interface shear contact stress components which contribute to the overall mechanical loading created at the surface of the skin when it contacts another body. However, some conclusions about the overall shear stress (and its consequences) can still be made. As part of their literature review, Sanders, Goldstein, and Leotta (1995) state that the skin response to shear loads mirrors its response to pressure loads: the duration skin can tolerate "rubbing" (sliding contact with another body) without experiencing damage (i.e., blistering) decreases as the magnitude of the shear stress increases. Of course, shear stress on the surface of the skin is produced by friction, which is a product of surface characteristics and normal (contact) stress. Thus, contact stress applied to the skin not only contributes to pressure-related injuries (i.e., pressure ulcers), but also to shear-related injuries. Reducing the magnitude of applied contact stress in an orthosis (again, through repositioning and/or design) thus has the potential to reduce the likelihood of both forms of injury.

3.5 REFERENCES

Bernardoni, G. P., & Gavin, T. M. (2006). Comparison between custom and noncustom spinal orthoses. *Physical Medicine and Rehabilitation Clinics of North America*, 17, 73-89. doi:10.1016/j.pmr.2005.10.005

Black, J., Baharestani, M., Cuddigan, J., Dorner, B., Edsburg, L., Langemo, D., Posthauer, M. E., Ratliff, C., & Taler, G. (2007). National Pressure Ulcer Advisory Panel's updated pressure ulcer staging system. *Dermatology Nursing*, 19(4), 343-349.

Brimacombe, J. M., Wilson, D. R., Hodgson, A. J., Ho, K. C. T., & Anglin, C. (2009). Effect of calibration method on Tekscan sensor accuracy. *Journal of Biomechanical Engineering*, 131(3), 034503-1-4. doi:10.1115/1.3005165

Chase, A. P., Bader, D. L., & Houghton, G.R. (1989). The biomechanical effectiveness of the Boston brace in the management of adolescent idiopathic scoliosis. *Spine*, 14(6), 636-642.

Edsberg, L. E., Natiella, J. R., Baier, R. E., & Earle, J. (2001). Microstructural characteristics of human skin subjected to static *versus* cyclic pressures. *Journal of Rehabilitation Research & Development*, 38(5), 477-486.

Flanagan, P., Gavin, T. M., Gavin, D. Q., & Patwardhan, A. G. (2000). Spinal orthoses. In M. Lusardi & C. Nielsen (Eds.), *Orthotics and Prosthetics in Rehabilitation* (pp. 231-252). Woburn, MA: Butterworth-Heinemann Medical.

Fourie, Z., Damstra, J., Gerrits, P. O., & Ren, Y. (2011). Evaluation of anthropometric accuracy and reliability using different three-dimensional scanning systems. *Forensic Science International*, 207(1-3), 127-134. doi:10.1016/j.forsciint.2010.09.018

Gefen, A. (2007). Risk factors for a pressure-related deep tissue injury: a theoretical model. *Medical & Biological Engineering & Computing*, 45, 563-573. doi:10.1007/s11517-007-0187-9

Hall, R. S., Desmoulin, G. T., & Milner, T. E. (2008). A technique for conditioning and calibrating force-sensing resistors for repeatable and reliable measurement of compressive force. *Journal of Biomechanics*, 41(16), 3492-3495. doi:10.1016/j.jbiomech.2008.09.031

Husain, T. (1953). An experimental study of some pressure effects on tissues, with reference to the bed-sore problem. *Journal of Pathology and Bacteriology*, 66, 347-363.

Leigh, I. H., & Bennett, G. (1994). Pressure ulcers: prevalence, etiology, and treatment modalities. A review. *The American Journal of Surgery*, 167(1A), 25S-30S.

Lou, E., Hill, D. L., & Raso, J. V. (2010). A wireless sensor network system to determine biomechanics of spinal braces during daily living. *Medical & Biological Engineering & Computing*, 48, 235-243. doi:10.1007/s11517-010-0575-4

Périé, D., Aubin, C. E., Lacroix, M., Lafon, Y., & Labelle, H. (2004). Biomechanical modelling of orthotic treatment of the scoliotic spine including a detailed representation of the brace-torso interface. *Medical & Biological Engineering & Computing*, 42(3), 339-344. doi:10.1007/BF02344709

Perner-Wilson, H., Buechley, L., & Satomi, M. (2010). Handcrafting textile interfaces from a kit-of-no-parts. In *Proceedings of the fifth international conference on Tangible, embedded, and embodied interaction (TEI '11)* (pp. 61-68). New York, NY: ACM.

Pham, V. M., Houilliez, A., Schill, A. Carpentier, A., Herbaux, B., & Thevenon, A. (2008). Study of pressures applied by a Chêneau brace for correction of adolescent idiopathic scoliosis.

Prosthetics and Orthotics International, 32(3), 345-355. doi:10.1080/03093640802016092

Reenalda, J., Van Geffen, P., Nederhand, M., Jannink, M., IJzerman, M., & Rietman, H. (2009). Analysis of healthy sitting behavior: Interface pressure distribution and subcutaneous tissue oxygenation. *Journal of Rehabilitation Research & Development*, 46(5), 577-586. doi:10.1682/JRRD.2008.12.0164

Remaley, D., & Jaeblon, T. (2010). Pressure ulcers in orthopaedics. *Journal of the American Academy of Orthopaedic Surgeons*, 18, 568-575.

Sanders, J. E., Goldstein, B. S., Leotta, D. F. (1995). Skin response to mechanical stress: adaptation rather than breakdown – a review of the literature. *Journal of Rehabilitation Research and Development*, 32(3), 214.

Susato, S. (2011). Development and application of portable manual non-contact-type anthropometric instruments for measuring human anatomical longitudinal parameters. *Journal of Physiological Anthropology*, 30(2), 55-67. doi:10.2114/jpa2.30.55

van den Hout, J. A. A. M., van Rhijn, L. W., van den Munckhof, R. J. H., & van Ooy, A. (2002). Interface corrective force measurements in Boston brace treatment. *European Spine Journal*, 11, 332-335. doi:10.1007/s00586-001-0379-1

Wywialowski, E. F. (1999). Tissue perfusion as a key underlying concept of pressure ulcer development and treatment. *Journal of Vascular Nursing*, 17,12-16.

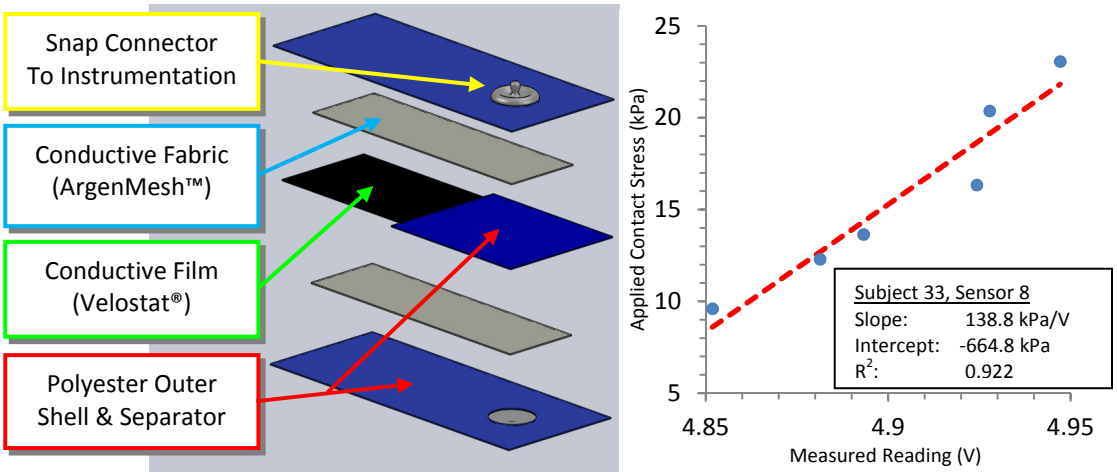

Figure 3.1: [Left] Example custom-made piezoresistive contact stress sensor, exploded view. The sensor layers are sewn together in final assembly. [Right] Example calibration data with resulting linear-fit calibration function.

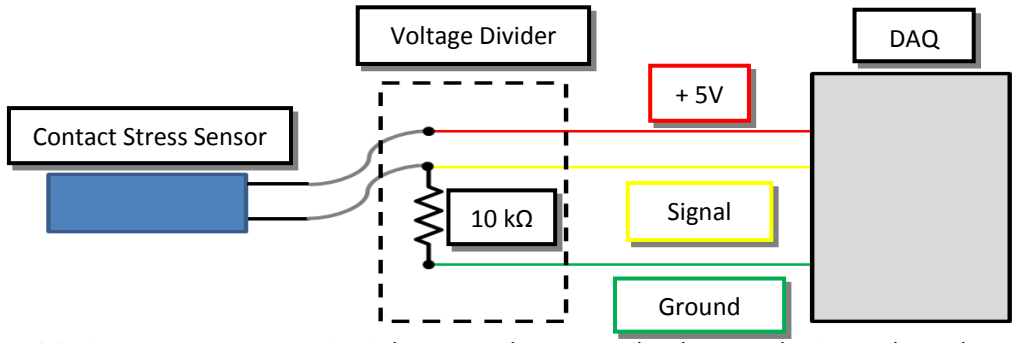

Figure 3.2: Contact stress sensor circuit layout. Each sensor utilized one analog input channel on the data acquisition unit (DAQ). Each sensor array (seven sensors) used one +5V and one ground channel, shared across each of its sensors.

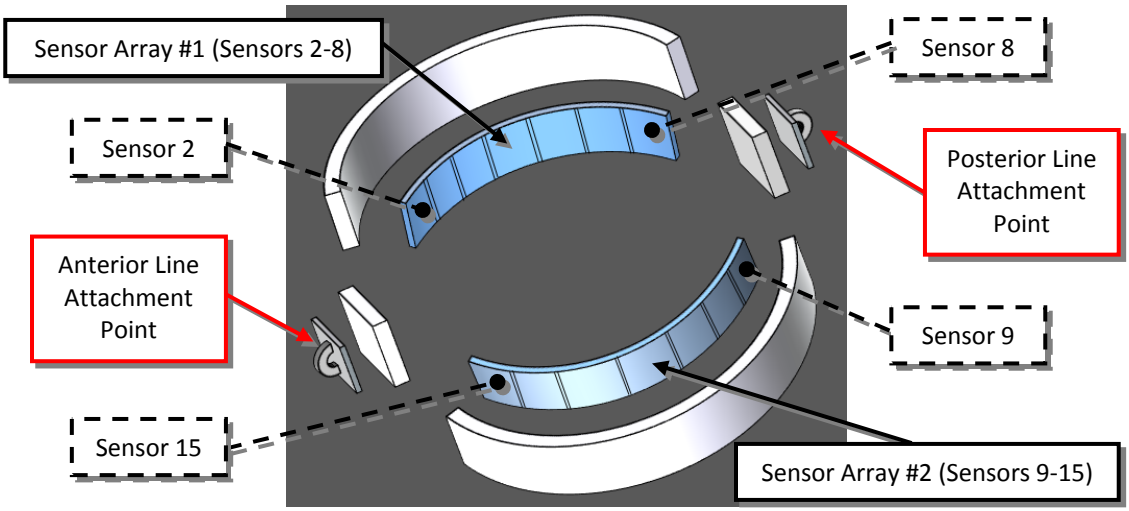

Figure 3.3: Test orthosis segments (shown in white), line attachment points, and sensor array placement, exploded view. Not shown: adjustable buckles and straps connecting each adjacent segment. Adhesive tape secured each sensor array during testing.

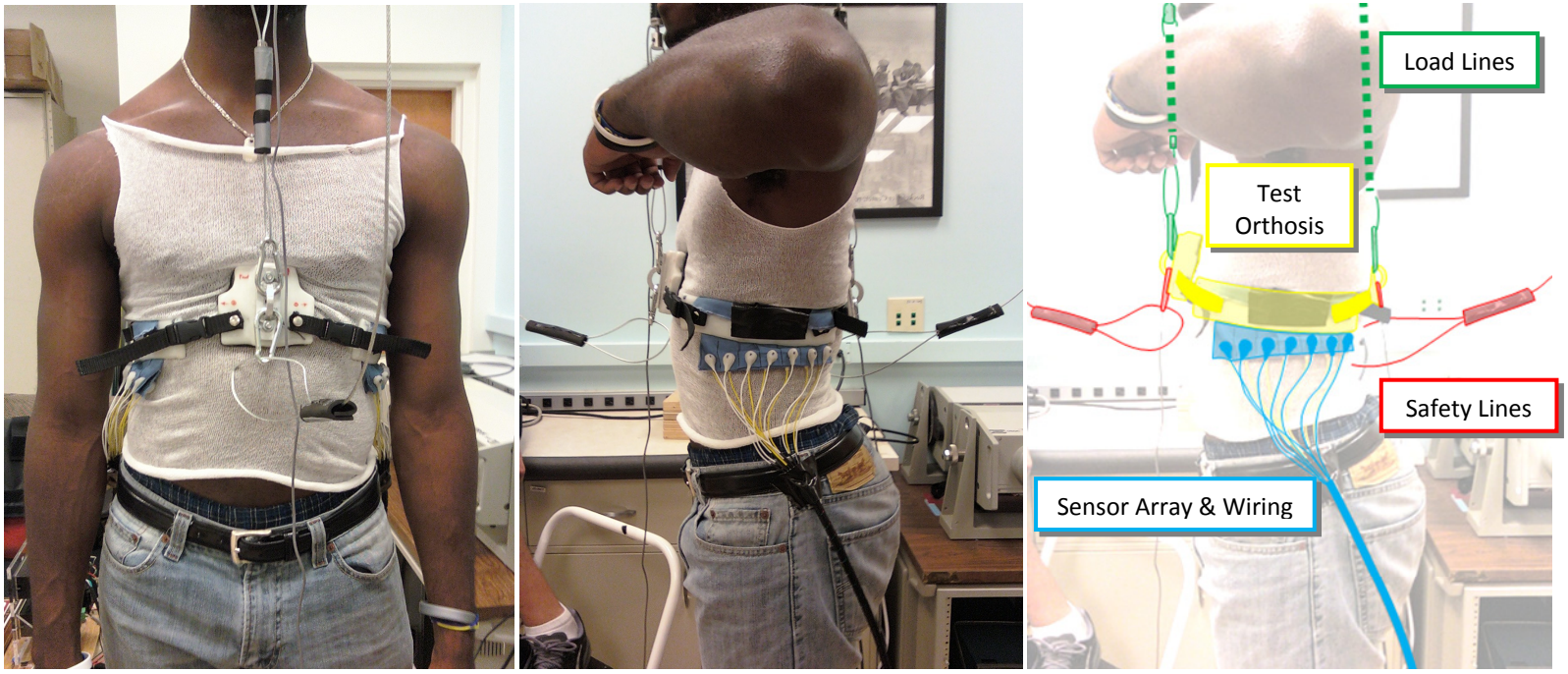

Figure 3.4: Test orthosis and sensor placement over stockinette shirt on a test subject. [Left] Anterior view. [Center] Lateral view. [Right] Lateral view with testing apparatus components labeled for visibility.

Figure 3.5: Distraction test battery results, all subjects, by sensor pair (right & left). Horizontal & vertical bars denote S.E.

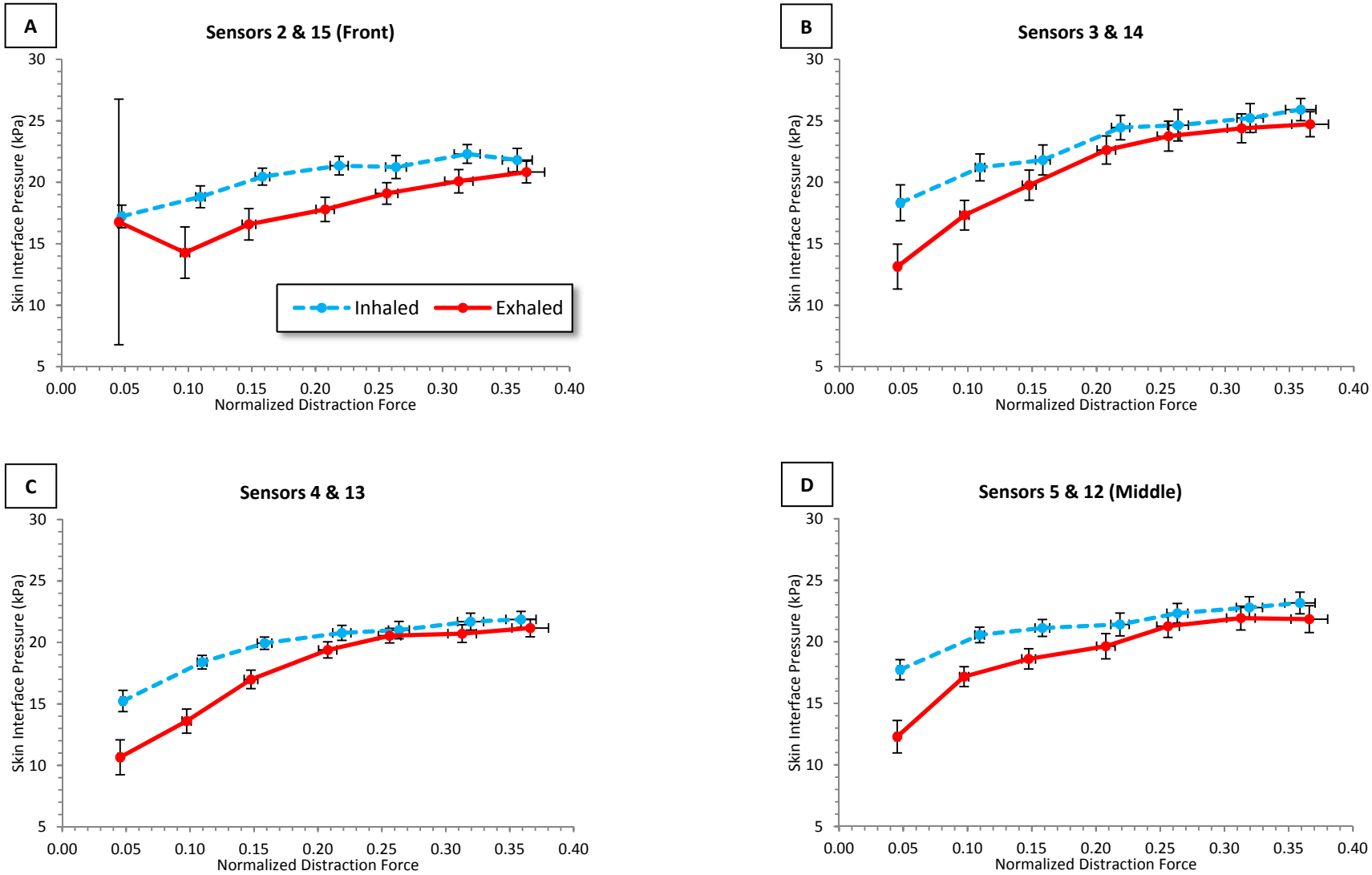

Figure 3.5 (Continued): Distraction test battery results, all subjects, by sensor pair (right & left). Horizontal & vertical bars denote S.E.

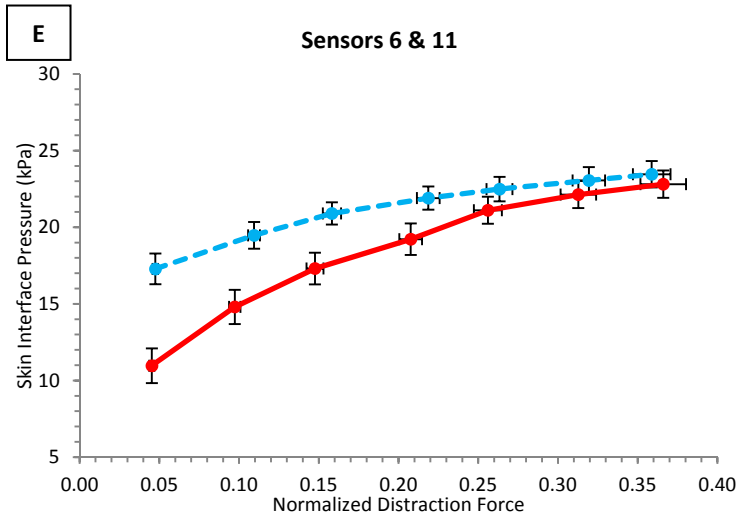

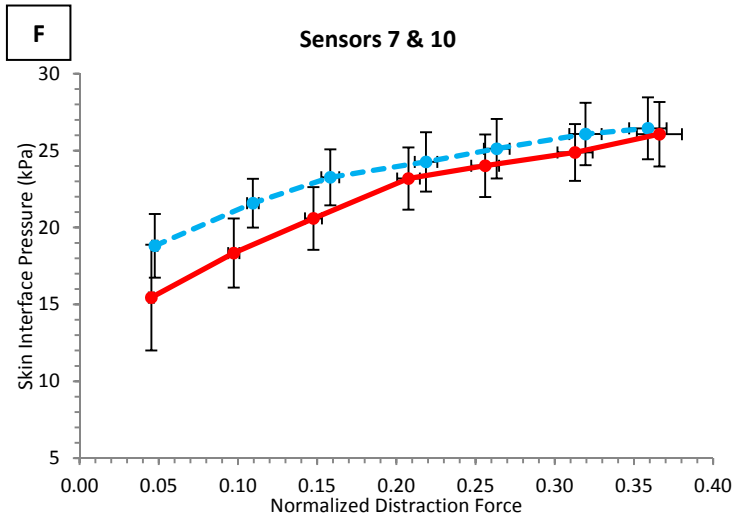

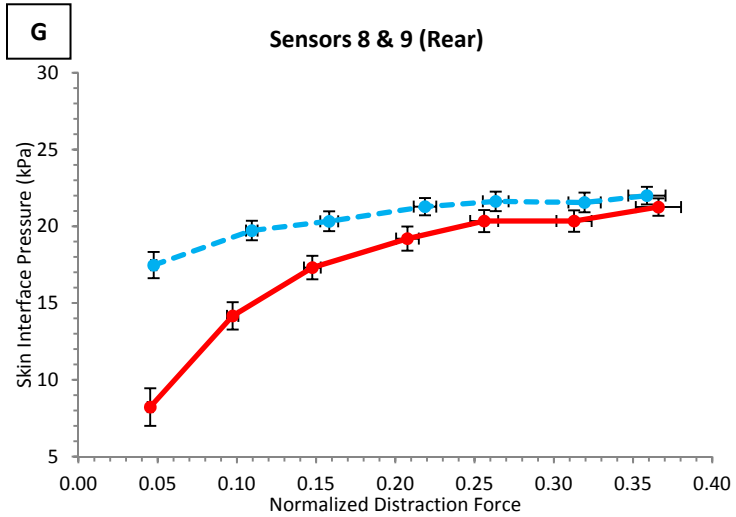

Figure 3.6: Moment test battery results, all subjects, by sensor pair (right & left). Horizontal & vertical bars denote S.E.

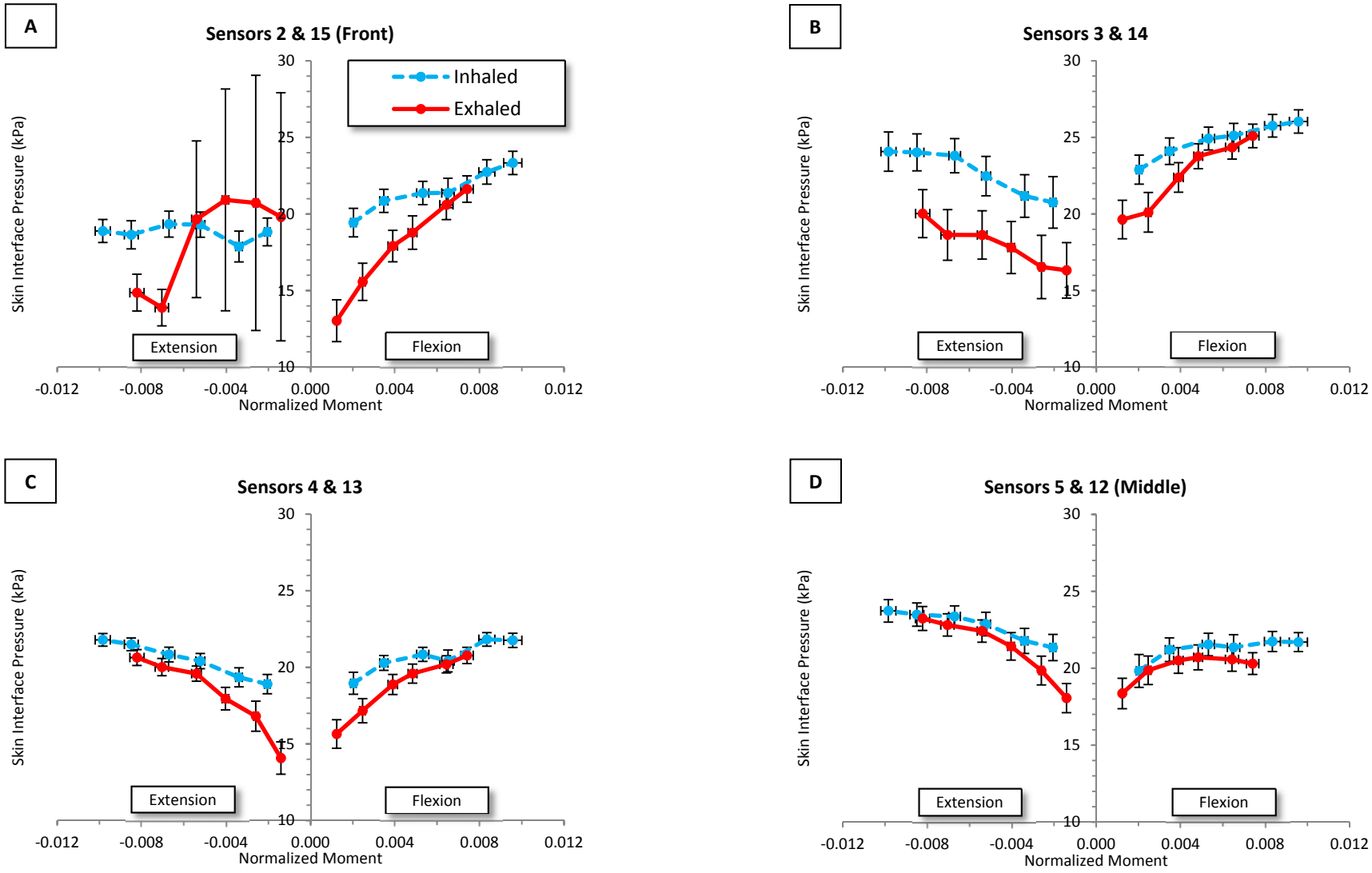

Figure 3.6 (Continued): Moment test battery results, all subjects, by sensor pair (right & left). Horizontal & vertical bars denote S. E.

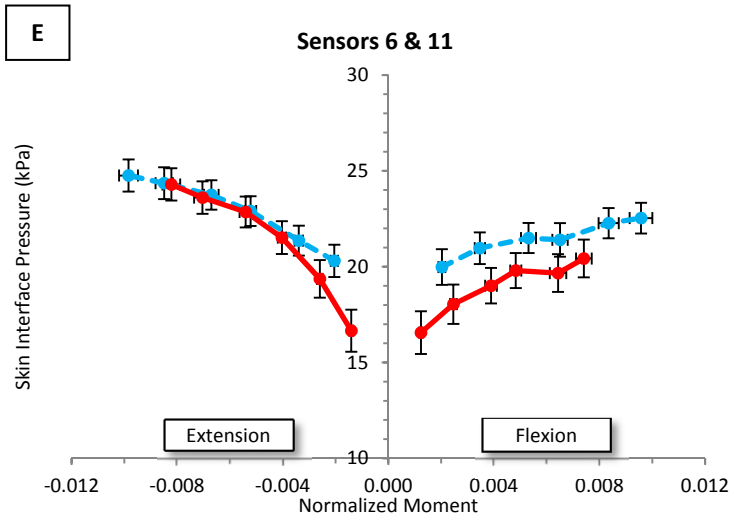

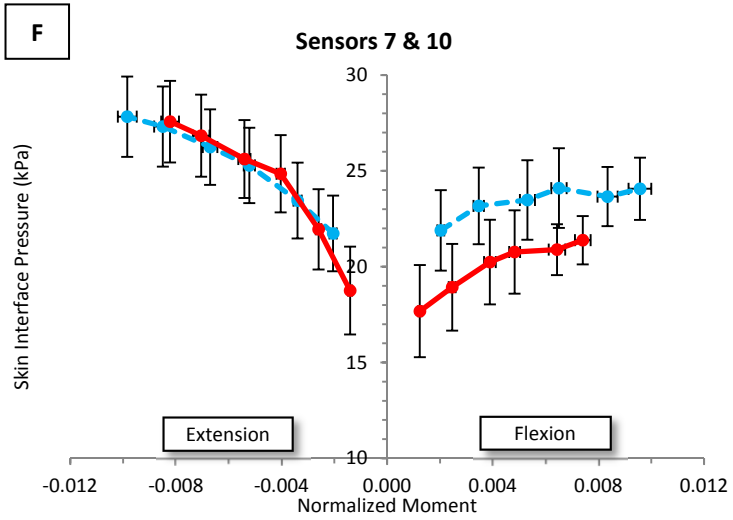

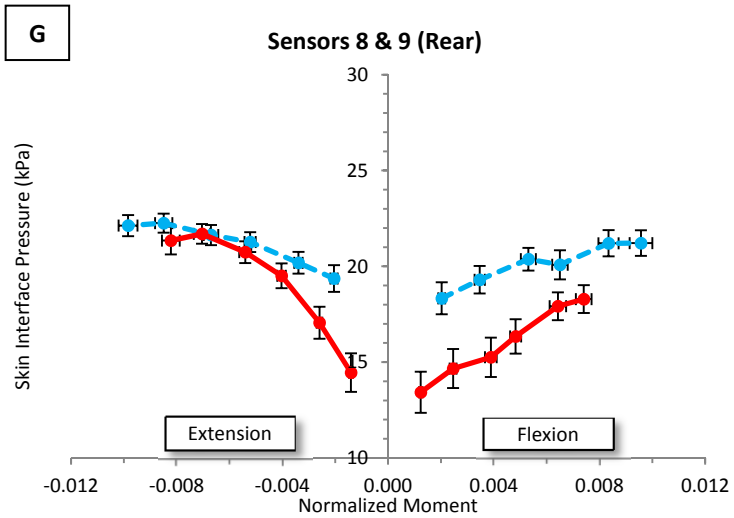

Table 3.1: Mixed linear model results.

Sensor	Test Statistic, F	Norm. Distraction	Norm. Moment	Respiration Phase	Avg. Thorax Eccentricity	p-Value	Norm. Distraction	Norm. Moment	Respiration Phase	Avg. Thorax Eccentricity	Fixed Effect Estimate	Norm. Distraction	Norm. Moment	Respiration Phase	Avg. Thorax Eccentricity
2		200.899	178.247	225.931	2.908		0.000	0.000	0.000	0.089		27.9	448.9	5.0	8.4
3		218.913	91.913	122.156	2.943		0.000	0.000	0.000	0.087		26.6	291.4	3.3	7.9
4		278.722	3.019	122.612	0.026		0.000	0.083	0.000	0.872		23.3	41.3	2.5	0.6
5		94.977	10.601	28.201	0.286		0.000	0.001	0.000	0.593		16.6	-98.7	1.5	-2.4
6		253.206	96.467	65.974	3.209		0.000	0.000	0.000	0.074		27.5	-288.9	2.3	-8.5
7		178.996	100.031	28.283	0.646		0.000	0.000	0.000	0.422		34.6	-444.3	2.3	-5.9
8		190.704	41.102	125.542	0.162		0.000	0.000	0.000	0.687		24.6	-193.9	3.3	-1.9
9		209.786	15.856	182.562	0.275		0.000	0.000	0.000	0.601		18.0	-84.7	2.8	1.4
10		108.593	18.737	55.487	5.297		0.000	0.000	0.000	0.022		14.9	-105.2	1.8	-9.0
11		148.292	9.139	102.877	0.438		0.000	0.003	0.000	0.509		14.9	-63.9	2.1	2.0
12		121.564	4.913	51.963	4.034		0.000	0.027	0.000	0.046		14.1	-49.1	1.5	6.2
13		171.695	1.058	48.317	5.289		0.000	0.304	0.000	0.023		18.4	24.6	1.6	7.8
14		12.501	3.109	0.113	0.002		0.001	0.083	0.738	0.964		14.7	138.9	0.2	-0.5
15		2.558	0.734	0.480	0.335		0.110	0.392	0.489	0.565		11.2	109.2	0.8	8.1

Chapter 4

Design and Preliminary Testing of a Novel Thoracopelvic Orthosis for Reducing Lumbar Spine Loading and Muscle Effort in Trunk Flexion with and without Weighted Garments

4.1 INTRODUCTION

Spinal orthoses are often prescribed to restrict spine motion and/or offload the spinal column following spine surgery or trauma (Flanagan, Gavin, Gavin, & Patwardhan, 2000; Edelstein, 1996). Spinal offloading is primarily achieved through two mechanisms: increasing intraabdominal cavity pressure, and the application of three-point bending to the trunk in the sagittal plane. Two examples of the latter are the CASH and Jewett hyperextension orthoses, which have apply two posteriorly-directed forces (at the thorax and pelvis) and one anteriorly directed force (at the lumbodorsal region of the trunk), offloading the anterior thoracolumbar vertebral bodies to promote the healing of compression fractures (Bussel, Merritt, & Fenwick, 1995). These two orthoses have been shown to generate counter-moments of up to 15.5 Nm and 14.5 Nm, respectively, which increase with flexion (Gilbertson *et al.*, 1991).

The spine is primarily loaded in compression, the magnitude of which can be measured invasively via the internal pressure developed in the nucleus pulposus of the intervertebral discs (Wilke, Neef, Caimi, Hoogland, & Claes, 1999). Örtengren, Andersson, & Nachemson (1981) showed that the magnitude of the pressure developed in the intervertebral disc is directly related to the degree of postural back muscle activation, as measured through electromyography. This suggests that any relative changes in spinal loading (such as those produced by the wearing of a spinal orthosis) can be evaluated through the use of non-invasive surface electromyography (SEMG). Indeed SEMG has been used to evaluate the relative changes in muscle activity of several common spinal orthoses (Lantz & Schultz, 1986-II). Lumbosacral orthoses have been demonstrated to reduce the muscle effort required to maintain a stable neutral posture (Cholewicki, Reeves, Everding, & Morrisette, 2007).

Outside of a clinical setting, the most commonly used forms of spinal orthosis are the soft/semi-rigid belts corsets, which are used with the intention of preventing and/or treating of low back pain by workers performing occupations with frequent bending and lifting. This population includes interventionalists, surgeons who perform minimally-invasive procedures with the aid of real-time radiography who must often assume sustained flexed postures while wearing bulky shielding garments known as "leads" (see Chapter 2). Theoretically, the soft belts and semi-rigid corsets can achieve spinal offloading by increasing intraabdominal pressure as well as serving as a kinesthetic reminder to the wearer to prevent excessive flexion during these tasks (Bussel, Merritt, & Fenwick, 1995). However, the work of Wassell, Gardner, Landsittel, Johnston, and Johnston (2000) showed that the use of such commercially-available "back belts" provided no reduction in the likelihood of injury (as quantified through compensation claims and reported low-back pain). Custom-made orthoses produced by a trained orthotist have been shown to be more biomechanically effective than common off-the-shelf models (Bernardoni & Gavin, 2006) but have several drawbacks: the individual manufacturing (and fitting) required are prohibitively expensive for common usage, the restricted maneuverability such orthoses create (Lantz & Schultz, 1986-I) could be disadvantageous in the workplace, and the increased back postural muscle activity some can produce (Lantz & Schultz, 1986-II) could promote muscle fatigue.

Since current back belts seem to be ineffective and clinical orthoses are impractical for workplace use, we wondered whether it was possible to design a non-custom orthosis which could reduce spinal compression and muscle effort in resisting gravitational bending moments (due to the mass of the trunk) while allowing multi-planer maneuverability within a set range of motion (ROM). In order to generate the desired effects, such an orthosis would have to function slightly differently from current designs. The following description describes the motion of flexion, although the same mechanisms apply for lateral bending as well (albeit with different combinations of muscles).

In order for the trunk to remain stationary, the postural muscles of the lower back (erector spinae, multifidi, and others) must contract with sufficient force to produce a corrective moment (red arrows, Figure 4.1 - left) which can counteract the moment produced by gravity, which arises due to the center of mass of the thorax resting anteriorly to the spinal column (black arrows, Figure 4.1 - left). Spinal orthoses can reduce the effort required of the postural muscles (and thus also the compressive load they add to the spine) by producing their own

corrective moment, created from normal contact stress applied to the skin of the wearer (blue arrows, Figure 4.1 - left). As long as the wearer is flexing against the orthosis, this corrective moment will exist and increase with the degree of flexion (if so designed, until the wearer is completely relying on the orthosis for support). For those orthoses which completely restrict motion to a single posture, this support mechanism is active at all times. In the case of those orthoses which allow a ROM, however, little or no support is provided until the wearer reaches the limits of the ROM (blue line, Figure 4.1 - right), where the structure of the orthosis comes into sustained contact with the wearer and support is applied. There is thus a "gap" in support when maneuverability is allowed. What if support, in the form of a corrective moment, could be continuously applied within a ROM, rather than just at the limits (green dashed line, Figure 1 - right)? Such an orthosis would necessarily be "active" in nature, meaning it would require a control system which could both monitor the corrective moment being applied to the wearer and also act on the structure of the orthosis to adjust the magnitude of that moment to a desired level.

The monitoring of corrective moments in spinal orthoses is not new; several studies have been performed to describe the magnitude and distribution of the normal contact stress (and thus forces and moments) developed between an orthosis and its wearer (see Chapter 3.1). Similarly, active orthotic devices (a.k.a. wearable robots or exoskeletons) already exist; recent examples include the Berkeley Lower Extremity Exoskeleton (Kazerooni & Steger, 2006) and the Raytheon/Sarcos XOS (Bogue, 2009). The orthosis proposed here is novel, however, for its focus on the spine (an area largely bypassed by existing active orthotic devices) and incorporation of a control system which reacts to the observed spinal moment(s) and alters the magnitude and distribution of the moment(s) to match desired specifications.

The purpose of this study is twofold:

First, this study a prototype of an active orthosis we have created. A description of each of the core structural/electromechanical and electronic components will be presented, as well as the general design rationale behind the final configuration of the prototype. Several design decisions were the result of this being very much a research platform rather than a final product, and those design elements will be described as well.

Second, a preliminary validation test of the prototype orthosis was performed in a healthy young subject to test the primary hypothesis that the orthosis will significantly reduce lumbar postural muscle activity in near neutral and slightly flexed postures with and without the

subject wearing a weighted lead vest ("lead"). The results of this preliminary test and a discussion are presented here.

4.2 METHODS

4.2.1 Prototype Description

Structural and Electromechanical Components. The structure of the prototype orthosis resembles a combination of a modified chairback LSO and a maneuverable robotic platform, commonly referred to as a "hexapod stage" (Figure 4.2). Two semi-flexible plastic segments (InstaMorph™; Happy Wire Dog, LLC, Scottsdale, AZ, USA); encircle the user at the lower thorax (around the lowermost "floating" ribs) and pelvis (making contact at the sacrum and iliac crests). Connecting the two segments, hereafter called the upper and lower interfaces (respectively), are four linear actuators (L12-100-210-06-P; Firgelli Technologies, Inc., Victoria, BC, CAN) which are rigidly mounted to the lower interface in aluminum brackets. The anterior and posterior actuators are mounted such that each is approximately 30° from the respective midline. Each actuator connects to the upper interface via a ball-and-socket joint fabricated from nylon and Delrin® (respectively), the socket of which is attached to the end of the linear actuator. The sockets are comprised of two Delrin® pieces held together with three nut-and-bolt assemblies; by tightening/loosening the nuts on each socket, the friction created with the ball can be increased/decreased (respectively). A buckle and adjustable-length straps, which allow the upper interface to be tightened around the thorax, are attached to the anterior of the upper interface with two Chicago-style screws embedded in the upper interface.

Electronic Components – Feedback. The monitoring of the corrective flexion-extension moment being applied to the wearer of the prototype is provided by means of conductive-fabric piezoresistive sensors (modified from those which appear in Chapter 3.2.2). Each sensor has an active sensing area of approximately 3.5 cm x 5.5 cm, and is secured to the inner surface of the upper interface using adhesive tape. The leads connecting each sensor to the rest of the control system are detachable and long enough to allow for each sensor to be repositioned anywhere on the perimeter of the upper interface.

As the microcontroller of the control system cannot measure resistance levels from each piezoresistive sensor directly, the resistance value from each sensor is converted into an analog voltage by means of a combination driver/filter/amplifier circuit situated on two circuit boards mounted to the posterior of the upper interface (see Appendix B for the schematics of all

three portions of the circuit). The active components are: twelve operational amplifiers (LM4091-2; Analog Devices, Inc., Norwood, MA, USA), two voltage regulators (LF90CV; STMicroelectronics, Geneva, CHE), and one voltage reference (ADR510; Analog Devices, Inc.). The driver portion is structured to place each sensor in a voltage divider; 100 mV is applied to each sensor, which is then in series with a 10 kΩ linear potentiometer that is set to approximately match the resistance of its associated sensor when under load (which adjusts the sensitivity). The "raw" sensor signal, which is affected by ambient electrical noise (from power lines, transmissions, etc.), next passes through the filter portion of the circuit: a fourth-order Butterworth type, arranged in a Sallen-Key topology, with the corner frequency f_c (-3 dB attenuation) set to 10 Hz and the stop frequency f_s (-30 dB) set to 60 Hz. Finally, in order to take advantage of the full measurement resolution of the microcontroller of the control system (1024 values in a range of 0-5 V), the filtered signal passes through a non-inverting amplifier with a tunable gain, which is adjusted such that the maximum value of the sensor signal is approximately 5 V (the maximum value which can be measured by the microcontroller). The entire feedback and control system (driver/filter/amplifier circuit and microcontroller), are all powered by a single 9 V battery contained with the microcontroller in an enclosure on the lower interface over the sacrum.

Finally, position feedback is provided from each actuator to the microcontroller by an internal potentiometer which outputs an analog voltage that varies linearly between 0-5 V, depending on the length the actuator is extended relative to its full stroke length (100 mm).

Electronic Components – Actuation. The four linear actuators have their speed and direction controlled by a pair of motor driver circuits (TB6612FNG; Toshiba Corp., Tokyo, JPN) re-packaged on secondary circuit boards for through-hole wiring (ROB-09457; SparkFun Electronics, Boulder, CO, USA). One motor driver unit is situated over each hip on the lower interface at approximately the midpoint between the front and back actuators on each side of the orthosis. The motor drivers and actuators are powered by a single battery pack (4 x AA-type) attached adjacent to the anterior left actuator.

Electronic Components – Microcontroller. The control system for the prototype orthosis is built around a single microcontroller (Arduino™ Nano v3; Gravitech, Claremont, CA, USA). The feedback signals are read in through six analog input channels, and control signals are sent out through twelve digital input/output channels. Each actuator is controlled by a set of three digital channels: two for direction, and one for the speed (varied using pulse-width-modulation). For

validation purposes, the microcontroller was set to induce flexion in the orthosis (i.e., the anterior actuators retract, while the posterior actuators extend) when the sensor signals exceeded a maximum threshold. If the sensor signals remained within a set "window" of permissible values or the actuators reached maximum extension/retraction, the orthosis would be held at the current level of flexion. If the sensor signals ever dropped below a minimum threshold, the microcontroller would induce extension in the orthosis (i.e., the anterior actuators extend, while the posterior actuators retract) until the orthosis reached its default erect posture (all actuators held at equal length).

4.2.2 Validation - Data Acquisition

Setup 1 - SEMG. After removing all upper body garments, the subject was fitted with 4 pairs of bipolar (2 cm spacing) SEMG electrodes (N00-S-25, Ambu®, Ballerup, DNK) over the muscles of the lower back and hips (Figure 4.3). The electrodes were attached bilaterally *ad modum* Chapter 2.2.3 at the L3 level, approximately 1 cm (the "medial" group) and 5 cm (the "lateral" group) from the midline. The subject was then fitted with a shirt made from a section of tubular stockinette (tg® Tubular, Lohmann & Rauscher, Inc., Topeka, KS, USA), which was worn for the duration of the testing. Each electrode pair was then connected to one of four differential-input amplifiers (MyoSystem 2000; Noraxon, Inc., Scottsdale, AZ, USA) and then sampled at 2 kHz via a 16-bit DAQCard-6024E (National Instruments, Inc., Austin, TX, USA) analog-to-digital converter board and notebook PC running LabVIEW™ (version 9.0, National Instruments, Inc., Austin, TX, USA).

Calibration 1 - Isometric maximum voluntary contraction (MVC). To measure this, the subject stood erect in front of a wall-mounted padded stand against which he placed his anterior iliac spine. A lightly padded seatbelt strap was then passed around the subject just under the armpits. The subject then extended his back against the strap, building to a maximum effort over 3-5 seconds and holding it for 5 seconds while the SEMG data were recorded. The strap and padded stand constrained the thorax and pelvis (respectively) of the subject, thus forcing him to maintain a nearly erect posture during the test.

Calibration 2 - Baseline. This was a measurement of baseline muscle activity with the subject relaxing all the muscle groups as much as possible while he lay in a supine posture on a mattress for approximately 1 minute taking slow, deep breaths. EMG data were recorded at the end of this period for 5 seconds.

Setup 2 - Posture Monitoring. The subject was fitted with two optoelectronic markers: one mounted to the end of a thin wooden strut secured at its base with adhesive tape at the level of T1, and one attached to a Velcro™ strap at approximately the L5/S1 (Figure 4.3, left). Two more markers were affixed to a vertical reference structure near the subject. The markers were tracked at 100 Hz using a three-camera, optical-measurement system (Optotrak® 3020, Northern Digital Inc., Waterloo, ONT, CAN). Both the markers and camera unit were controlled by a desktop PC running NDI ToolBenchTM (version 3.00.39, Northern Digital Inc., Waterloo, ONT, Canada). A real-time numerical readout from the software reported the absolute angle between the lines connecting the fixed and torso pairs of markers on a computer monitor fixed approximately 1 m off of the floor in front of the subject. These angle measurements were not recorded but only used as a visual aid for assisting test subject in reaching and maintaining the proper torso flexion angle for the test duration. At each test posture, the subject stood with arms relaxed and hanging vertically, and data were recorded for 5 seconds.

Test Battery 1 - Normal. The subject initially assumed a normal erect (neutral, 0° flexion) posture. Data were recorded for three, consecutive 5 second intervals as the subject held the posture. Next the subject assumed and maintained 5° of flexion in the sagittal plane, and data were again recorded for three, consecutive 5 second intervals as the subject held the posture. Finally, the subject assumed and maintained 10° of flexion in the sagittal plane, and data were again recorded for three, consecutive 5 second intervals as the subject held the posture.

Test Battery 2 - Lead Vest. The subject was assisted in donning the vest portion of a typical lead (mass: 3.70 +/- 0.05 kg; LB 16 Rev. D, BMS, Newport News, VA, USA). The subject then again assumed and maintained postures of 0° (neutral), 5°, and 10° flexion, with data being recorded for three, consecutive 5 second intervals at each posture.

Test Battery 3 - Prototype Orthosis. The subject was assisted in removing the lead vest and in donning the prototype orthosis. After the prototype orthosis was activated and its functionality verified, the subject again assumed and maintained postures of 0° (neutral), 5°, and 10° flexion, with data being recorded for three, consecutive 5 second intervals at each posture.

Test Battery 4 - Prototype Orthosis & Lead Vest. The subject was again assisted in donning the lead vest, this time over the prototype orthosis. After the functionality of the prototype orthosis was verified once more, the subject again assumed and maintained postures

of 0° (neutral), 5°, and 10° flexion, with data being recorded for three, consecutive 5 second intervals at each posture.

4.2.3 Validation - Data Analysis

All data post-processed *ad modum* Chapter 2.2.4 using MATLAB® (version 7.0.0.19920 with Signal Processing Toolbox installed, The Mathworks, Inc., Natick, MA, USA) with some changes: only the single baseline test was used for this study, the mean root-mean-square (RMS) value of each channel was used for the isometric MVC calibration data, and only the single root mean square RMS values for each channel in each test were output. Final normalization to %MVC and averaging of corresponding left/right channels was performed using Excel (version 2007, Microsoft Corp., Redmond, WA, USA). As there was only the single test subject for the validation, only the mean %MVC value and standard deviation were calculated for each test configuration and posture.

4.3 RESULTS

The mean %MVC data (and standard deviations) for the lateral and medial muscle groups are shown in Figures 4 and 5, respectively. No data were dropped from the analysis. Despite the differences in mean %MVC visible in the graphs, when the standard deviations are taken into account, the primary hypothesis (the prototype orthosis will significantly reduce lumbar postural muscle activity) must be rejected. The term “significant” here does not imply the statistical meaning. Here, it means outside the bounds of standard error; for a single subject (n = 1), standard error is the standard deviation.

Looking only at the mean values, several key features and trends can be noted. The maximum %MVC values for both muscle groups occur when the prototype orthosis and lead vest were worn: 36.6 %MVC for the lateral group (neutral posture) and 35.1 %MVC for the medial group (10° flexion). The minimum %MVC values for both muscle groups occur when only the prototype orthosis is worn: 20.3 %MVC for the lateral group (10° flexion) and 3.0 %MVC for the medial group (5° flexion). The maximum and minimum standard deviations both occur in the medial group when the prototype orthosis and lead vest are worn: 13.9 %MVC at 5° flexion and 0.04 %MVC at 10° flexion, respectively. The maximum and minimum differences in activity levels between two postures in the same test configuration both occur between 0° (neutral) and 5°

flexion when only the prototype orthosis is worn: - 28.7 %MVC in the medial group, and +0.9 %MVC in the lateral group.

4.4 DISCUSSION

This is the first description of an active, reconfigurable spinal orthosis which monitors and reacts to the applied normal contact stress (and thus the resulting applied moments) on the wearer. Despite the limited scope of the validation test, the results suggest that the prototype orthosis could produce a reduction in postural muscle effort when compared to normal loading (no external load on the trunk) or that produced by a weighted garment. The details of the validation test results and the limitations of the testing warrant further discussion, however.

There are two primary visible trends in the %MVC results for each muscle group with flexion: a general decrease in muscle activity levels with flexion for the lateral group (Figure 4.4), and a decrease from neutral to 5° flexion followed by an increase from 5° to 10° flexion. These trends contrast with what might be expected: a positive trend with flexion for both groups. The observed results might be explained by the combination of the electrode placement and postures adopted during the test. The lateral group of electrodes primarily captured parts of the erector spinae, as well as the quadratus lumborum and (possibly) portions of the rectus abdominus, while the medial group primarily captured the erector spinae (sacrospinalis, spinalis dorsi, longissimus dorsi) and multifidii, the primary extensor muscles. The lower value of observed %MVC for most of the test conditions at 5° flexion in the medial group suggests that the so-called “neutral” posture of the validation test might have actually been slight hyperextension. The actual neutral posture most likely occurred somewhere in between the “neutral” test posture and 10° flexion; the exact point cannot be determined from only the three postures used in the test. The lateral group trend may be a result of the slight hyperextension at the “neutral” posture: the rectus abdominus and other anterior trunk muscles may have been contracting in order to maintain spinal stability and counter the hyperextension of the extensor muscles, and their contraction would lessen/stop as the extensor muscles took over all load-bearing in flexion.

While the mean activity levels suggest possible trends, the large standard deviations observed (especially for the tests where the prototype orthosis and lead vest were worn) do not allow any definitive conclusions to be made about the magnitudes of any differences in muscle activity observed, even for the single test subject; in fact, the magnitudes of the standard

deviations observed in the orthosis & lead test make all of that data highly questionable. Variability is to be expected with the use of SEMG (see Chapter 2.4), and the large variation observed here could be a product of many factors, including slight impingement/displacement of electrodes between tests (especially when donning the test orthosis and lead vest), skin conductivity changes, and even the onset of fatigue (despite the short testing duration).

Aside from the lack of an accurate neutral posture and large standard deviations, there are several other key limitations to this study. First, the limited number of postures doesn't show enough data to find true %MVC vs. flexion angle trends; a larger number of postures (or synching the SEMG and postural tracking data in real-time) would allow not only the location of a true neutral posture, but also allow comments to be made about how the orthosis not only affected the magnitude of postural muscle effort, but also the shape of any trend it produced in the data. Second, to reduce the standard deviation (or standard error), more subjects and/or more tests at each posture need to be recorded; the prototype described here is best fit to the test subject used in the preliminary validation test, so increasing the number of tests at each posture would be simpler to analyze than the addition of multiple test subjects (where factors of fit and anthropometry would have to be separated out). Third, the normal contact stress (or pressure) "window" used with the orthosis to initiate motion or hold at a level of flexion should be varied to find which values best balance comfort/safety with corrective moment magnitude; this variation could include holding the thresholds static over the entire ROM (as in this study), or having them vary with degree of flexion. Fourth, different motion "behaviors" should be tested, i.e. varying the limits of the ROM as well as the velocities of the anterior/posterior linear actuators (which could allow adjustment of the center of rotation). Finally, the measurement of normal contact stress alone does not give a complete picture of the state of mechanical loading of the skin in contact with the orthosis. In particular, shear stress was not measurable with the current piezoresistive sensors. This would mean that the measurement of contact stress in this dissertation systematically is underestimated because it lacks the two orthogonal shear stress components. These would be important to monitor because they are known to be primary risk factors for abrasions and burns, and secondary risk factors for pressure ulcers (Sanders, Goldstein, & Leotta, 1995).

4.4.1 Conclusions

While the active spinal orthosis presented here was initially developed for a very specific section of the workforce (interventionalists), the underlying technology could allow the creation of devices which could benefit anyone who performs an occupation with frequent bending and lifting by offloading the spinal column and reducing the muscle effort required to assume and maintain non-neutral postures (i.e., flexion, extension, and lateral bending). By producing spinal and muscular offloading, such devices could potentially reduce the incidence of lower back fatigue, pain, and injury, thus reducing the cost associated with lost productivity and medical care.

4.5 REFERENCES

Bernardoni, G. P., & Gavin, T. M. (2006). Comparison between custom and noncustom spinal orthoses. *Physical Medicine and Rehabilitation Clinics of North America*, 17, 73-89. doi:10.1016/j.pmr.2005.10.005

Bogue, R. (2009). Exoskeletons and robotic prosthetics: a review of recent developments. *Industrial Robot: An International Journal*, 36(5), 421-427. doi:10.1108/01439910910980141

Bussel, M., Merritt, J., & Fenwick, L. (1995). Spinal Orthoses. In J. B. Redford, J. V. Basmajian, & P. Trautman (Eds.), *Orthotics: Clinical Practice and Rehabilitation Technology* (pp. 71-101). Philadelphia, PA: Churchill Livingstone.

Cholewicki, J., Reeves, N. P., Everding, V. Q., & Morrisette, D. C. (2007). Lumbosacral orthoses reduce trunk muscle activity in a postural control task. *Journal of Biomechanics*, 40, 1731-1736. doi:10.1016/j.jbiomech.2006.08.005

Edelstein, J. E. (1996). Orthoses for Spinal Pain. In B. Goldberg & J. D. Hsu (Eds.), *Atlas of Orthoses and Assistive Devices* (3rd ed., pp. 243-250). St. Louis, MO: Mosby.

Flanagan, P., Gavin, T. M., Gavin, D. Q., & Patwardhan, A. G. (2000). Spinal Orthoses. In M. Lusardi & C. Nielsen (Eds.), *Orthotics and Prosthetics in Rehabilitation* (pp. 231-252). Woburn, MA: Butterworth-Heinemann Medical.

Gilbertson, L., Goel, V. K., Patwardhan, A. G., Havey, R., Morris, T., & Gavin, T. (1991). The Biomechanical Function of “Three-Point” Hyperextension Orthoses. *The American Society of Mechanical Engineers, Bioengineering Division (Publication)*, 20, 269-271.

Kazerooni, H., & Steger, R. (2006). The Berkeley Lower Extremity Exoskeleton. *Journal of Dynamic Systems, Measurement, and Control - Transactions of the ASME*, 128(1), 14-25. doi:10.1115/1.2168164

Lantz, S. A., & Schultz A. B. (1986). Lumbar spine orthosis wearing. I. Restriction of gross body motions. *Spine*, 11(8), 834-837.

Lantz, S. A., & Schultz A. B. (1986). Lumbar spine orthosis wearing. II. Effect on trunk muscle myoelectric activity. *Spine*, 11(8), 838-842.

Örtengren, R., Andersson, G., & Nachemson, A. (1981). Studies of relationships between lumbar disc pressure, myoelectric back muscle activity, and intra-abdominal (intragastric) pressure. *Spine*, 6(1), 98-103.

Sanders, J. E., Goldstein, B. S., Leotta, D. F. (1995). Skin response to mechanical stress: adaptation rather than breakdown – a review of the literature. *Journal of Rehabilitation Research and Development*, 32(3), 214.

Wassell, J. T., Gardner, L. I., Landsittel, D. P., Johnston, J. J., & Johnston, J. M. (2000). A prospective study of back belts for prevention of back pain and injury. *The Journal of the American Medical Association*, 284(21), 2727-2732.

Wilke, H., Neef, P., Caimi, M., Hoogland, T., & Claes, L. (1999). New *in vivo* measurements of pressures in the intervertebral disc in daily life. *Spine*, 24(8), 755-762.

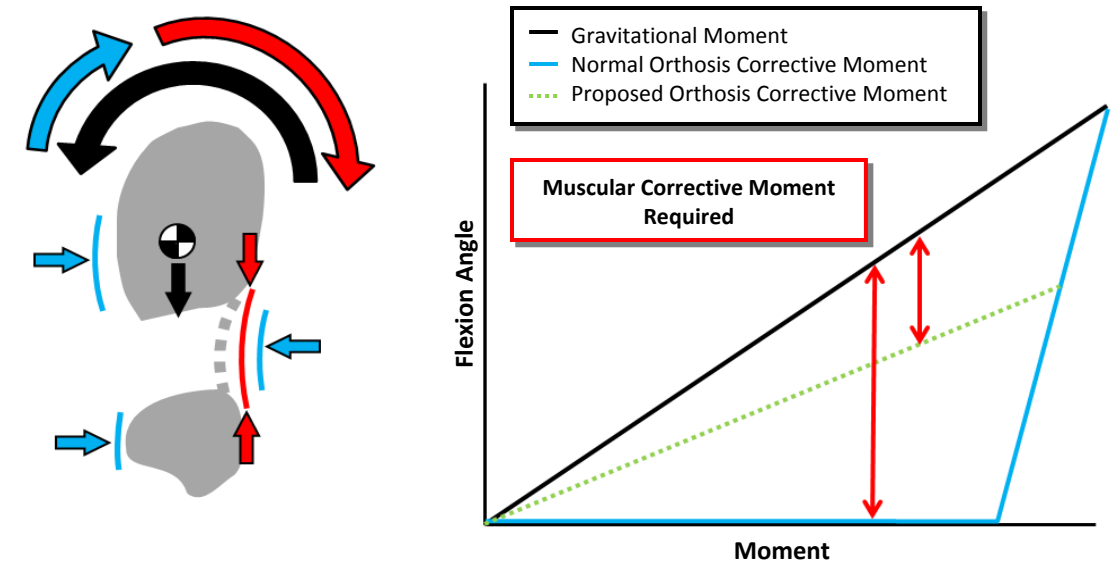

Figure 4.1: Underlying biomechanical function of the proposed active thoracopelvic orthosis. [Left] Free-body diagram of forces acting on the trunk. Black = gravitational forces/moments, Red = postural muscle forces/moments, Blue = orthosis forces/moments. [Right] Graphical depiction of typical moment vs. flexion angle relationships for a body-orthosis system. The gravitational moment must be exactly counterbalanced by the corrective moments produced by the postural muscles and an orthosis (if present). The proposed orthosis would require a smaller muscular corrective moment, and thus less muscle effort.

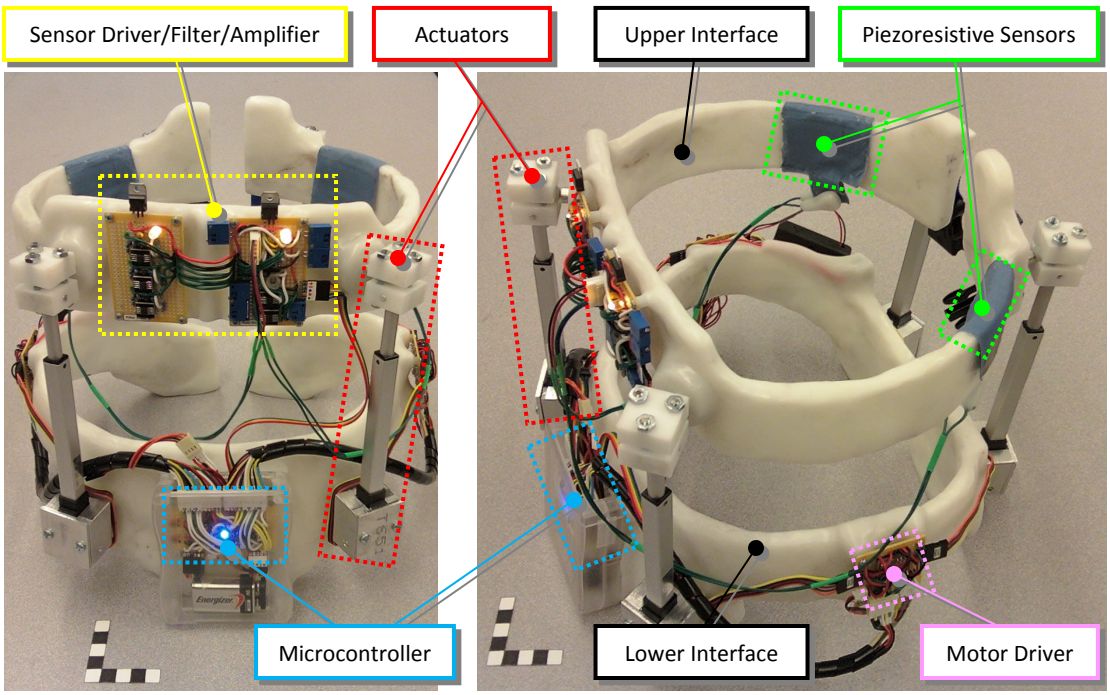

Figure 4.2: The prototype active thoracopelvic orthosis, posterior [Left] and isometric [Right] views, with major components labeled. The scale shown is demarcated in cm.

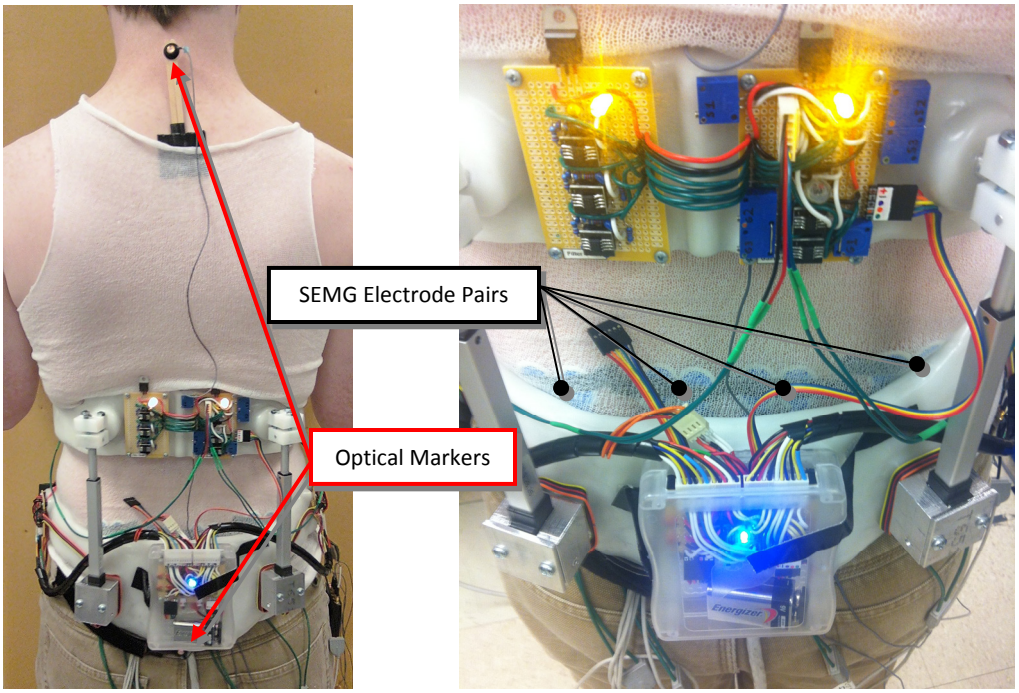

Figure 4.3: [Left] Optical marker, prototype orthosis, and SEMG electrode placement during validation testing. [Right] Detail of SEMG electrode and prototype orthosis placement.

Figure 4.4: Mean (bars denote std. deviation) of %MVC for all test configurations, lateral muscle group.

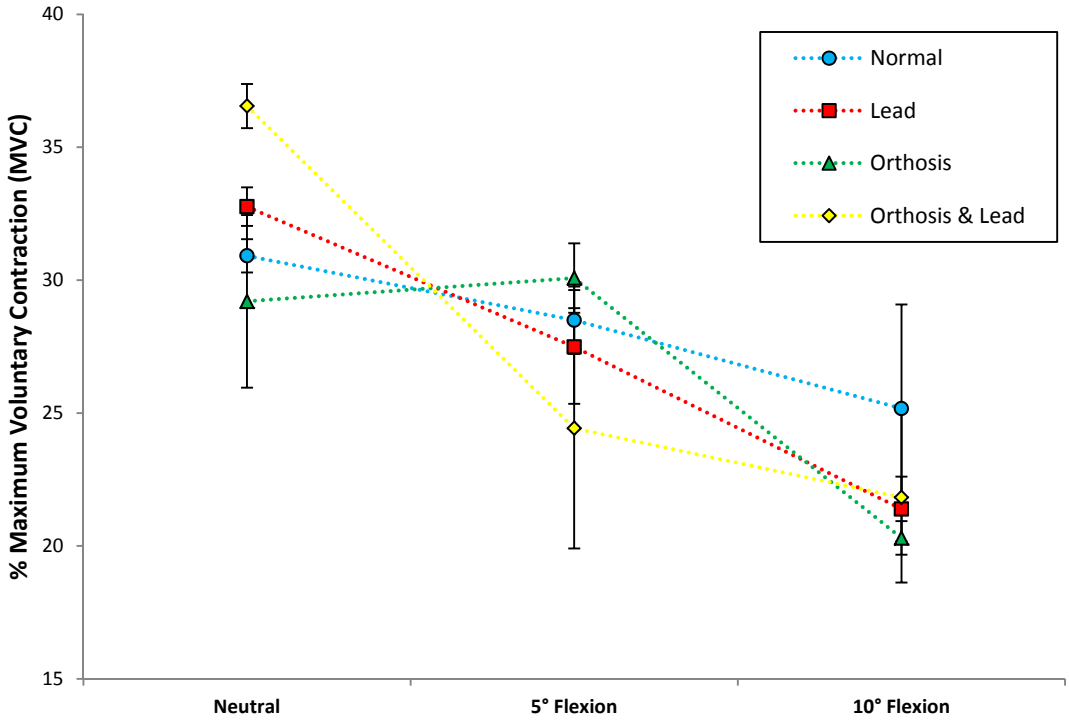

Figure 4.5: Mean (bars denote std. deviation) of %MVC for all test configurations, medial muscle group.

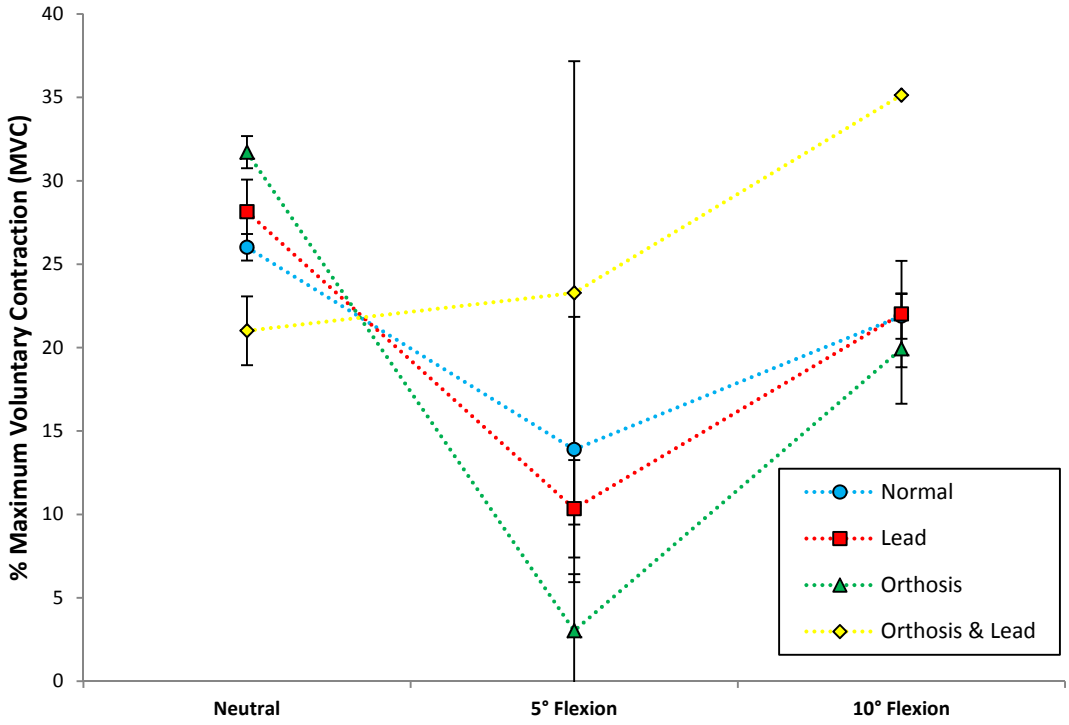

Chapter 5

General Discussion

The overall goal of the work described in the previous chapters of this thesis was to first gain a better understanding of the causes of lower back pain, fatigue, and potential injury in interventionalists, as well as investigate one potential means of reducing the likelihood of developing those conditions via offloading of the lumbar spine and postural muscles through the application of a corrective moment produced by distraction forces. First, some of the most likely factors influencing the amount of muscle effort were investigated (Chapter 2). Next, the relative magnitudes of (and factors influencing) the normal stress distributions arising from the imposition of various external distraction forces and moments on the skin of the lower thorax (where any applied postural support forces may first contact the body) were described (Chapter 3). Finally, the design and preliminary validation of a novel thoracopelvic orthosis which could produce controlled corrective moments over a range of motion was described, a device which could represent one possible means of reducing the muscle effort and compressive forces in the lower back of interventionalists (Chapter 4). This chapter describes some of the primary conclusions which can be made from each of the previous chapters and how they collectively relate to the overall goal of this thesis.

5.1 PER-CHAPTER REVIEW

Chapter 2. The work of Chapter 2 showed that while use of lead vests in the operating room is anecdotally blamed for the incidence of back pain/injury among interventionalists and does eventually induce fatigue in the neck and shoulders (Aarås, 1994), it does not significantly affect the effort required of the postural muscles of the lower back (at least in acute loading). Rather, posture proved to be the most influential factor. The observed changes in muscle effort with posture were expected and agree with the literature (Andersson, Örtengren, & Herberts, 1977; Schultz, Haderspeck-Grib, Sinkora, & Warwick, 1985; Andersson, Oddsson, Grundström, Nilsson, & Thorstensson, 1996). Prolonged loading could not be fully analyzed, but even the

acute loading results suggest that any potential means to reduce the effort required of the postural muscles of the lower back (erector spinae and multifidi, esp.) must focus on applying some form of corrective support in a flexed posture. Previous support devices which functioned solely by offloading the mass of the lead (Pelz, 2000) do not address the primary cause of postural muscle effort, and while more effective designs have been developed, they tend to still intrude into the operating space and restrict the mobility of the physician (Albayrak et al., 2007). A support device which could be worn under the surgical gown (such as an orthosis) is thus an attractive alternative.

Chapter 3. The exploratory study of Chapter 3 described the normal contact stress (i.e., pressure) distribution developed between the interior surface of a "test orthosis" and the skin of the lower thorax when various external distraction forces and moments were imposed on the orthosis; even at the lowest imposed external distraction force (approximately 44 N), the minimum observed contact stress was 8.2 kPa, which exceeds the average contact stress of 4.27 kPa (32 mmHg) required to occlude epidermal capillaries, resulting in ischemia (Remaley & Jaeblon, 2010; Leigh & Bennett, 1994). Contact stress levels above this threshold can be tolerated for some time, but eventual skin and deep tissue damage will develop which may not be reversible (Husain, 1953). Any device which thus applies sustained support to the trunk, which is ultimately conveyed to the trunk through contact stress developed at the skin/support interface, must continually redistribute/readjust itself to ensure no single area remains loaded for prolonged periods. Of course, if the contact stress is simple removed, the beneficial support effect also vanishes.

Chapter 4. The design and validation of a prototype orthosis was described in Chapter 4, a device which is novel for its ability to monitor and react to the contact stress developed between itself and the thorax of its wearer, thus being able to create a regulated applied corrective moment to the trunk over a range of motion. A reduction in mean muscle effort (as measured by the same SEMG technique as in Chapter 2) was observed for slight flexion while wearing only the prototype orthosis, but mean muscle activity increased when a lead vest was worn in conjunction with the device. Large bounds of standard error were also observed for the three trials conducted at each test point, and the overlap between test configurations makes the results inconclusive. Thus, in order to make any definitive claims about the efficacy of the prototype orthosis, a more extensive validation test protocol needs to be conducted.

5.2 LIMITATIONS

Of course, there were several limitations to each portion of the work described in this thesis, some of which encompass the work of more than one chapter; a discussion of the limitations specific to the design of the prototype is included in the next chapter (Chapter 6). First, all three studies made all observations in acute loading conditions only; the effect of time (and results such as muscle fatigue) could not be parsed from the these data. Second, statistical power could be improved for all three experiments. For the first experiment (Chapter 2), a priori power analysis indicated that at least 22 subjects would be required for sufficient statistical power. A similar number of test subjects were recruited for the second experiment (Chapter 3), however large magnitudes of standard error were observed, making the results from some sensors questionable. The third experiment (the validation test of Chapter 4) included a very limited number of trials at each point, which contributed to the large magnitudes of the observed standard deviations at each point. Third, the use of SEMG, while convenient and noninvasive, is easily influenced by factors including ambient electrical "noise", cross-talk, and conductivity variations of the electrode-skin contact sites (Tassinary & Cacioppo, 2000). Fourth, the placement of SEMG electrodes used in Chapters 2 and 4 also may not adequately capture enough postural muscle activity due to misalignment with some muscle fiber orientation. As discussed in Chapter 2, the most superficial layer of the erector spinae is inclined approximately 10° from the vertical (the sagittal plane), the next deepest layer is inclined approximately 20°, and the multifidi have the opposite inclination (Sobotta, 1974). Ideally, SEMG electrodes are aligned parallel to muscle fiber orientation; the orientation used was a compromise to allow adequate spacing between adjacent electrode pairs. Fifth, the force-sensitive resistor (FSR) sensors used in the test and prototype orthoses (Chapters 3 and 4, respectively) have the same limitations as any sensor of that type, including hysteresis and drift with use (Hall, Desmoulin, & Milner, 2008). The limitations of FSRs only exacerbated the variation in each measurement observed in the second experiment (Chapter 3).

5.3 OVERALL ANALYSIS

The work described in this thesis initially began as an effort to understand and address the needs of interventionalists for some means to reduce the likelihood of back fatigue, pain, and potential injury from the conditions they experience in the operating room. The largest contributor to lower back postural muscle effort (and thus also spinal compressive forces) was

the adoption and maintenance of a flexed posture. In order to allow maximum range of motion and accessible workspace volume (without increasing sterilization requirements), an orthotic support meant to be worn under the surgical gown was selected as the most attractive potential solution. Any device for supporting the trunk, including an orthosis, produces corrective/support forces through contact stress on the skin. Unfortunately, even small external forces applied to the trunk produce potentially damaging contact stress on the skin, thus requiring the support be periodically removed or redistributed. If a support device were to apply corrective forces/moments over an entire range of motion, it would have to carefully monitor and adjust the contact stresses it produced in order to balance biomechanical efficacy with risk of injury. The final result of the initial two experiments was a functional prototype orthosis which could produce a corrective moment over a range of motion, which it accomplished by monitoring of the contact stress distribution it developed with its wearer and adjusting its electromechanical structure to best maintain that contact stress distribution (and resulting applied moment) within set limits. While the preliminary validation test was not definitive, a beneficial result was suggested.

The Exoskeletal Spinal Support (ESS) is thus at a relatively early stage of development, but shows promise as a potential means to alleviate some of the spinal and muscular loading experienced by interventionalists in the operating room. Perhaps more importantly, the core concept and technology created in its design (i.e., active orthotics) has a much larger potential impact than with interventionalists alone. The ESS could supplement orthotic treatment in a clinical setting as well as the workplace. An active spinal orthosis could initially be programmed to fully immobilize the patient, but gradually reintroduce motion and decrease applied support over the course of treatment, until near-normal mobility is restored. This would help to wean the patient from the orthosis in a systematic manner and perhaps shorten the duration of any remaining physical therapy. The onboard control system could allow a clinician to remotely monitor and adjust the treatment regimen, thus reducing the time required from patient and clinician by repeated visits. Modifications that could be programmed into the microcontroller include altering the perceived flexural stiffness and damping of the orthosis, something which is impossible with current designs. The reconfigurable and modular nature of the structure could allow a wider variety of patients to be treated with a single design for the orthosis, thus reducing the time, labor, and cost involved with the custom manufacture of one or more orthoses for each patient (current practice). It would also allow an orthotist to change the size

of one or both interfaces if a patient's obesity changes over the course of treatment. This would obviate the need for new custom orthoses and their associated costs. In summation, by making orthotic treatment of the spine "smart", both the cost and quality of this type of care could benefit immensely.

5.4 REFERENCES

Aarås, A. (1994). Relationship between trapezius load and the incidence of musculoskeletal illness in the neck and shoulder. *The International Journal of Industrial Ergonomics*, 14 (4), 341-348.

Albayrak, A., van Veelan, M. A., Prins, J. F., Snijders, C. J., de Ridder, H., & Kazemier, G. (2007). A newly designed ergonomic body support for surgeons. *Surgical Endoscopy*, 21, 1835-1840. doi:10.1007/s00464-007-9249-1

Andersson, E. A., Oddsson, L. I. E., Grundström, H., Nilsson, J. & Thorstensson, A. (1996). EMG activities of the quadratus lumborum and erector spinae muscles during flexion-relaxation and other motor tasks. *Clinical Biomechanics*, 11(7), 392-400.

Andersson, G.B., Örtengren, R. & Herberts, P. (1977). Quantitative electromyographic studies of back muscle activity related to posture and loading. *Orthopedic Clinics of North America*, 8(1), 85-96.

Hall, R. S., Desmoulin, G. T., & Milner, T. E. (2008). A technique for conditioning and calibrating force-sensing resistors for repeatable and reliable measurement of compressive force. *Journal of Biomechanics*, 41(16), 3492-3495. doi:10.1016/j.jbiomech.2008.09.031

Husain, T. (1953). An experimental study of some pressure effects on tissues, with reference to the bed-sore problem. *Journal of Pathology and Bacteriology*, 66, 347-363.

Leigh, I. H., & Bennett, G. (1994). Pressure ulcers: prevalence, etiology, and treatment modalities. A review. *The American Journal of Surgery*, 167(1A), 25S-30S.

Pelz, D. M. (2000). Low back pain, lead aprons, and the angiographer [letter]. *American Journal of Neuroradiology*, 21(7), 1364.

Remaley, D., & Jaeblon, T. (2010). Pressure ulcers in orthopaedics. *Journal of the American Academy of Orthopaedic Surgeons*, 18, 568-575.

Sobotta, J. (1974). *Atlas of Human Anatomy* (Vol. 1). F. H. J. Figge, (Ed.). New York, NY: Hafner Press.

Tassinary, L. G. & Cacioppo, J. T. (2000). The skeletomuscular system: surface electromyography. In J. T. Cacioppo, L. G. Tassinary and G. G. Berntson (Eds.), *Handbook of psychophysiology* (2nd ed.) (pp. 163-199). New York: Cambridge University Press.

Chapter 6

General Conclusions

1. The use of a weighted garment on the upper body (i.e., the vest portion of a protective "lead") in acute loading does not significantly affect the activity levels of muscular activity produced in the muscle groups of the lower back and shoulders studied in the population of healthy young subjects; the results of prolonged loading (i.e., the effect of time) could not be conclusively analyzed.
2. Among the factors studied as contributors to muscle activity levels observed in the lower back and shoulders (lead vest use, posture, gender) under acute lading, posture was the largest contributor to increases in muscle activity in a flexed posture.
3. Interventionalists should avoid sustained flexed postures in the operating room in order to most-effectively reduce lower back muscle effort (and its muscular contribution to spinal compressive loading) and thus decrease the likelihood of back fatigue, pain, and injury in this population.
4. When external distraction forces and moments are imposed on the lower thorax via an orthosis, the resulting normal contact stress (or "pressure") distribution developed at the skin-orthosis interface increases in proportion to the external force/moment (normalized across multiple subjects) and exceeded dermal capillary internal pressure at every loading configuration tested.
5. Apart from external loading conditions, respiration phase (full inhalation vs. full exhalation) was also found to significantly affect the observed normal contact stress magnitudes; the magnitude of this effect decreased with external loading (both distraction force and moment) but remained significant.
6. The novel prototype thoracopelvic orthosis described in this thesis (Chapter 6) produced a reduction in observed activity levels in the postural muscles of the lower back in slight flexion when worn by the single test subject; when worn in conjunction with a lead vest, however, muscle activity levels were greater than when the lead vest was worn by itself.

7. While mean muscle activity levels suggest a possible beneficial trend for one loading configuration (i.e., the prototype orthosis worn by itself), the large variation in the observed readings does not allow definitive conclusions to be made as to the efficacy of the prototype orthosis in reducing the muscle activity levels of the muscles of the lower back in a variety of postures; more trials at each test configuration and/or more test subjects are needed.

Chapter 7

Future Work

7.1 INTRODUCTION

The prototype orthosis described in Chapter 4 (a.k.a. the Exoskeletal Spinal Support, or ESS) is still at a very early stage of development. Several design changes will have to be made in order for the ESS to be considered robust enough for preliminary clinical trials, let alone release as a final product. The device most likely has two main markets: a prophylactic aid in the workplace (where frequent bending and lifting is required), and a therapeutic rehabilitation device for use in a clinical setting (such as in recovery from lumbar spine fracture or surgical intervention). These two different markets would necessitate two divergent development processes, culminating in two very different versions of the orthosis. A workplace version would most likely have to be relatively low in cost to be widely adopted, as well as being light and agile to try to mimic normal spinal maneuverability as closely as possible. A clinical version, by contrast, would have to be extremely robust and maximally effective in order to be adopted, but could be more costly and (potentially) require less maneuverability (since the wearers would actually require constrained spinal maneuverability).

If the ESS is ever to exist as a final product in one or both of the proposed versions, it must first be redesigned to be a more effective research platform. Both markets would require more extensive validation testing in order to accept the device. Thus, even before one or both markets are addressed, both a new prototype version of the ESS and a protocol to validate it must be designed. This chapter describes some of the most urgent design changes that would be required in any “test” version of the ESS, as well as a tentative protocol for a pilot clinical study. It is hoped that the development of the ESS will continue at least through a thorough validation test to accurately determine its efficacy. If that first step can be completed, the ESS may yet become a mature device that could spawn a whole new generation of orthotics.

7.2 DEVICE DESIGN

Any future version of the ESS which would be used for final validation testing would require extensive design changes in order to improve three core design attributes: performance, robustness, and (to a lesser extent) versatility. Performance entails basic functional capabilities such as actuation (range of motion, moment/force magnitude, speed) control (sensor accuracy, control system behavior), energy efficiency and capacity, and (for unsupervised use outside of a laboratory environment) communications. Robustness entails the ability to survive prolonged regular use as well as occasional extremes (of loading, fault, etc). Versatility is one of the key design goals of a final version of the ESS, but a prototype version would benefit as well; here it means the ability to fit a wide variety of test subjects comfortably without custom fabrication or adjustment, which would drastically reduce material costs of validation testing. The prototype ESS described in Chapter 4 used primarily off-the-shelf components, and many of the design changes suggested here focus on creating components specifically-tailored for use in the ESS. The following is by no means an exhaustive list, but should address some of the key design elements requiring improvement.

7.2.1 Performance

Actuation. Linear actuators were chosen for use in the prototype ESS due to their many beneficial characteristics when compared to alternative candidate actuation technologies such as pneumatics or hydraulics, such as not requiring a pressurized working fluid (which would entail incorporation of a bulky and potentially hazardous fluid handling system) and the ability to hold position even when unpowered (a result of the internal screw mechanism at the heart of the unit). The specific Firgelli actuators (L-12 series) chosen for the prototype provided useful force and displacement levels, as well as low mass and volume requirements, but they suffered in one major area of performance: speed.

The relatively slow speed of the actuators is a result of their high gearing ratio (210:1), a necessity due to the small size of the DC motors at the heart of each actuator. If a new actuator were designed, a lower gear ratio could be chosen and speed would improve, but a larger motor (with larger electrical current requirements to produce correspondingly more torque) would be required. An alternative solution would be to redesign the actuators to incorporate a much faster DC motor. A faster motor might emit more noise and decrease the functional life of the actuator due to increased wear, however. More exotic electromechanical actuation

technologies could be explored (i.e., linear motors), but issues of cost, energy use, and safety would most likely be even more pronounced than with a potential fluidic system. Regardless of what form a redesigned actuation system would take, it would have to move many times faster than the current linear actuators in order to approximate normal trunk motion.

Control. The control system for the prototype ESS (microcontroller, sensors, and motor drivers) was primarily selected for its simplicity and low cost. Even if identical components (integrates circuits and passive components) were used, the overall volume required for the circuitry and corresponding wiring could be greatly reduced by designing all of the control system circuits onto a single printed circuit board using surface-mount components. Using surface mount components makes repair/replacement of components much more difficult than the current through-hole type (and may require the fabrication of a new printed circuit board), but the beneficial size reduction far outweighs this concern.

The open-source piezoresistive sensors which measure normal contact stress (or "pressure") developed between the orthosis and wearer are low cost, simple devices, but they suffer the same limitations as other force-sensitive resistors (FSRs, Chapter 4) which make them unreliable and complicated to use properly. One alternative pressure-monitoring technology is the use of transducers embedded in a gel or fluid bladder, such as the P161 (General Electric Co., Fairfield, CT, USA) used I conjunction with an auto-balancing Wheatstone bridge (Microbridge, Montreal, QC, CAN). The small form factor of these circuits could allow multiple sensing units to be placed throughout any of the areas of the orthosis in sustained contact with the wearer (thorax, iliac crests, sacrum).

If FSRs are selected to be used in the next iteration of the ESS, the circuitry which "drives" them (Chapter 4, Appendix B) should be redesigned to include an offset adjustment stage in conjunction with the adjustable sensitivity and gain. By using an adjustable offset, the "zero" point of the loading range for each sensor could be tuned such that the sensors would only register a signal past certain stress thresholds. This would allow higher resolution measurements to be taken by the microcontroller, making smaller fluctuations in load to be detectable. For instance, the null could be set such that each sensor only registers any contact stress beyond that equivalent to the minimum surface capillary pressure of skin (Chapter 3); any applied stress below that is known to not cause occlusion and eventual ischemia, so it can be disregarded.

As mentioned in Chapter 4, the measurement of normal contact stress alone does not give a complete picture of the state of mechanical loading at the skin-orthosis interface. Measuring both shear and normal contact stress is now possible with recent sensor technologies (for example, Cheng, Lin, Lai, & Yang, 2010); minimizing the magnitudes of both would reduce the likelihood of blisters and abrasions, as well as pressure ulcers. Additional parameters could also be measured with sensors embedded within the ESS in order to gain a better assessment of the likelihood of skin or deep-tissue injury, including temperature, moisture levels (via relative humidity or changes in skin conductivity due to the presence of salts from sweat).

Energy Efficiency & Capacity. The current prototype of the ESS, which is powered by 1 x 9V and 4 x AA batteries, can only maintain function for a few hours, based on typical usage experience in the laboratory. This would have to be dramatically improved if the device were to be worn long term. Recharging/replacing batteries is permissible, but each charge must last long enough that the task doesn't interfere excessively with normal activity. Lithium ion batteries are commonly used in many electronic devices due to their versatility, but they require more complicated regulating circuitry in order to perform consistently and safely (i.e., to prevent bursting from overcharging). The most acceptable solution might be several permanently attached battery units which the wearer must periodically recharge by connecting to a wall outlet (such as when sleeping). Energy efficiency can be partly addressed through circuit design and partly through the behavior of the control system: actuators could be shut off completely during periods of prolonged inactivity, the processor of the microcontroller could only be powered at certain intervals, etc.

Communications. The current prototype of the ESS is used exclusively in a laboratory setting, so reprogramming the microcontroller via a cable connection to a PC is not excessively cumbersome. In order for the device to be used unsupervised for extended periods, however, some degree of wireless communications with the research staff/clinicians would be required. Short range communication (such as in the laboratory) could be handled through technologies such as Bluetooth or X-Bee wireless serial communication. Long range communications would require the use of standard wireless internet (such as 802.11b, which would require an access point with a broadband connection in proximity to the wearer) or cellular protocols. All communications would also have to include some form of password protection and/or encryption to prevent unauthorized access to data or rewriting of the control data. Fortunately,

many of these technologies exist in off-the-shelf units/platforms which could be easily incorporated into the next version of the ESS.

7.2.2 Robustness

One of the most obvious problems with the current prototype of the ESS is its fragility, and this is largely due to the design of the linear actuators and their connections to the interfaces. The Firgelli L-12 actuators have an extruded aluminum shaft enclosing the screw mechanism, but the motor and transmission are only loosely constrained in a thin plastic housing. When subjected to bending moments, the mechanical components of each actuator are prone to moving out of alignment, which can lead to jamming. Also, the position feedback sensor in each actuator (used to keep the actuator within acceptable bounds of its stroke) is built into a thin plastic ribbon, the electrical contacts of which easily separate when subjected to any torque. Currently, the actuators are mounted such that the plastic portion of the outer housing is contained entirely within an aluminum bracket (the attachment points for the actuators on the lower interface). These brackets do not, however, adequately protect the actuators from bending moments. A more robust actuator design should incorporate an all-metal housing, including for the motor, gearing, and position feedback circuitry. If off-the-shelf actuators such as the L-12 units are to be used, new brackets would have to be designed to constrain the actuators more adequately, such as with a metal truss attaching to the aluminum portion of the actuator housing. Reinforcing the actuators thus may increase the bulk of the ESS as a whole, but a more robust design is absolutely critical if the ESS is to be used for any extended period of time.

The piezoresistive sensors of the current prototype are also prone to wear, and must be periodically “re-conditioned” to remain functional, a process which usually entails disassembly, cleaning, replacement of damaged layers, and re-assembly. All FSRs are prone to performance degradation from repeated use, another factor which might make an alternative technology more attractive in future iterations of the ESS. The added cost of the transducer-type system described above would be offset by its potentially longer-life and more stable performance.

7.2.3 Versatility

One key feature of the ESS, which is partially incorporated into the current prototype, is versatility. The current prototype not only incorporates flexible interface pieces which can

conform to various thorax/pelvis geometries, but can also have its default distraction (the separation between thorax and pelvis) adjusted by varying the default position of the linear actuators. In order to be truly versatile and fit a large variety of body types, however, the shapes of the upper and lower interfaces (and where they contact the wearer) must be much more variable. Gripping the wearer around the lowermost ribs may simply not be viable for some wearers (i.e., the obese), so the orthosis may have to contact the wearer at other loading points, such the sternum or subclavicular region (as in so-called "cowhorn" triplanar control orthoses, Chapter 4). Apart from which regions can be loaded, the relative position of the load application sites to one another may have to be adjusted to accommodate varying skeletal morphology and subcutaneous fat distribution. One example means to allow reconfiguration of the interfaces could be through the use of multiple interconnected segments; load application regions (the segments) could be connected through adjustable trusses and hinges, much like the structure of a desk lamp suspends the light socket relative to the weighted base unit.

7.3 VALIDATION TESTING PROTOCOL

In order to obtain more definitive results quantifying the biomechanical effectiveness of the ESS, the initial validation test described in Chapter 4 should be modified and performed again, with several improvements to the protocol. In order to truly remove any effect loading duration might have had over the course of the testing duration, all testing sequences (i.e., the order of postures assumed) should be completely randomized. Also, to prevent the onset of fatigue, the test subject should maintain a relaxed neutral posture when data are not being recorded. The validation test could benefit from more than one subject (*ad modum* Chapter 2), however the standard deviations observed could be reduced in magnitude even with a single test subject by conducting more trials at each test point. The minimum number of trials required for a high statistical power could be assessed using a priori power analysis, but would have to remain below the maximum number of trials which could be reasonably conducted in one testing session. More-invasive implanted electromyography (EMG) electrodes may offer reduced measurement volumes and thus improved parsing of individual muscle activity when compared to the surface type used here (Chapters 2 and 4). Measurement of intervertebral disc pressure, such as that performed by Wilke, Neef, Caimi, Hoogland, and Claes (1999) is too invasive to be practical, and thus must continue to be indirectly assessed by its correlation to EMG activity levels (Örtengren, Andersson, & Nachemson, 1981).

If the ESS is to be developed into a clinically-accepted medical device, a preliminary clinical trial would also have to be conducted; the following example protocol for a parallel randomized trial (shown schematically in Figure 7.1) was submitted as part of an NIH-STTR grant proposal submitted in order to fund such a study. At least six healthy patients (male or female, ages 21 to 40 years, BMI < 30 kg/m2) would be recruited who are scheduled for a lumbar microdiscectomy (single-level) for sciatica. Within one day of the surgery, patients would be randomized to one of three groups , organized by orthotic support given as part of treatment: 1) ESS (the experimental group), 2) over-the-counter (OTC) soft/semi-rigid textile lumbar support (the positive control), or 3) no support (negative control, standard of care). At the Entry and Exit laboratory visits, weekly opiate use (the primary outcome), a McGill Pain Questionnaire, pain on downward reach measured using an visual-analog scale (VAS), downward reach distance (cm), lumbar postural muscle EMG (*ad modum* Chapter 2), and trunk range of motion and postural changes per day, Yale Physical Activity Questionnaire (secondary outcomes) will be measured. Both the ESS and OTC supports would record activity levels, compliance, and postural history for the duration of treatment through embedded low-profile inertial measurement units (IMUs). As mentioned, the amount of opiate use would be the primary measurement compared between each group. It is expected that the ESS group would demonstrate a statistically-significant reduction in opiate use over both controls.

7.4 REFERENCES

Cheng, M., Lin, C., Lai, Y., & Yang, Y. (2010). A polymer-based capacitive sensing array for normal and shear force measurement. *Sensors*, 10(11), 10211–10225. doi:10.3390/s101110211

Örtengren, R., Andersson, G. & Nachemson, A. (1981). Studies of relationships between lumbar disc pressure, myoelectric back muscle activity, and intra-abdominal (intragastric) pressure. *Spine*, 6(1), 98-103.

Schulz, K.F., Altman, D. G., & Moher, D.; for the CONSORT Group. (2010). CONSORT 2010 statement: Updated guidelines for reporting parallel group randomized trials. *Annals of Internal Medicine*, 152 (11), 1-7.

Wilke, H., Neef, P., Caimi, M., Hoogland, T., & Claes, L. (1999). New in vivo measurements of pressures in the intervertebral disc in daily life. *Spine*, 24(8), 755-762.

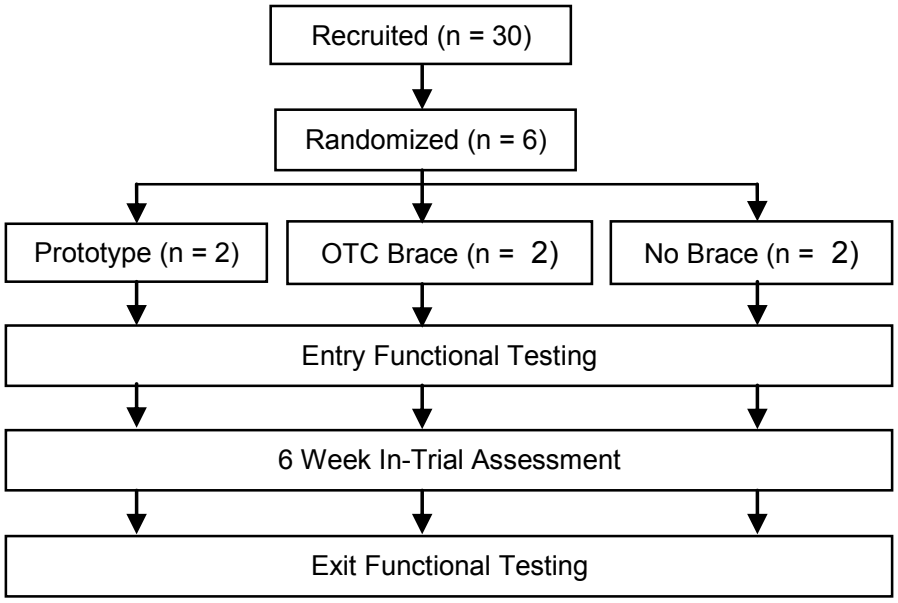

Figure 7.1: Proposed preliminary clinical trial test structure. Adapted from Schulz., Altman, and Moher (2010).

Appendix A

MATLAB Post-Processing Script (Chapter 2)

```
%************************************************************************
%Data Analysis Script for Experiment 1 - Version 7
%By Daniel D. Johnson (with assistance from Anne E. Kirkpatrick)
%Written for MATLAB v7.0.0.19920, with Signal Processing Toolbox
%
%This script runs Experiment 1 data through the following steps, in order:
%(NOTE: Steps 1-5 run for all test data before the script moves to Step 6)
%
%1.) Reads the .txt file for the designated subject & test into an array
%named "Raw_Data", which is reset for each .txt file (i.e. each test).
%2.) Removes any startup transients by removing a set number of
%data points (the "Trim Window", specified in the "Script Inputs" section)
%from the beginning of the raw data (to convert, 2000 data points =
%1 second). This step produces the "Trimmed_Data" array.
%3.) Removes any offset in each channel by finding the mean of the data
%points in that channel and subtracting it from each point, creating the
%"Centered_Data" array.
%4.) Passes the centered data through two Butterworth filters: a bandpass
%filter from 30-1000 Hz, followed by a bandstop filter centered at 60 Hz
%(to remove AC power noise). The order and frequency boundaries of each
```

```
%filter are specified in the "Script Inputs" section. This step produces
%the "Filtered_Data" array.
%5.) Produces a single, representative RMS value for each channel of each
%test. To do this, it first finds the RMS of a small subset of the data
%(an "RMS window") and stores that value in the "Channel_RMS_Values"
%array. It then advances the RMS window (by an increment less than the
%full size of the RMS window) to a new subset of the data and repeats,
%each time appending the calculated RMS value to the Channel_RMS_Values
%array. The size of the RMS window and the increment of advancement are
%both specified in the "Script Inputs" section. Depending on the type of
%test being analyzed, it next finds one of the following in the
%Channel_RMS_Values array: 1) for a "Baseline" test, it finds the minimum
%of the RMS values of the channel, 2) for a "Max Effort" test, it finds
%the maximum of the RMS values of the channel, and 3) for all others, it
%finds the mean of the RMS values of the channel. These single,
%representative RMS values are finally collected into the 9x6 "RMS_Data"
%array.
%6.) Converts the single RMS values (for tests 4-8) to effort values by
%using the following formula:
%                    (Test RMS Value - Min RMS Value)
%   Test Effort # = --------------------------------
%                    (Max RMS Value - Min RMS Value)
%This step produces the 5x6 "Effort_Data" array.
%7.) Averages the left and right channel effort values (removing any side
%bias), which produces the 5x3 "Avg_Effort_Data" array.
%8.) Displays the results in a bar plot for each test, either showing all
```

```
%channels or averaged left & right (1 & 4, 2 & 3, 5 & 6).
%************************************************************************
clear all


%*******************
%***Script Inputs***
%*******************
%---Test Subject Number---
Subject = '01';
%---The Code and Data Folder Paths---
Code_Folder = 'C:\Documents and Settings\Username\My Documents\Matlab Work';
Data_Folder = ['C:\Documents and Settings\Username\My Documents\Matlab
Work\Data\Subject ', Subject];
%---For Step 2: Size of the Trim Window (in # of data points) to be removed---
Trim_Window_Size = 500;
%---For Step 4: Filter 1 (F1) Specifications; Butterworth Bandpass---
F1_Order = 3; %The order of the Butterworth filter
F1_Low = 30; %Lower frequency boundary (Hz)
F1_High = 999.999; %Upper frequency boundary (Hz)
%---For Step 4: Filter 2 (F2) Specifications; Butterworth Bandstop---
F2_Order = 3; %The order of the Butterworth filter
F2_Low = 59.5; %Lower frequency boundary (Hz)
F2_High = 60.5; %Upper frequency boundary (Hz)
%---For Step 5: Moving RMS Window Specifications---
RMS_Window_Size = 100; %Size of the window (in # of data points)
RMS_Window_Increment = 10; %Advancement increment (in # of data points)
```

```
%---For Step 8: Plot mode (1 = All Channels, 2 = Averaged L & R)---
Plot_Mode = 1;
%**************************
%***End of Script Inputs***
%**************************

%Change the current working directory to the one containing the test data
addpath(Code_Folder)
cd(Data_Folder)
%Specify which data file is to be processed (out of 9 total)
%test = test index
for test = 1:9 %<--The start of the "for" loop encompassing Steps 1-5 for all
test data
%--------------------------------------
%---Step 1: Reading In the Raw Data---
%--------------------------------------
       if test == 1
           %Test 1: Start Baseline
           Data_File = [Subject, '-StartBaseline.txt'];
    elseif test == 2
        %Test 2: Max Effort, Back
           Data_File = [Subject, '-MaxEffortBack.txt'];
    elseif test == 3
        %Test 3: Max Effort, Trapezius
           Data_File = [Subject, '-MaxEffortTrap.txt'];
    elseif test == 4
```

```
        %Test 4: No Lead, Erect

           Data_File = [Subject, '-NoLeadErect.txt'];

    elseif test == 5

        %Test 5: No Lead, 25-Degrees Flexion

           Data_File = [Subject, '-NoLeadFlexed.txt'];

    elseif test == 6

        %Test 6: With the Lead Vest, Erect

           Data_File = [Subject, '-LeadErect.txt'];

    elseif test == 7

        %Test 7: With the Lead Vest, 25-Degrees Flexion

           Data_File = [Subject, '-LeadFlexed.txt'];

    elseif test == 8

        %Test 8: With the Lead Vest, 25-Degrees Flexion, Up to 30 Minutes

        Data_File = [Subject, '-30Min.txt'];

    elseif test == 9

        %Test 9: End Baseline

        Data_File = [Subject, '-EndBaseline.txt'];

    end

       %Read in the raw data file

       [Time,Chan1,Chan2,Chan3,Chan4,Chan5,Chan6] = textread(Data_File,'%f %f %f
%f %f %f %f %f');

    %Store the raw data in an array where each column corresponds to an

    %SEMG channel

       Raw_Data = [Chan1,Chan2,Chan3,Chan4,Chan5,Chan6];

%-------------------

%---End of Step 1---
```

```
%-------------------

%----------------------------------------

%---Step 2: Removing Initial Transients---

%----------------------------------------

    %In the Raw_Data array, move to the row after the end of the

    %Trim Window and keep that and all subsequent rows' points, in

    %all columns (i.e. ignore all points within the Trim Window).

    Trimmed_Data = Raw_Data((Trim_Window_Size+1):end,:);

%-------------------

%---End of Step 2---

%-------------------


%--------------------------------------

%---Step 3: Removing Channel Offsets---

%--------------------------------------

    %Initialize an array for the results of this section (the centered data)

    Centered_Data = [];

    %Each channel may have a different offset, so they are processed
individually

    %chan = channel index

    for chan = 1:6

        %For the current channel, subtract the mean of the trimmed data from
the trimmed data

        Centered_Data(:,chan) = Trimmed_Data(:,chan)-
mean(Trimmed_Data(:,chan));

    end
```

```
%-------------------

%---End of Step 3---

%-------------------



%------------------------

%---Step 4: Filtering---

%------------------------

    %Initialize an array for the results of this section (the filtered data)

       Filtered_Data = [];

       %Find the Nyquist frequency (1/2 of the sampling frequency)

       Nyquist_Freq = 0.5*1/Time(2);

       %Create the first filter (Filter 1)

       %Type: Butterworth, bandpass (30-1000 Hz)

    %The order and frequency range are taken from "Script Inputs" section

       %F1_N = Filter 1 numerator, F1_D = Filter 1 denominator

       [F1_N, F1_D] = butter(F1_Order,[F1_Low/Nyquist_Freq
F1_High/Nyquist_Freq],'bandpass');

       %Create the second filter (Filter 2)

       %Type: Butterworth, bandstop (centered at 60 Hz)

       %The order and frequency range are taken from "Script Inputs" section

       %F2_N = Filter 2 numerator, F2_D = Filter 2 denominator

       [F2_N, F2_D] = butter(F2_Order,[F2_Low/Nyquist_Freq
F2_High/Nyquist_Freq],'stop');

       %Apply the filters to the centered data,

    %producing a filtered data array with the same number of points

    %chan = channel index

       for chan = 1:6
```

```
        %Apply Filter 1 to the current channel's points
        Filtered_Data(:,chan) = filter(F1_N,F1_D,Centered_Data(:,chan));
        %Apply Filter 2 to the current channel's points
        Filtered_Data(:,chan) = filter(F2_N,F2_D,Filtered_Data(:,chan));
      end
%-------------------
%---End of Step 4---
%-------------------

%--------------------------------------
%---Step 5: Min/Max/Mean RMS Finding---
%--------------------------------------
      %For each channel, find RMS of the points in each window and then the
    %max/min/mean of those RMS values.
      %chan = channel index, point = point index
      for chan = 1:6
        %Initialize an array to collect the RMS values of each window for the
        %current channel
        Channel_RMS_Values = [];
        %Start at the first data point, iterate by the chosen window size, and
end
        %when the current point is the first in the last possible window
        for point = 1:RMS_Window_Increment:(length(Filtered_Data(:,chan))-
(RMS_Window_Size-1))
            %Create the temporary data window of the specified size
            Current_RMS_Window = Filtered_Data(point:point+(RMS_Window_Size-
1),chan);
```

```
            %Get the RMS value of just the points in the window
            Current_RMS_Value = norm(Current_RMS_Window)/sqrt(RMS_Window_Size);
            %Appending the RMS to the collection of the others
            Channel_RMS_Values = [Channel_RMS_Values;Current_RMS_Value];
        end
        %Finding the representative RMS value for each channel of a test
        %from the collection stored in "Channel_RMS_Values"
        if (test == 1 || test == 9)
            %For the Baseline tests, use the *MINIMUM* RMS found
            RMS_Data(test,chan) = min(Channel_RMS_Values);
        elseif (test == 2 || test == 3)
            %For the Max Effort tests, use the *MAXIMUM* RMS found
            RMS_Data(test,chan) = max(Channel_RMS_Values);
        else
            %For all others, use the *MEAN* RMS found
            RMS_Data(test,chan) = mean(Channel_RMS_Values);
        end
      end
%-------------------
%---End of Step 5---
%-------------------
end %<--The end of the "for" loop encompassing Steps 1-5 for all test data


%-----------------------------------------------------------
%---Step 6: Converting Single RMS Values to Effort Values---
%-----------------------------------------------------------
```

```
%Subtracting out the baseline readings and dividing by amplitude range
%test = test index, chan = channel index
%base = baseline data location, max = max effort data location
for test = 4:8
       %For the 30-Min test, use the End Baseline data
       if test == 8
             base = 9;
    %Otherwise, use the Start Baseline data
       else
             base = 1;
       end
       for chan = 1:6
        %For trapezius channels (5 & 6), use the Max Effort, Trapezius data
        if (chan == 5) | (chan == 6)
            max = 3;
        %Otherwise, for the lateral & medial lumbar channels (1-4), use the
        %Max Effort, Back data
        else
            max = 2;
        end
        %Effort Reading = (RMS - Baseline)/(Max - Baseline)
        Effort_Data(test-3,chan) = ((RMS_Data(test,chan)-
RMS_Data(base,chan))/(RMS_Data(max,chan)-RMS_Data(base,chan)));
   end
end
%Convert the results to percents
```

```
Effort_Data = 100*Effort_Data;

%-------------------

%---End of Step 6---

%-------------------



%--------------------------------------------------

%---Step 7: Averaging Left & Right Effort Values---

%--------------------------------------------------

%row = row index (row 1 = test 4, row 5 = test 8)

for row = 1:5

    %Averaging channels 1 and 4 (lateral lumbar)

    Avg_Effort_Data(row,1) = (Effort_Data(row,1) + Effort_Data(row,4))/2;

    %Averaging channels 2 and 3 (medial lumbar)

    Avg_Effort_Data(row,2) = (Effort_Data(row,2) + Effort_Data(row,3))/2;

    %Averaging channels 5 and 6 (trapezius)

    Avg_Effort_Data(row,3) = (Effort_Data(row,5) + Effort_Data(row,6))/2;

end

%-------------------

%---End of Step 7---

%-------------------



%----------------------------------

%---Step 8: Plotting the Results---

%----------------------------------

figure
```

```
if Plot_Mode == 1

    %---Plotting Non-Averaged Results (All Channels)---

    bar(Effort_Data)

    legend('Lateral Lumbodorsal (L)','Medial Lumbodorsal (L)','Medial
Lumbodorsal (R)','Lateral Lumbodorsal (R)','Trapezius (L)','Trapezius (R)')

elseif Plot_Mode == 2

    %---Plotting Averaged L & R Results (By Muscle Group)---

       bar(Avg_Effort_Data)

       legend('Lateral Lumbodorsal','Medial Lumbodorsal','Trapezius')

end

ylim([-10 40])

xlabel('Test')

ylabel('Percent of Max Effort')

title(['Experiment 1 Results for Subject ',Subject])

text(0.75,-5,'No Lead, Erect')

text(1.75,-5,'No Lead, Flexed')

text(2.75,-5,'Lead, Erect')

text(3.75,-5,'Lead, Flexed')

text(4.55,-5,'Lead, Prolonged Flexion')

%-------------------

%---End of Step 8---

%-------------------
```

Appendix B

Driver/Filter/Amplifier Circuit Schematics and Filter Performance

B.1 CIRCUIT SCHEMATICS

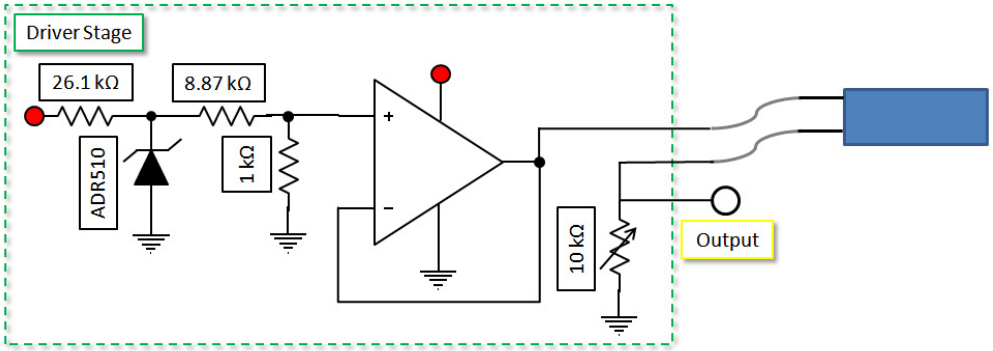

Figure B.1: Driver stage. The piezoresistive sensor (which has two leads) is shown in blue.

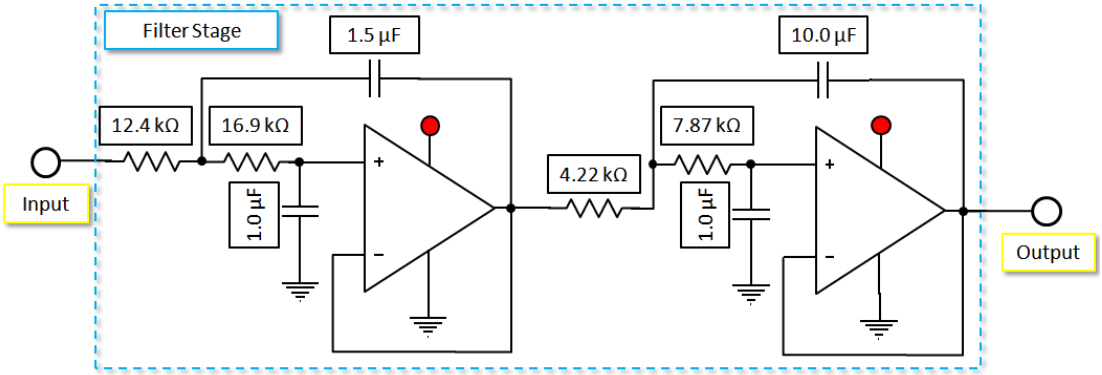

Figure B.2: Filter stage. The input for this stage is the output of the driver stage.

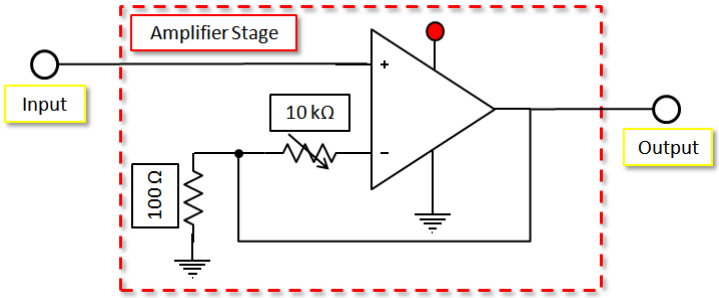

Figure B.3: Amplifier stage. The input for this stage is the output of the filter stage. The output of this stage is connected to an analog input channel on the microcontroller.

B.2 FILTER PERFORMANCE

To test the actual response of the filter, we used a function generator to create sine wave signals at varying frequencies (1-100 Hz) with one of three amplitude/ DC-offset combinations: 100 mV_{p-p} amplitude with +100 mV DC offset (the "AC = DC" configuration, Test 1), 200 mV_{p-p} amplitude with +100 mV DC offset (the "AC > DC" configuration, Test 2), and 100 mV_{p-p} amplitude with +200 mV DC offset (the "AC < DC" configuration, Test 3). The AC V_{RMS} values of both the input (from the function generator) and output (from the filter stage) signals were then measured using an oscilloscope. The resulting DC gain performance, AC gain performance, and phase shift for each test are shown in Figures B.4, B.5, and B.6, respectively.

As Figure B.5 shows, there is a small positive gain in each scenario between 4-8 Hz: approximately 0.6 at the maximum. The attenuation curves also diverge near 60 Hz, where the attenuation values plateau at --31.28 dB, -32.69 dB, and -27.56 dB (AC = DC, AC > DC, and AC < DC, respectively). Thus, the filter attenuates higher frequency noise (anything past ≈ 56 Hz, where the responses diverge) more effectively as the amplitude of the noise increases.

Figure B.4: D.C. gain performance of the filter stage for all three test configurations.

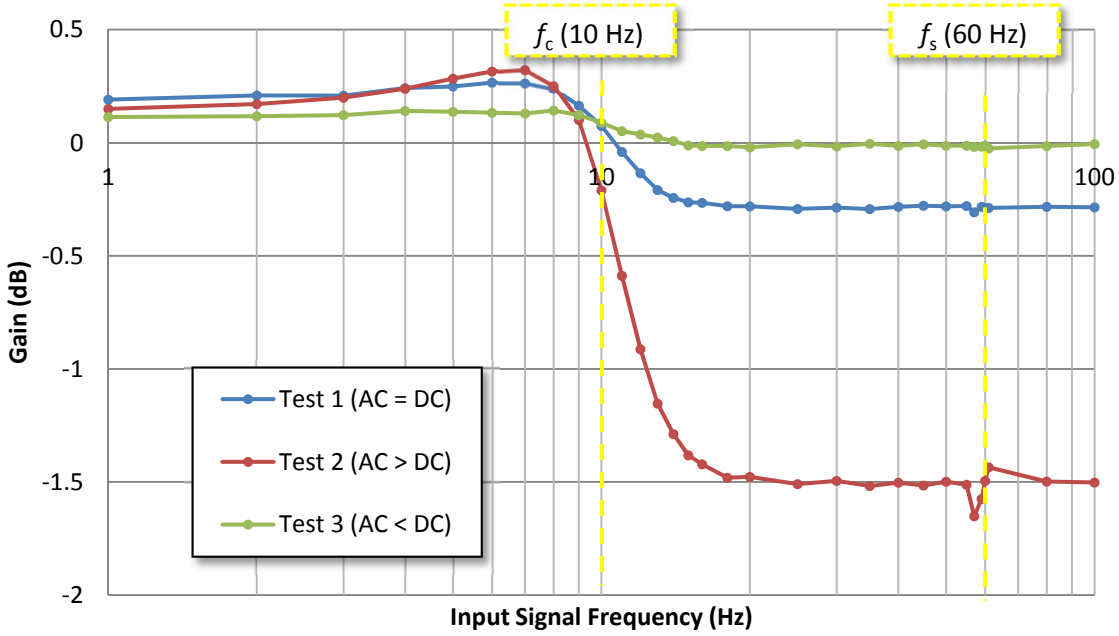

Figure B.5: AC gain performance of the filter stage for all three test configurations.

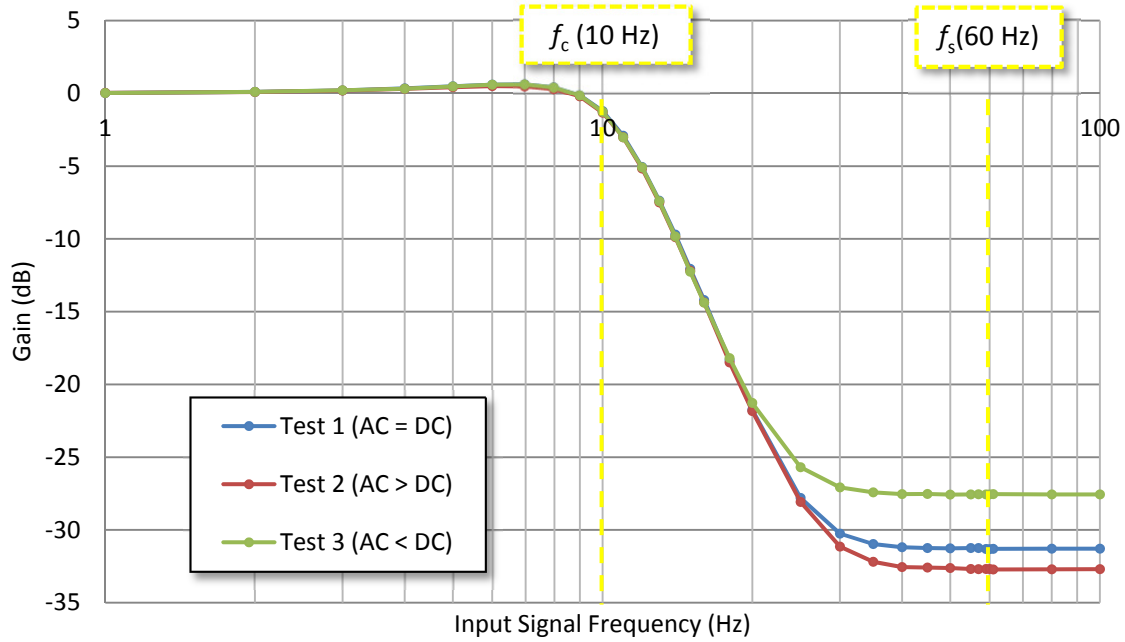

Figure B.6: Phase shift response of the filter stage for all three test configurations; the trendlines are 3rd-order polynomials.